ABSTRACT

Title of Dissertation: INTERCEPTING CYCLIC DINUCLEOTIDE SIGNALING WITH SMALL MOLECULES

Yue Zheng
Doctor of Philosophy
2016

Dissertation directed by: Professor Herman O. Sintim
Department of Chemistry and Biochemistry
University of Maryland, College Park
Department of Chemistry
Purdue University

Bacterial infections, especially the ones that are caused by multidrug-resistant strains, are becoming increasingly difficult to treat and put enormous stress on healthcare systems. Recently President Obama announced a new initiative to combat the growing problem of antibiotic resistance. New types of antibiotic drugs are always in need to catch up with the rapid speed of bacterial drug-resistance acquisition. Bacterial second messengers, cyclic dinucleotides, play important roles in signal transduction and therefore are currently generating great buzz in the microbiology community because it is believed that small molecules that inhibit cyclic dinucleotide signaling could become next-generation antibacterial agents. The first identified cyclic dinucleotide, c-di-GMP, has now been shown to regulate a large number of processes, such as virulence, biofilm formation, cell cycle, quorum sensing, etc. Recently,

another cyclic dinucleotide, c-di-AMP, has emerged as a regulator of key processes in Gram-positive and mycobacteria. C-di-AMP is now known to regulate DNA damage sensing, fatty acid synthesis, potassium ion transport, cell wall homeostasis and host type I interferon response induction. Due to the central roles that cyclic dinucleotides play in bacteria, we are interested in small molecules that intercept cyclic dinucleotide signaling with the hope that these molecules would help us learn more details about cyclic dinucleotide signaling or could be used to inhibit bacterial viability or virulence.

This dissertation documents the development of several small molecule inhibitors of a cyclic dinucleotide synthase (DisA from *B. subtilis*) and phosphodiesterases (RocR from *P. aeruginosa* and CdnP from *M. tuberculosis*). We also demonstrate that an inhibitor of RocR PDE can inhibit bacterial swarming motility, which is a virulence factor.

INTERCEPTING CYCLIC DINUCLEOTIDE SIGNALING WITH SMALL MOLECULES

by

Yue Zheng

Dissertation submitted to the Faculty of the Graduate School of the
University of Maryland, College Park, in partial fulfillment
of the requirements for the degree of
Ph.D. in Biochemistry
2016

Advisory Committee:
Professor Dr. Herman O. Sintim, Chair
Dr. Douglas Julin
Dr. Paul Paukstelis
Dr. Kwaku Dayie
Dr. Sergei Sukharev

Dedication

This is dedicated to my dear husband Changyang Weng. I could never have done this without your constant encouragement and support. I would like to dedicate my dissertation to my beloved parents and grandparents.

Acknowledgements

I would never have been able to finish my dissertation without the guidance of my advisor Dr. Herman O. Sintim and my committee members, the help and cooperation of my co-workers, and the support from my family. I owe my gratitude to all those people who have made this dissertation possible.

First of all, I would like to express my sincere gratitude to my advisor Dr. Herman O. Sintim for his excellent guidance and continuous support of my Ph.D. study and related research. I could not imagine finishing my Ph.D study and this dissertation without his great motivation and immense knowledge.

I would like to acknowledge my committee members Dr. Douglas Julin, Dr. Paul Paukstelis, Dr. Kwaku Dayie, Dr. Surgei Sukharev and Dr. Shuwei Li. Dr. Julin is also my academic advisor, who not only helped me with my Ph.D. projects , but also provided me with invaluable suggestions on my graduate course selections and English test. Dr. Paukstelis is also my independent proposal advisor, who gave me great advices about topic selection, presentation preparation and proposal writing.

A special thank you goes to Sintim group members. Dr. Shizuka Nakayama set a good example for me as a hard working scientist. Dr. Yiling Luo trained me on protein purification and radiolabelling assays in the short period we overlapped. Dr. Jie Zhou always gave me insightful suggestions and kindly help for my research and my personal life. I also thank Dr. Min Guo, Dr. Benjamin Roembke, Dr. Genichiro Tsuji, Dr. Stefan M. Cooper Jr. and Dr. Changhao Wang for synthesizing important compounds for my Ph.D. projects. I am grateful to my colleagues Clement Opoku-Temeng for giving me a hand with protein purification and bacteria culture.

I thank my collaborators in the Center for Tuberculosis Research at Johns Hopkins University, Dr. William Bishai and his postdocs and students Dr. Ruchi Jain Dey, Dr. Bappa Dey and Laurene Chueng for protein purification, LC-MS/MS analysis, *Mtb* culture and mouse study.

I would like to thank for the professors and researchers who kindly provided their plasmids for my research. I am grateful to Dr. Zhao-Xun Liang for RocR and YybT plasmids, Dr. Karl-Peter Hopfner for DisA plasmid, Dr. Angelika Gründling for DisA and GdpP plasmids, Dr. Mark Gomelsky for YahA plasmid, Dr. Vincent Lee for WspR and RocR plasmids, Dr. Karin Sauer for DipA plasdmid, Dr. Francesca Cutruzzolà for PA4108 and PA4781 plasmids, Dr. Nicole Frankenberg-Dinkel for NbdA and MucR plasmids. I would also like to thank Dr. Nicole LaRonde for allowing me to do radiolabeling experiments in her laboratory before we set up our own radioactive laboratory.

Last but not least, I want to express me gratitude to the persons and organizations that provide significant financial support to my scientific research. I thank National Science Foundation (CHE 1307218). I thank the Graduate school of the University of Maryland for Dean's Fellowship (2011 and 2012) and Graduate Dean's Dissertation Fellowship (2015). I thank Dr. Ruchi Mehta and Dr. Amit Mehta for the Mehta research award (2013). I thank the dean of the College of Computer, Mathematical, and Natural Sciences (CMNS) Dr. Jayanth Banavar for the Kraybill Biochemistry Award (2014). I also thank Dr. Joseph Sampugna and ACS Division of Biological Chemistry for the Sampugna/Keeney travel award and ACS travel award (2015).

Table of Contents

List of Tables

List of Figures

List of Schemes

List of Abbreviations

2’3’-cGAMP	cyclic [G(2’,5’)pA(3’,5’)p]
3’3’-cGAMP	cyclic [G(3’,5’)pA(3’,5’)p]
ADPRT	ADP-ribosyltransferase
AMP	adenosine monophosphate
ATP	adenosine triphosphate
BMDC	bone marrow-derived primary dendritic cells
BMDM	bone marrow derived macrophages
c-di-AMP	cyclic diadenosine monophosphate
c-di-GMP	cyclic diguanylate monophosphate
CAUTI	catheter-associated urinary tract infection
CDN	cylic dinucleotide
CF	cystic fibrosis
cGAS	cyclic GMP-AMP synthase
CSP	cytosolic surveillance pathway
DAC	diadenylate cyclase
DAMP	danger associated molecular pattern
DGC	diguanylate cyclase
DisA	DNA integrity scanning protein
DNA	deoxyribonucleic acid
ENPP1	ectonucleotide pyrophosphatase/phosphodiesterase 1
EPS	extracellular polymeric substance

GAP	GTPase-activating protein
GMP	guanosine monophosphate
GTP	guanosine triphosphate
GTS	glycosidic triterpenoid saponin
HIV	human immunodeficiency virus
HPLC	high-performance liquid chromatography
IFN	interferon
IRF3	interferon regulatory factor 3
ITC	isothermal titration calorimetry
MLV	murine leukemia virus
MRSA	Methicillin-resistant Staphylococcus aureus
MTD	median time to death
PAMP	pathogen associated molecular pattern
pApA	5’-phosphoguanylyl-(3’-5’)-adenosine
PDB	protein databank
PDE	phosphodiesterase
pGpG	5’-phosphoguanylyl-(3’-5’)-guanosine
PRR	pattern recognition receptor
SIV	simian immunodeficiency virus
STING	stimulator of interferon genes
T3SS	type III secretion system
TBK1	TANK-binding kinase 1
TCS	two component signaling

TEAA	triethylammonium acetate
TLC	thin layer chromatography

Chapter 1 : Introduction

1.1.Introduction to cyclic dinucleotide

Humanity has always fought with pathogens and bacteria have been especially problematic to counter. Bacterial epidemics have led to the deaths of millions of people over the years. For example the bubonic plaque, caused by the bacterium *Yersinia pestis*, killed over 50 million people in the Roman Empire. The discovery of many antibiotics in the 50s and 60s ushered in an optimism that deaths due to bacterial infections would be a thing of the past but many of these drugs and derivatives thereof have succumbed to bacterial resistance, rendering them ineffective.[3] Recently President Obama announced a new initiative to combat the growing problem of antibiotic resistance.[4] New types of antibiotics are in urgent need to curb the threats posed by methicilin-resistance *Staphylococcus aureus* (MRSA) and other infections that are continually claiming lives. The ability to sense the surrounding environment and regulate cellular processes to adapt to environmental changes is critical for bacterial survival. It is widely accepted that understanding the bacterial signaling and regulation system will lead to the discovery of new druggable targets. Cyclic dinucleotides have emerged as important second messengers and regulate diverse processes.[5] The structures of four types of cyclic dinucleotides are shown in Figure 1.1. C-di-GMP mainly regulates lifestyles of Gram-negative bacteria.[6] C-di-AMP is essential for Gram-positive bacterial survival.[7] 3'3'-cGAMP is found in *Vibrio*[8] and 2'3'-cGAMP, which has a non-canonical 2',5'-phosphodiester linkage, is produced by mammalian cells[9].

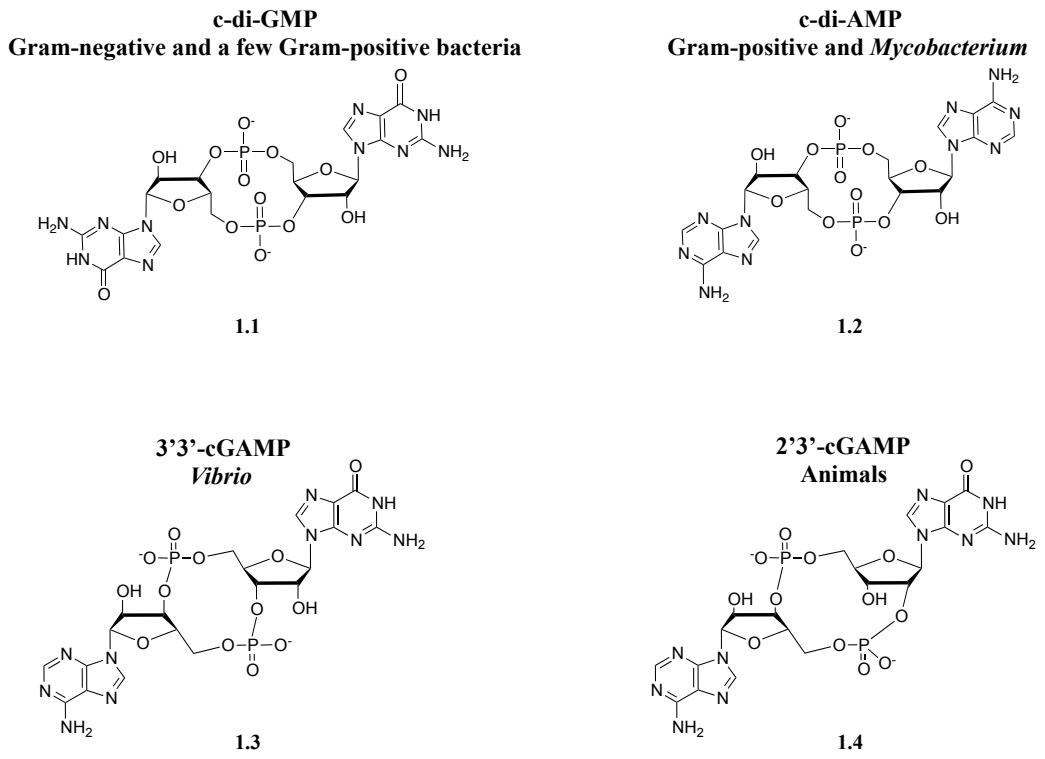

Figure 1.1. Structures of four types of cyclic dinucleotides.

1.2.C-di-GMP

Bis-(3'-5') cyclic diguanylic acid (c-di-GMP) was originally discovered by Benziman and colleagues in the 1987 as an activator of cellulose synthase in Gram negative bacterium *Gluconoacetobacter xylinus* (formerly named *Acetobacter xylinum*).[10] They also showed the existence of diguanylate cyclase (DGC) that enzymatically generated the signaling molecule c-di-GMP from two molecules of guanosine triphosphate (GTP) and phosphodiesterase (PDE) that degraded c-di-GMP.[10] So far, c-di-GMP has been widely identified in a wide variety of Gram-negative, such as *Pseudomonas aeruginosa*, *Caulobacter crescentus*, *Escherichia coli*, *Salmonella typhimurium* and *Vibrio cholerae*, and a few Gram-positive bacteria,

such as *Bacillus subtilis* and *Listeria monocytogenes*.[5] The discovery of different types of c-di-GMP binding proteins discloses its important roles in bacterial lifestyle (planktonic or sessile).[11] When the intracellular concentration of c-di-GMP is high, it induces extracellular polymeric substance (EPS) production and promotes biofilm formation.[12] When c-di-GMP concentration is low, flagella biosynthesis is upregulated and bacterial motility significantly increases.[13] C-di-GMP also represses acute virulence gene transcription.[14] In 2008, Breaker and colleagues reported that c-di-GMP could bind to a new type of receptor, RNA riboswitches and control expression of genes.[15] A general overview of c-di-GMP metabolism and the pathways regulated by c-di-GMP is shown in Figure 1.2.

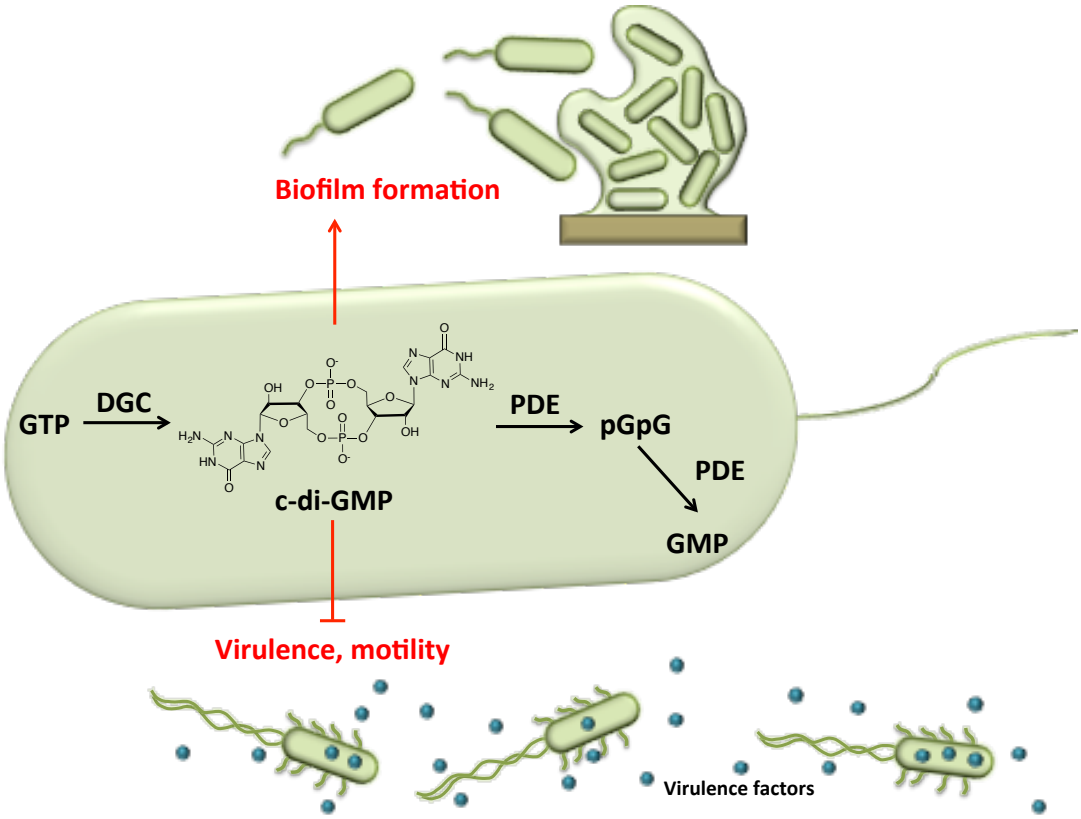

Figure 1.2. An overview of c-di-GMP metabolism and pathways regulated by c-di-GMP. C-di-GMP is synthesized by DGC and degraded by PDE. C-di-GMP promotes biofilm formation and inhibits bacterial motility and acute virulence factor production.

1.2.1. Diguanylate cyclase and phosphodiesterase

The intracellular concentration of c-di-GMP is fine-tuned by its metabolism enzymes, diguanylate cyclase (DGC) and phosphodiesterase (PDE). DGCs cyclize 2 molecules of GTP to c-di-GMP and release 2 molecules of pyrophosphates. DGC was first purified and tested *in vitro* by Benziman.[10] In 1995, Newton and colleagues characterized the gene of a DGC PleD in *Caulobacter crescentus* and identified a novel GGDEF (Gly-Gly-Asp-Glu-Phe) domain at C terminal.[16] PleD is a part of the

PleC-PleD two component signaling (TCS) system. Upon the phosphorylation by histidine kinase PleC, PleD synthesizes the second messenger c-di-GMP.[17] The crystal sctructure of PleD was solved by Schirmer and colleagues in 2004 (Protein Data Bank (PDB) entry 1W25).[18] The conserved GGDEF or GGEEF (Gly-Gly-Glu-Glu-Phe) motifs were confirmed to be commonly shared by most DGCs.[19-21] Some well characterized examples are WspR[20] from *Pseudomonas aeruginosa* (PDE entry 3I5A) and DosC[22] (also known as YddV) from *Escherichia coli* (PDB entry 4ZVE). Some non-canonical domains also display DGC functions, such as AGDEF domain in *Vibrio cholerae* VCA0965[23] and SGDEF domain in *Pectobacterium atrosepticum* ECA3270[24]. Besides the active site (A-site), some DGCs also contain an inhibitory site (I-site). When c-di-GMP binds to the DGC I-site, which usually consists an RxxD (x refers to any amino acid), c-di-GMP synthesis is allosterically inhibited.[25]

The hydrolysis of c-di-GMP is conducted by two types of phosphodiesterases (PDEs), EAL (Glu-Ala-Leu) domain PDE and HD-GYP (His-Asp and Gly-Tyr-Phe) domain PDE. The major product of EAL domain PDE is 5'-phosphoguanylyl-guanosine (pGpG) and the step of degradation of pGpG to Guanosine monophosphate (GMP) is slow. RocR (PDB entry 3SY8[26]) from *Pseudomonas aeruginosa* cleaves c-di-GMP to pGpG in the presence of Mg^{2+} or Mn^{2+} and it is inhibited by Ca^{2+} and Zn^{2+}.[27] The crystal structure of YahA from *Escherichia coli* in complex with c-di-GMP and Ca^{2+} was solved by Schirmer and colleagues in 2014 (PDB entry 4LJ3).[28] Graperin and colleagues predicted the functions of HD-GYP in c-di-GMP hydrolysis by bioinformatic studies[29] and the biochemical evidence for this hypothesis was reported by Dow and colleagues[30]. The HD-GYP domain PDE RpfG from

Xanthomonas campestris pv. Campestris directly cleaves c-di-GMP to GMP.[30] There are a few crystal structures of HD-GYP PDEs. Bd1817 from *Bdellovibrio bacteriovorus* (PDE entry 3TMD), which lacks the tyrosine in the GYP active site, presents a bi-iron center.[31] However, the structure of another HD-GYP protein PmGH from *Persephonella marina* shows a different trinuclear iron active site (PDB entry 4ME4).[32] In 2015, the structure of PA4781 from *Pseudomonas aeruginosa* was reported (PDB entry 4R8Z) and the bimetallic active site binds to Mn^{2+}, Ni^{2+} and some other transition metals with similar affinities.[33]

1.2.2. C-di-GMP binding proteins and riboswitches

The regulation functions of c-di-GMP rely on the downstream receptors, including c-di-GMP binding proteins and riboswitches.[5] There are three major types of c-di-GMP binding proteins: 1) PilZ domain c-di-GMP receptor; 2) DGC I-sites and inactive EAL and HD-GYP domains; 3) other types of c-di-GMP receptors.[11]

The first type of c-di-GMP binding domain PilZ (Pfam: PF07238) was predicted by Amikam and Gaperin by bioinformatics studies.[34] This hypothesis was proved by Gomelsky and colleagues in the same year.[35] The purified PilZ domain protein YcgR from *Escherichia coli* showed a dissociation constant (K_d) of 0.84 ± 0.16 μM to c-di-GMP and the C terminus of BcsA from *Gluconacetobacter xylinus* also binds to c-di-GMP with a lower affinity.[35] The PilZ domain is widely spread in many bacteria. Alg44 from *Pseudomonas aeruginosa*[36], DgrA protein from *Caulobacter crescentus*[37], PlzC and PlzD from *Vibrio cholerae*[38] are typical PilZ domain c-di-GMP receptors. The conserved sequence $RxxxR_{20\text{-}30}$(D/N)x(S/A)xxG (x refers to any

amino acid) in PilZ domain, which is responsible for c-di-GMP binding, was disclosed by the crystal structures and biochemical experiments.[11, 35, 36]

As mentioned previously, c-di-GMP binds to the I-site of DGC and allosterically inhibits DGC activity. C-di-GMP strongly inhibits PleD from *Caulobacter crescentus* with a K_i of 0.5 μM.[18] Protein with degenerate GGDEF or EAL domains is another kind of c-di-GMP receptor. For example, FimX from *Pseudomonas aeruginosa* with GGDEF-EAL domain does not have DGC or PDE activity (PDB entry 3HV8).[39] Its EAL domain binds to c-di-GMP with 104.2 nM affinity and regulates twitching motility.[39] Another example is the GGDEF domain of PopA from *Caulobacter crescentus*. Instead of synthesizing c-di-GMP, its GGDEF domain binds to c-di-GMP and mediates movement toward cell pole.[40]

Some c-di-GMP receptors are transcription factors that upregulate or downregulate target gene transcription upon c-di-GMP binding, such as the major flagella gene regulator in *Pseudomonas aeruginosa* FleQ (PDB entry 4WXM).[41] C-di-GMP binds to the Walker A motif of FleQ with stoichiometry of 2:1 and K_d of about 4.1 μM and results in the repression of flagella biosynthesis and increase of EPS production.[42] VpsT is a transcription factor in *Vibrio cholerae* that regulates biofilm formation. C-di-GMP dimer binds to VpsT and induces VpsT dimerization, so the stoichiometry is 1:1 and the affinity was measured as 3.2 μM.[43]

Breakers and Collegues reported the first type of c-di-GMP binding RNA riboswitch Vc2 in 2008.[15] Riboswitch is a noncoding segment of messenger RNA, which adopts specific secondary structures. Upon binding to the small molecular

ligand c-di-GMP, RNA riboswitch secondary structure changes and regulates transcription of downstream genes. Vc2 riboswitch binds to c-di-GMP specifically with about 1 nM affinity.[15] In 2010, the same group identified c-di-GMP-II riboswitch.[44] C-di-GMP-II riboswitch senses c-di-GMP with ≤ 200 pM affinity and regulates self-splicing.[44] In 2012, Sintim and colleagues reported a hybrid Spinach-Vc2 RNA aptamer, which contains a c-di-GMP binding region and a fluorescent reporter region.[45] In the presence of fluorophore DFHBI, Spinach-Vc2 RNA aptamer detects as low as 320 nM c-di-GMP.[45]

1.2.3. Cellular processes regulated by c-di-GMP

C-di-GMP was first discovered as an allosteric activator of cellulose synthase in *Gluconoacetobacter xylinus*.[10] Although discovered almost 30 years ago, it is only in the last decade that the many cellular processes that are regulated by c-di-GMP have been elucidated. The major function of c-di-GMP is the regulation of motility-to-sessility transition.[5] It is also a key player in cell cycle and virulence factor production.[5]

Bacteria have two common lifestyles, planktonic cells and sessile biofilm. Biofilm is a group of microorganisms adhere to a solid surface and it is a common mode of bacterial growth in natural enviroment.[46] Biofilm cells are embedded within a self-produced matrix of extracellular polymeric substance (EPS).[46] EPS matrix consists of exoplolysacchrides, extracellular proteins, DNA and some other macromolecules.[47] EPS protects bacterial cells from harsh environment and antibiotic killing. It also facilitates attachment and adhesion to host cells and contributes to pathogenicity.[47] Biofilm causes different kinds of health problems, such as wound infection, cystic

fibrosis lung infection and dental plaque.[48] Biofilm colonizes implanted medical devices, like Catheter, Mechanical heart valves and Prosthetic joints.[49] Biofilms are difficult to eradicate, leads to complications during infections and are also a threat to food industry.[50] Many outbreaks of foodborne diseases were associated with biofilm. Interest is currently high regarding c-di-GMP signaling because it has emerged as it is a master biofilm regulator.[12] Research studies about different bacteria have shown that inactivation of c-di-GMP synthase dramatically abolished biofilm formation, rendering c-di-GMP as a new target for biofilm eradication.[51, 52] The mechanism of how c-di-GMP regulates biofilm formation has been studied in details. There are plenty of c-di-GMP receptor proteins participating in the EPS biosynthesis system. C-di-GMP promotes biofilm formation by binding to these receptors and facilitate EPS synthesis and transportation.[53] Cellulose is a key component of EPS matrix. It provides structural support to biofilm and promotes attachment to surfaces.[54] C-di-GMP is a cellulose biosynthesis regulator. In *Gluconoacetobacter xylinus*, c-di-GMP binds to the PilZ domain of cellulose synthase subunit A (CeSA) and induces the production of cellulose.[55] Alginate is an exopolysaccharide produced by *Pseudomonas aeruginosa* to enhance bacterial adhesion to solid surface and host tissues.[56] C-di-GMP binds to a PilZ domain receptor protein Alg44 and promotes alginate secretion.[36] Pel polysaccharide is produced by *Pseudomonas aeruginosa* during biofilm formation.[57] It not only helps adhesion, but also provides resistance to aminoglycoside antibiotics.[58] Dimeric c-di-GMP binds to the inactive GGDEF domain of PleD protein and stimulates Pel production.[59] C-di-GMP also regulates Pel and another *Pseudomonas aeruginosa* exopolysaccharide Psl via the transcription

factor FleQ.[60] FleQ represses the expression of *pel* and *psl* genes.[60] When c-di-GMP binds to FleQ, the repression effect is relieved.

Bacterial motility is essential for the infection process, because it enables bacteria to move toward host cells. Nurminen and colleagues showed that urinary tract infection of *Salmonella enterica* serovar Typhimurium relied on its motility.[61] Guentzel and Berry reported that *Vibrio cholerae* infection and virulence was associated with its motility. The mortality rate of mice infected with non-motile *Vibrio cholera* was much lower than the ones infected with wild-type strains.[62] Most bacteria move via rotation of flagella, which is a long rigid structure protruded from the cell surface. Flagellum enables bacteria to swim in the water and sometime swarm on the semi-solid surface. Hughes and coleagues showed that urinary tract infection caused by *Proteus mirabilis* was related to the flagella mediated swarming activity. Lost of flagella abolished its ability to enter urothelial cells and the non-swarmer cells were 25-fold less invasive into the urothelial cells than wild-type cells.[63] Inhibition of bacterial motility is considered as a promising way to reduce infection. C-di-GMP stands out because of its key role in flagella regulation in various bacteria. In *Escherichia coli* and *Salmonella enterica*, c-di-GMP impedes flagella rotation and swimming motility by binding to the PilZ domain protein YcgR. (Figure 1.3)[64] The rotation of flagella depends on the torque generated by the stator protein MotA and the rotor component FliG.[65] Research reported showed that c-di-GMP bound YcgR disrupted the electrostatic interaction between MotA and FliG/M and resulted in inefficient swimming.[66]

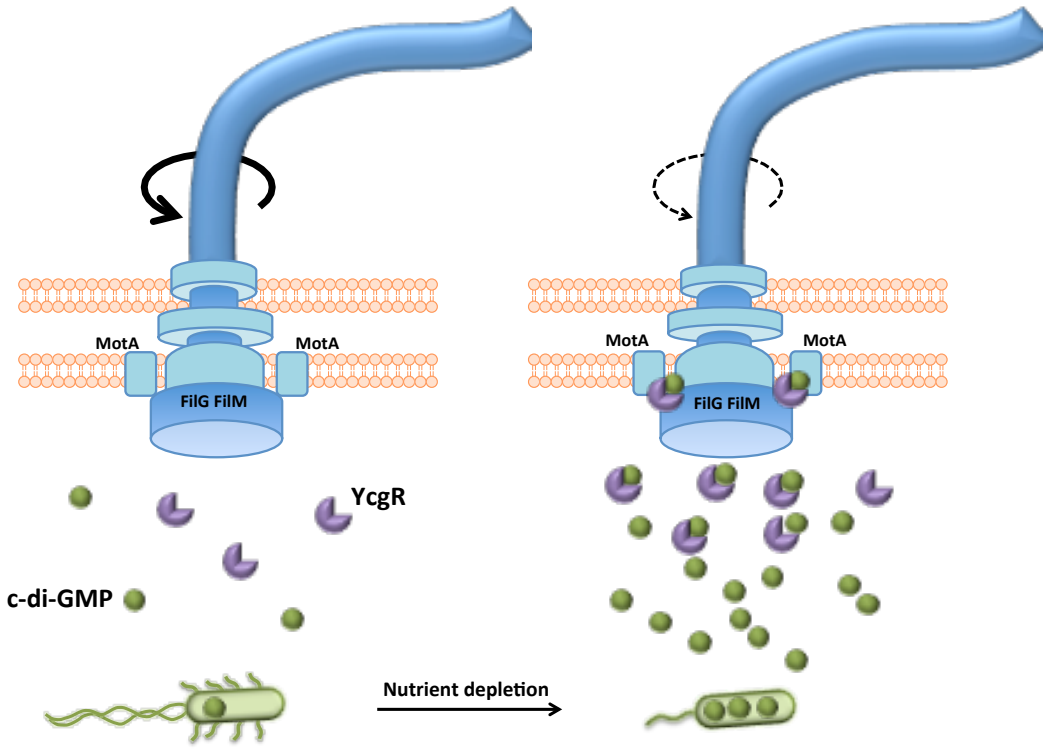

Figure 1.3. C-di-GMP impedes motility of *Escherichia coli*. When c-di-GMP concentration is low, *Escherichia coli* swims by rotation of flagella, which is powered by the torque generated by MotA and FilG. When c-di-GMP intracellular concentration is high, it binds to the PilZ domain protein YcgR. C-di-GMP bound YcgR interrupts the interaction between MotA and FilG/M and slows down swimming.

In *Pseudomonas aeruginosa*, c-di-GMP binds to the Walker A motif of FleQ, which is the activator of flagella genes, and leads to the repression of flagella synthesis. C-di-GMP mediates flagella biosynthetic gene repression via binding to a key transcription factor FleQ.[67] *P. aeruginosa* encodes two stator complexes, MotAB (PA4954/4953) and MotCD (PA1460/1461).[68] These stators are cytoplasmic membrane channels that generate flagella rotation torque by proton conduction. The

numbers of MotAB and MotCD in a motor is dynamic. Both MotAB and MotCD stators can provide energy for swimming motility. Disability of one stator does not completely vanish swimming. However MotAB and MotCD have opposite functions in swarmer cells.[69] MotCD generates torque for swarming, but MotAB impedes it. With unknown mechanism, c-di-GMP downregulates the proportion of MotCD in a motor and slows down swarming.[70]

Bacterial virulence factors make significant contribution to their pathogenicity. Virulence factors enable bacteria to attach to and invade into host cells and tissues, escape from host immune response and cause damage to host tissues. C-di-GMP is involved in virulence factor production regulation. Tischler and Camilli found that c-di-GMP repressed the expression of the cholera toxin produced by *Vibrio cholerae*. The c-di-GMP phosphodiesterase VieA activity is essential for *Vibrio cholerae* virulence. VieA mutant leads to high intracellular concentrations of c-di-GMP, which attenuated *Vibrio cholerae* virulence in the infant mouse model.[71] Klose and colleagues also showed that elevated c-di-GMP concentration in *Francisella novicida*, a Gram-negative pathogen, increased biofilm formation and decreased virulence in mice infection.[72] *Pseudomonas aeruginosa* utilizes its type III secretion system (T3SS) to directly inject effector proteins into host cells. ExoS and ExoU are the two most toxic effector proteins. ExoS has both GTPase-activating protein (GAP) activity and ADP-ribosyltransferase (ADPRT) activity and disrupts of host cell actin skeleton.[73] ExoU is a phospholipase, which has acute cytotoxicity in epithelial cells and macrophages and is involved in killing neutrophils.[74] Overexpression of *Pseudomonas aeruginosa* DGC WspR or PA1120 dramatically decreased the delivery

of T3SS needle tip structural protein PcrV, indicating that c-di-GMP represses T3SS.[75] Figure 1.4 shows the regulation of virulence factors in *Pseudomonas aeruginosa* regulated by c-di-GMP signaling system and quorum sensing.

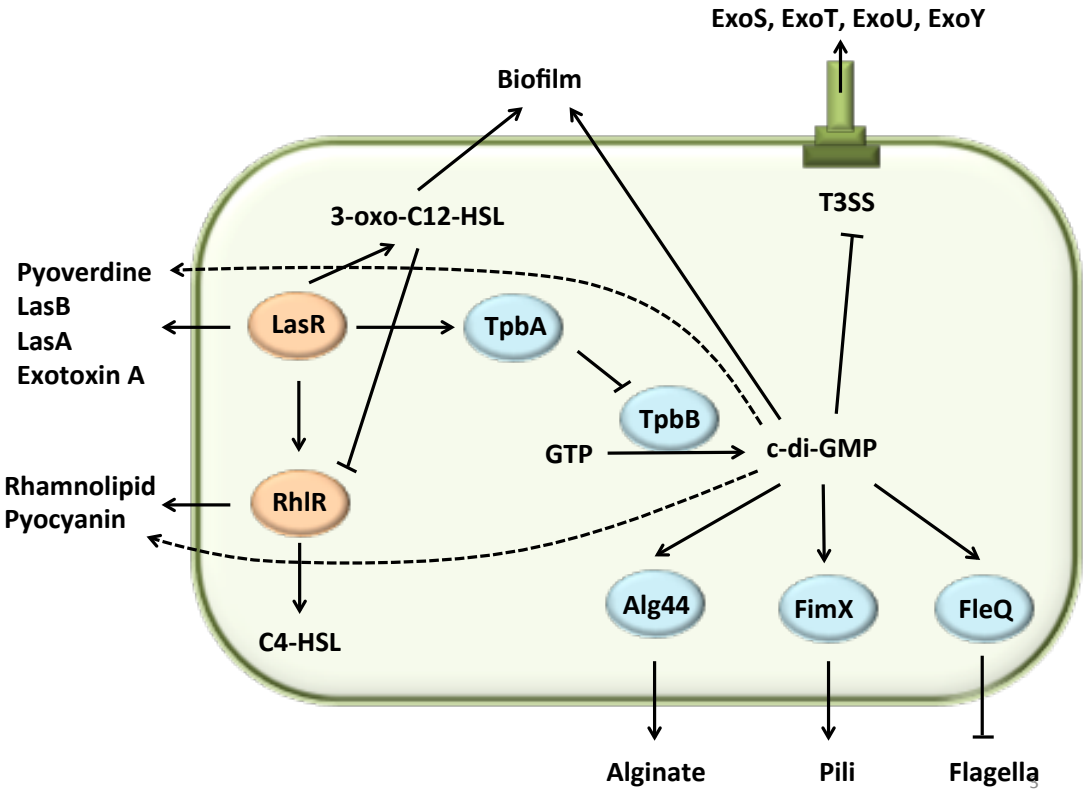

Figure 1.4. Virulence factor production in *Pseudomonas aeruginosa* regulated by c-di-GMP signaling system and quorum sensing. C-di-GMP inhibits the expression of acute virulence genes, such as T3SS, which directly delivers toxins to host tissues. C-di-GMP promotes chronic infection, such as exopolysaccharide production and biofilm formation. QS and c-di-GMP are linked by TpbA and TpbB. LasR activates *tpbA* gene expression and TpbA inhibits TpbB, which is a diguanylate cyclase.

1.2.4. Inhibitors of c-di-GMP signaling

A lot of efforts have been put into the discovery of c-di-GMP signaling inhibitor. The pioneer work was done by Benziman, who discovered c-di-GMP. Benziman group isolated Glycosidic triterpenoid saponin (GTS) from *Pisum sativum* and showed that GTS was a specific inhibitor for DGC in *Gluconoacetobacter xylinus* with a K_i of 5 μM.[76] Papulacandin B, which is an antifungnal compound from *Papularia sphaerosperma*, also inhibits DGC with less promising K_i (70 μM).[77] Recently more small molecule inhibitors of DGCs have been discovered. Waters and colleagues reported seven *Vibrio cholerae* DGC inhibitors that also inhibited biofilm formation.[52] They also identified four molecules that inhibited DGC activity and biofilm formation by *Pseudomonas aeruginosa* and *Acinetobacter baumannii*.[51] However, researchers only focus on DGC inhibitors because c-di-GMP increases biofilm formation. There is a paucity of c-di-GMP PDE inhibitors. In 1990, Benziman and colleagues synthesized a series of 13 cyclic dinucleotides or cyclic trinucleotides. These nucleotides were subject to *Gluconoacetobacter xylinus* PDE-A cleavage and they inhibited the cleavage of c-di-GMP by PDE-A.[78] Sintim and colleagues synthesized an analog of c-di-GMP with a bridging sulfur in the phosphodiester linkage. This analog, named endo-S-c-di-GMP inhibits c-di-GMP cleavage by *Pseudomonas aeruginosa* PDE RocR.[79] These PDE inhibitors are all nucleotides that harbor negative charged phosphodiester linkage. Thus the cell permeability of these inhibitors is low and they hardly have *in vivo* activities. During my Ph.D., I was interested in the identification of cell permeable PDE inhibitors, which can be utilized to analyze the intracellular functions of PDE. In Chapter 5, I

described the identification of a RocR inhibitor, which modulated the swarming activity and virulence factor production of *Pseudomonas aeruginosa*.

1.3. C-di-AMP

In 2008, Hopfner discovered another cyclic dinucleotide second messenger, Cyclic diadenosine monophosphate (c-di-AMP) in *Bacillus subtilis* along with its synthase DNA integrity scanning protein (DisA).[80] DisA scans DNA and searches for DNA breaks.[81] During DNA scanning by DisA, the enzyme converts ATP into c-di-AMP. When DisA finds a DNA break, such as Holiday junction, it stays at the damage site, c-di-AMP synthesis is halted and the enzyme recruits other enzymes to repair DNA.[80] C-di-AMP serves as a signal to report the DNA breaks and causes a delay in sporulation.[82] Now c-di-AMP has emerged as a key regulator of key processes in Gram-positive and mycobacteria, such as *Staphylococcus aureus*, *Streptococcus pneumonia*, *Streptococcus pyogenes*, *Listeria monocytogenes*, *Mycobacterium smegmatis*, *Mycobacterium tuberculosis*, etc.[7] C-di-AMP is now known to regulate DNA damage sensing[80], fatty acid synthesis[83], potassium ion transport[84], cell wall homeostasis[85] and host type I interferon response induction[86] (See Figure 1.5). Interestingly bacterial DNA and cell wall are important targets for antibiotics that are currently used in the clinic. Therefore it is likely that inhibitors of c-di-AMP signaling could potentiate the actions of these traditional antibiotics.

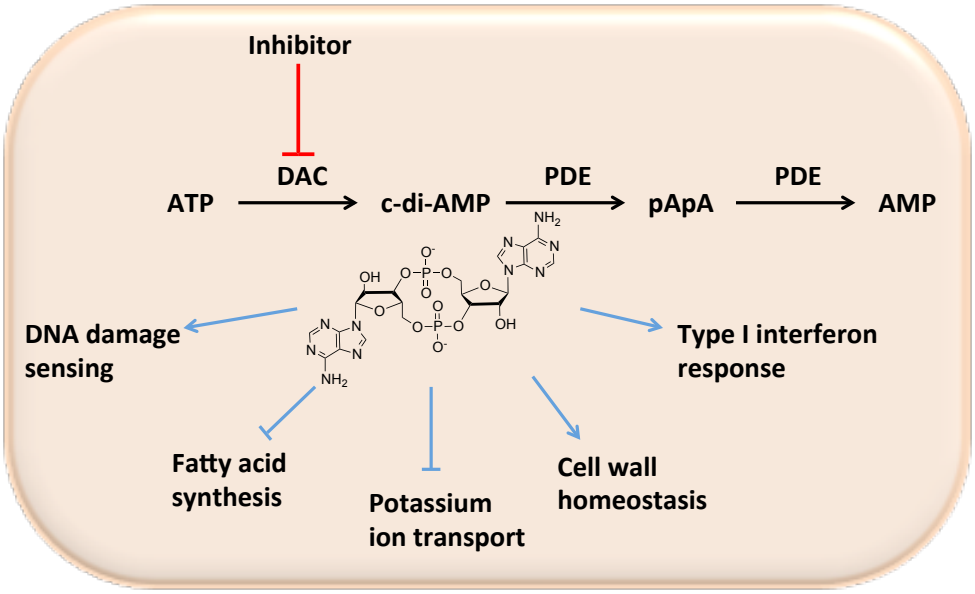

Figure 1.5. An overview of c-di-AMP metabolism and pathways regulated by c-di-AMP. C-di-AMP is synthesized by DAC and degraded by c-di-AMP specific PDE. C-di-AMP regulates DNA damage sensing, cell wall homeostatic, fatty acid synthesis and potassium ion transport. C-di-AMP is able to induce host type I interferon response.

1.3.1 Diadenylate cyclase and phosphodiesterase

Unlike c-di-GMP, for which the metabolic and regulatory pathways have been largely explored, c-di-AMP metabolism enzymes, receptor proteins and RNAs remain largely uncharacterized. C-di-AMP is synthesized from two molecules of ATP by diadenylate cyclase (DAC), which contains a DAC domain. DAC domain proteins have been reported in *Bacillus subtilis* (DisA[80] and CdaS[87]), *Streptococcus pyogenes* (spyDAC)[88], *Streptococcus pneumoniae* (DacA)[89] and *Mycobacterium tuberculosis* (Rv3586)[90]. C-di-AMP is degraded by phosphodiesterase (PDE) to linear 5'- phosphoadenylyl adenosine (pApA) or adenosine monophosphate (AMP).

Most of c-di-AMP PDE contains DHH/DHHA1 domain. C-di-AMP PDEs have been reported in *Bacillus subtilis* (YybT)[91], *Staphylococcus aureus* (GdpP)[92], *Streptococcus pneumoniae* (Pde1 and Pde2)[89], *Mycobacterium tuberculosis* (Rv2837c)[93] and *Borrelia burgdorferi* (DhhP)[94]. Recently a novel HD(His-Asp)-domain PDE from *Listeria monocytogenes* was reported to hydrolyze c-di-AMP by Woodward and colleagues.[95]

1.3.2 C-di-AMP effector proteins

As a second messenger, c-di-AMP binds to receptors and regulates downstream cellular processes. The receptors of c-di-AMP include proteins or RNA riboswitches.[7] The first identified c-di-AMP receptor was DarR, a TetR family transcription factor in *Mycobacterium smegmatis*.[83] C-di-AMP binding enhances DarR DNA binding activity and represses the expression of target genes, including the gene encoding a cold shock protein CspA and two genes associated with fatty acid metabolism and transportation.[83] C-di-AMP binding proteins KtrA in *Staphylococcus aureus*[96] and CabP in *Streptococcus pneumoniae*[84] enable bacterial survival under low-potassium conditions and elevated c-di-AMP impairs potassium uptake. For some other c-di-AMP binding proteins in *Staphylococcus aureus*, histidine kinase KdpD was also predicted to involve in potassium homeostasis and CpaA was predicted to be a cation/proton antiporter[96]. The PII-like signal transduction protein PstA[97] in *Staphylococcus aureus* and DarA[98] in *Bacillus subtilis* also showed c-di-AMP binding affinity. RNA riboswitches also serve as c-di-AMP receptors. A common riboswitch class ydaO was reported to bind to c-di-AMP with subnanomolar affinity[99] and the c-di-AMP bound structures showed two c-di-AMP binding pockets[100, 101] and

fluorescent riboswitch biosensors were also developed to detect c-di-AMP in live cells.[102]

1.3.3 Inhibitors of c-di-AMP signaling

Although c-di-GMP is an important second messenger, bacteria are usually able to tolerate the overexpression or mutation of c-di-GMP metabolism enzymes.[5] However, c-di-AMP intracellular concentration is rigidly controlled. If c-di-AMP level is either lower or higher than an appropriate range, it impairs the growth of *Bacillus subtilis*.[103] Woodward and colleagues showed that c-di-AMP is very important for cell wall metabolism and viability of *Listeria monocytogenes*.[85] Low concentration of c-di-AMP caused by depletion of DAC or overexpression of PDE led to decreased bacterial growth and bacteriolysis.[85] C-di-AMP is also involved in virulence production. Mutation of *dhhP* gene (a c-di-AMP PDE in *Borrelia burgdorferi*) significantly decreased the production of the major bacterial virulence factor OspC.[94] *Mycobacterium tuberculosis* c-di-AMP PDE CnpB is critical for its virulence.[104] Macrophages infected with ΔcnpB strain, which produces higher concentrations of c-di-AMP, expressed more type I interferon. ΔcnpB strain was less virulence in a mice infection model than the wild-type strain.[104]

Since c-di-AMP concentration needs to be maintained at a certain level for bacterial survival, its metabolism enzymes are considered as good targets for new antibiotic development. So far only a few inhibitors of c-di-AMP metabolic enzymes have been reported in literature. DNA integrity scanning protein A (DisA) is a diadenylate cyclase from *Bacillus subtilis*.[81] DNA damage sensing and c-di-AMP synthesis are performed simultaneously. Sintim and colleagues established a high-

throughput fluorescent assay for c-di-AMP detection named the coralyne assay.[105] Coralyne is prepared in a buffer containing halogens (Br^- or I^-), which quenches the fluorescence of coralyne. In the presence of c-di-AMP, coralyne forms complex with c-di-AMP and this complex protects coralyne from halogen quenching effect (see Figure 1.6). Coralynce fluorescence is resumed and correlated to the c-di-AMP concentration.[105] During my Ph.D., I participated in the development of coralyne assay and optimized this method for DAC inhibitor screening. In Chapter 2, I described the identification of the first inhibitor for DisA from a 1000-compound library.[106] Hopfner and colleagues found that 3'-dATP inhibited DisA with an IC_{50} of 3 μM.[107] Recently, Sintim group identified another DisA inhibitor suramin, which is an antiparasitic drug, from a screening of a library of 2000 known drugs.[108] For c-di-AMP PDE, Liang and colleagues showed that the stringent stress alarmone ppGpp was an inhibitor for YybT in *Bacillus subtilis*.[91] ppGpp competitively inhibited YybT cleaving c-di-AMP with a K_i of about 36 μM.[91] ppGpp also inhibits GdpP in *Staphylococcus aureus* with a K_i of 129.7 ± 42.8 μM[109] and PgpH in *Listeria monocytogenes* with a IC_{50} of 200 ~ 400 μM[95]. There are no literature reports for inhibitors for c-di-AMP receptor proteins and riboswitches.

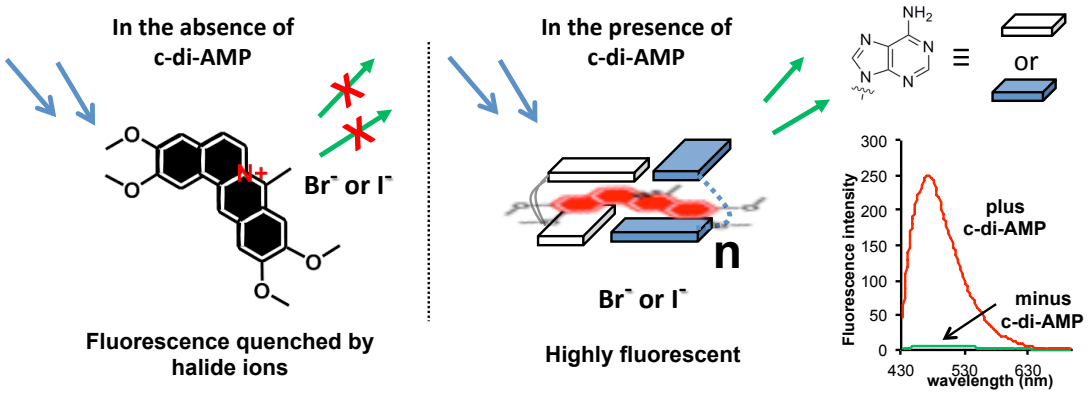

Figure 1.6. C-di-AMP detection by the coralyne assay. Halide ions (Br^- or I^-) in the solution quench coralyne fluorescence in the absence of c-di-AMP. In the presence of c-di-AMP, it forms complexes with coralyne. C-di-AMP protects coralyne from quenchers and c-di-AMP-coralyne complex's fluorescence can be detected.

C-di-AMP production is critical for bacterial viability. It is expected that the inhibitors of c-di-AMP signaling would have the potential to be developed into potent antibacterial agents against important human pathogens. In Chapter 4, I described the characterization of a *Mycobacterium tuberculosis* c-di-AMP PDE CdnP and showed its unexpected cleavage against host derived second messenger 2'3'-cGAMP. The cleavage activity of CdnP is critical for *Mycobacterium tuberculosis* virulence. We designed and synthesized a small molecule Ap(S)A, which inhibits CdnP activity *in vitro* and attenuated virulence *in vivo*.

1.4. 3'3'-cGAMP

In 2012, Mekalanos and colleagues explored the contribution of the Vibrio 7(th) pandemic island-1 (VSP-1) to pathogenesis and they discovered a new type of cyclic dinucleotide with hybrid bases, cyclic AMP-GMP (3'3'-cGAMP), in Vibrio

cholerae.[8] This new bacterial second messenger is synthesized by a novel class of di-nucleotide cyclase DncV,[8] which contains a conserved G[G/S]$X_{9\text{-}13}$DX[D/E] motif. DncV was required for the intestinal colonization and it also repressed *V. cholerae* chemotaxis. Three years later, Jiang and colleagues reported three cGAMP-specific PDEs in Vibrio cholerae with HD-GYP domains, named V-cGAP1/2/3.[110] All of V-cGAP1/2/3 are able to degrade 3'3'-cGAMP to the linear 5'-pApG and V-cGAP1 can cleave 5'-pApG to 5'-ApG in a second step, due to its 5'-nucleotidase activity.[110] The protein receptors for 3'3'-cGAMP are still unclear. The first 3'3'-cGAMP riboswitch was developed based on the class I c-di-GMP riboswitch. In 2011, Strobel and colleagues found that a single C92U mutation in the ligand binding pocket enables c-di-GMP class I riboswitch to bind to 3'3'-cGAMP.[111] In 2015, Hammond showed that Gram-negative bacterium *Geobacter sulfurreducens* produced 3'3'-cGAMP and GEMM-I (Genes for the Environment, Membranes, and Motility) class riboswitch was a 3'3'-cGAMP receptor that regulates electrophysiology genes.[112] At the same time, Breaker and colleagues also reported 3'3'-cGAMP riboswitch in *Deltaproteobacteria* that controls exoelectrogenesis.[113]

1.5. 2'3'-cGAMP

In 2013, cyclic dinulcleotide second messenger in mammals was brought to light by Ablasser, Hornung and colleagues.[114] One of the two phosphodiester bonds has a special linkage between 2'-OH of GMP and 5'-phosphate of AMP, which distinguished mammalian 2'3'-cGAMP from cyclic dinucleotides in bacteria.[115] 2'3'-cGAMP is synthesized from GTP and ATP by a cytoplasmic nucleotidyl transferase, named cyclic GMP-AMP synthase (cGAS).[114] The 2'3'-cGAMP synthesis was

postulated in a two-step manner. Firstly GTP and ATP forms the linear intermediate pppGp(2'-5')A and in the second step, pppGp(2'-5')A is cyclized to 2'3'-cGAMP.[116] The enzymatic activity of cGAS is stimulated by foreign or self DNA in the cytoplasm. When cGAS binds to cytoplasmic DNA, it synthesizes the signaling molecule 2'3'-cGAMP and induces immune response.[117, 118] In 2014, Mitchison and colleagues identified an glycoprotein on the plasma membrane and endoplasmic reticulum ENPP1 that degrades 2'3'-cGAMP into AMP and GMP (k_{cat} = 12 s^{-1}, K_m = 20 μM).[119] ENPP1 was originally reported to be an ATP hydrolase (k_{cat} = 16 s^{-1}, K_m = 46 μM). Crystal structure of ENPP1 (PDB entry 4HTW) revealed a Ca^{2+}-binding domain and ENPP1 is able to chelate two Zn^{2+} ion in its active site.[120]

1.6. Cyclic dinucleotides induce Type I interferon response in a STING-dependent manner

One of the efficient methods for the host innate immune system to detect intracellular pathogens is to sense cytoplasmic DNA. As described previously, upon binding to cytoplasmic double stranded DNA, cGAS synthesizes the signaling molecule 2'3'-cGAMP.[121] 2'3'-cGAMP binds to and activates STING (Stimulator of Interferon Genes, also known as MITA, MPYS and ERIS), which is a 5 transmembrane domain protein that predominantly resides in the endoplasmic reticulum.[114] Activated STING triggers the phosphorylation of transcriptional factor IFN regulatory factor (IRF3) by the kinase TANK-Binding Kinase 1 (TBK1).[122, 123] Phosphorylated IRF3 then translocates into the nucleus to induce the transcription of type I interferon genes (See Figure 1.7). The affinity of 2'3'-cGAMP for human STING has been shown to be very high, with a dissociation constant of 4.59 nM.[115]

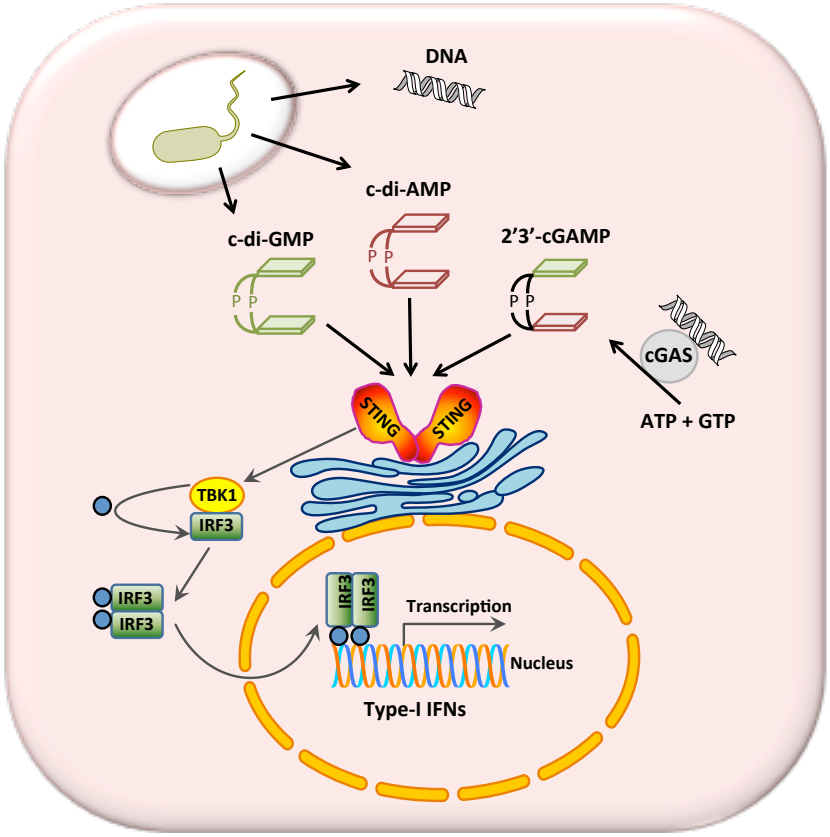

Figure 1.7. Cyclic dinucleotides induce type I interferon response. cGAS detects cytoplasmic DNA and synthesizes 2'3'-cGAMP. 2'3'-cGAMp and c-di-AMP and c-di-GMP from bacteria bind to STING. Activated STING mediates the phosphorylation of IRF3 by TBK1. Phosphorylated IRF3 induces the transcription of type I interferon genes in nucleus.

STING is able to sense cytoplasmic DNA directly[124], as well as the bacterial cyclic dinucleotides[125]. Vance and colleagues showed the direct binding of STING to c-di-GMP and dissociation constant K_d of 5 μM was obtained by equilibrium dialysis.[125] C-di-AMP is capable to induce type I interferon response in a STING-dependent manner but with a lower binding affinity.[126] Chen and colleagues measured the binding affinity of STING to 3'3-cGAMP and synthetic analogs 3'2'-cGAMP and

2’2’-cGAMP by ITC. K_d was measured as 1.04 μM, 1.61 μM and 287 nM. Their binding affinities are much lower than host derived 2’3’-cGAMP.[115]

Chapter 2 : Identification of Bromophenol Thiohydantoin as an Inhibitor of DisA and Structure-activity Relationship Studies of Bromophenol Thiohydantoin

2.1. Identification of bromophenol thiohydantoin as an inhibitor of DisA, a c-di-AMP synthase, from a 1000 compound library, using the coralyne assay

This section (2.1.) was originally published as: Zheng, Y.; Zhou, J.; Sayre D.; Sintim H.O. "Identification of bromophenol thiohydantoin as an inhibitor of DisA, a c-di-AMP synthase, from a 1000 compound library, using the coralyne assay." *Chem. Commun*., 2014, 50, 11234-11237.

2.1.1. Introduction

The ability to sense the environment and communicate with co-inhabitants of an ecosystem is critical for the survival of any organism. Consequently intricate sensing and regulatory mechanisms have evolved in organisms to regulate physiological processes, in response to a changing environment. In 2008, Hopfner showed in a seminal paper that DisA, a *Bacillus subtilis* protein that controls sporulation checkpoint when DNA double strand break occurs, has a nucleotide-binding domain that binds to ATP to make a novel cyclic dinucleotide, c-di-AMP.[80] It turned out that the presence of c-di-AMP signaled the presence of DNA structures that would interfere with proper chromosome segregation. Hopfner also predicted that many bacteria harbored proteins that contained the diadenylate cyclase (DAC) domain and hence c-di-AMP could have a wider role in bacteria, beyond reporting DNA strand breaks.[80] The importance of Hopfner's discovery became apparent when soon

thereafter many reports by other laboratories confirmed that c-di-AMP is indeed produced in other bacteria, some of which are of clinical relevance.[7, 82, 86, 93, 99, 103, 127-131] C-di-AMP has now been shown to control a dazzling array of processes in bacteria (see Figure 1.5), including cell wall formation[85, 132], cell size regulation[92], heat stress[133], virulence[94, 134], ion transport[84], resistance to acid[85, 91] etc. Additionally, when c-di-AMP is introduced into the cytoplasm of eukaryotic cells, for example when intracellular pathogens secret the nucleotide or during endocytosis of bacteria, it binds to STING to elicit type I interferon response[86, 88, 126, 135-137].

The modulation of bacterial cell wall synthesis by c-di-AMP is particularly interesting because a high percentage of antibiotics, in clinical use, target components of the bacterial cell wall, suggesting that small molecules that could perturb the intracellular concentrations of c-di-AMP could synergize with antibiotics such as the b-lactams or vancomycins to kill pathogenic bacteria.[138] An obvious way to reduce intracellular concentration of c-di-AMP would be to inhibit c-di-AMP synthases. High-throughput assays that could be used to monitor the production of c-di-AMP by DAC enzymes would facilitate the discovery of c-di-AMP signaling inhibitors.

2.1.2 Result and discussion

Recently, we described a surprisingly simple detection of c-di-AMP using commercially available coralyne and halide quenchers.[105] In this assay, the fluorescence of coralyne is quenched by a bromide or iodide anion but when coralyne becomes entrapped by a supramolecular aggregate of c-di-AMP, iodide can no longer quench the fluorescence and hence enhancement of fluorescence occurs only when c-di-AMP is present (see Figure 2.1). In our prior disclosure, the synthesis of c-di-AMP

by DisA was monitored as an end-point assay, that is aliquots of the enzymatic reaction were taken at different time points and analyzed using coralyne and KI. For high-throughput assay, this format was obviously not ideal so we wondered if we could add the coralyne and KI to the DisA reaction and monitor the progress of c-di-AMP formation in "real-time". Pleasingly, the presence of coralyne or KI did not affect the enzymatic proficiency of DisA to a great extent and so we could use the coralyne assay to screen for the inhibition of 1000 compounds (obtained from TimTec and Sigma, see Appendix for compounds ID). The TimTec compounds were part of a general ATP kinase inhibitor set as we had postulated that because DisA also binds to ATP, using a kinase library would increase our chances of getting a hit. The Sigma compounds were randomly selected by us from the Sigma website but our selection was biased by compounds that were drug-like or known to be kinase inhibitors.

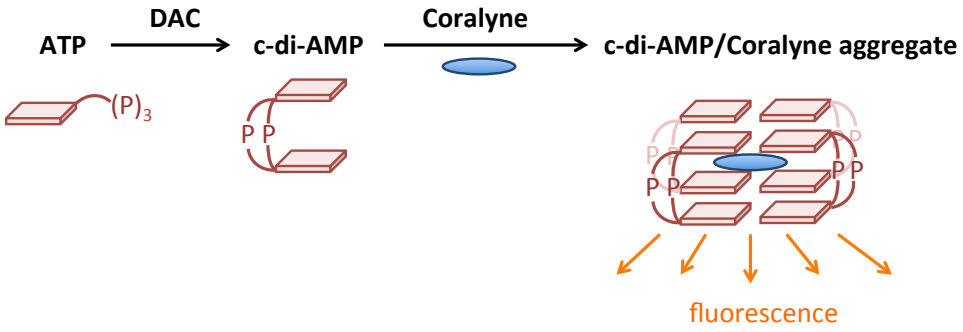

Figure 2.1. Coralyne detection of c-di-AMP formation. DAC converts ATP to c-di-AMP. Once c-di-AMP is formed, it can form complexes with coralyne. I^- in the solution quenches coralyne fluorescence in the absence of c-di-AMP. c-di-AMP protects coralyne from quenchers and c-di-AMP-coralyne complex's fluorescence can be detected.

The majority of the tested compounds, 99%, did not affect the synthesis of c-di-AMP by DisA to any meaningful extent (see Appendix and Figure 2.2). However, about 11 out of the 1000 compounds reduced the fluorescence of the coralyne assay, implying that these compounds either inhibited the DisA enzyme or competed with the synthesized c-di-AMP for binding to coralyne or both. Conceivably the compounds could form a p-complex with coralyne leading to a "dark" aggregate. This would be especially true for compounds that contain heavy halogens, which are known to be fluorescence quenchers[139]. We therefore investigated the extent to which the fluorescence of coralyne was reduced by the 11 apparent "hits" in the presence and absence of c-di-AMP. We also used HPLC to monitor the synthesis of c-di-AMP by DisA in the presence of the 11 apparent hits, see Figure 2.3.

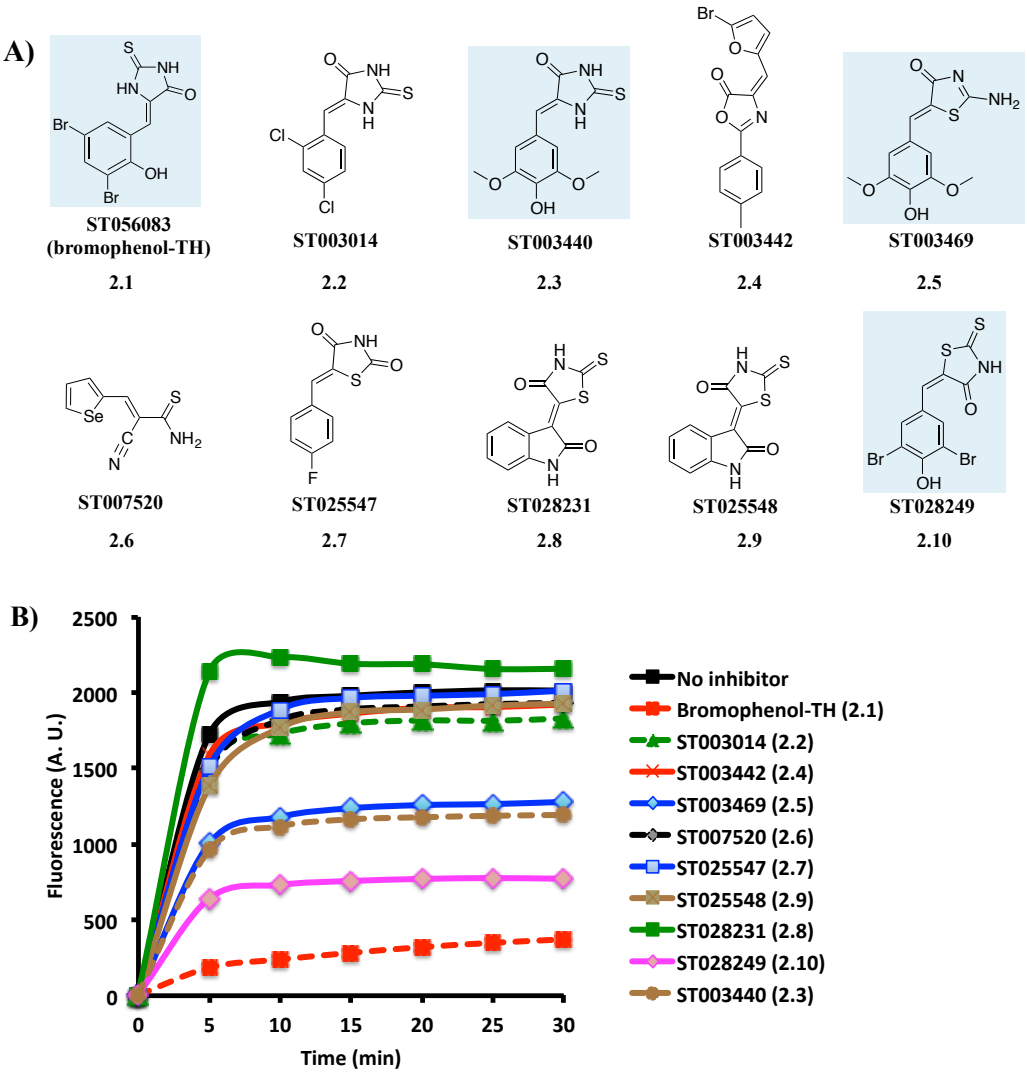

Figure 2.2. A) Structures of bromophenol-TH and molecules in the 1000 compound library that have similar structures. B) Realtime coralyne-based fluorescent detection of DisA reaction.

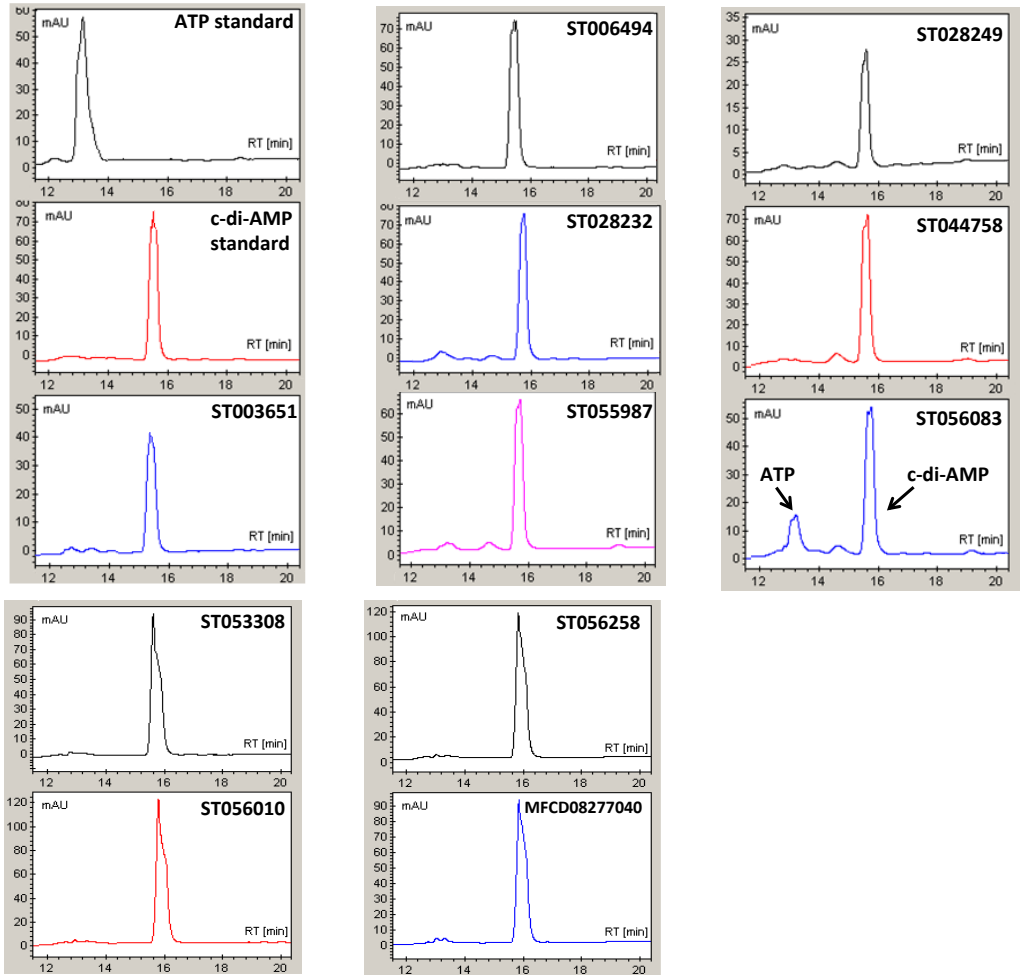

Figure 2.3. HPLC graphs of selected hits affecting DisA reactions. 50 μM hits from Timtec ActiTarg-K library and 100 μM MFCD08277040 from Sigma-Aldrich library were mixed with 100 μM ATP and 10 μM DisA. Reactions were stopped after 30 min. Enzymes were removed by filtration. ATP and c-di-AMP were used as HPLC standards. The compound added was indicated at the upper right corner of each graph.

Out of the 11 apparent hits, only one ST056083 (5-[(3,5-dibromo-2-

hydroxyphenyl)methylene]-2-thioxo-1,3-diazolidin-4-one,[140] referred to as Bromophenol-TH in this manuscript, see Figure 2.2 for structure) could inhibit c-di-AMP synthesis, judged by HPLC analysis (see Figure 2.3). It therefore appears that the coralyne assay has some false positives due to the direct quenching of coralyne's fluorescence by some small molecules. But this problem is not unique to the coralyne assay and in fact would exist in all turn-off assays as the potential for library members to affect the fluorescence of an assay would always exist. An excellent paper by Inglese has documented the problem of false positives that arise from fluorogenic library members.[141] Nonetheless, because there are hardly any false-negatives (that is if the fluorescence of coralyne in the presence of an inhibitor is similar to when no small molecule was added, control, then it implies that that small molecule is definitely not an inhibitor; 25 compounds that were negative for the coralyne assay were retested using HPLC assay and none showed inhibition, see Figure 2.4), the assay is still very useful because it reduced a large library size of 1000 to 11, which could then be investigated in detail using traditional low-throughput assays, such as HPLC and radioactive labelling assays.

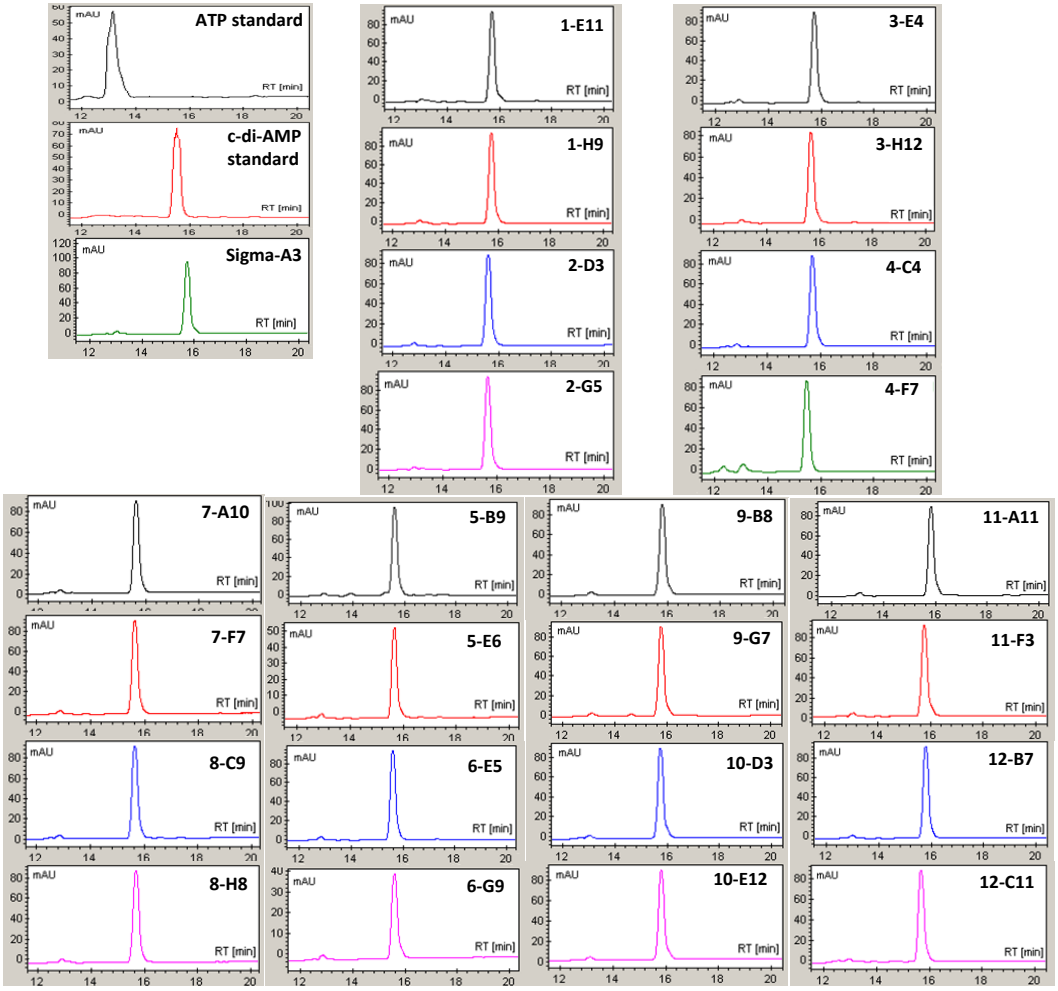

Figure 2.4. HPLC analysis of DisA reaction in the presence of 25 randomly selected library compounds that did not affect c-di-AMP synthesis, as judged by the coralyne assay. This re-testing, using HPLC analysis confirms that compounds that were judged by the coralyne assay as not inhibitors indeed do not inhibit DisA.

Bromophenol-TH contains both a halogenated phenol and thiohydantoin groups, however it appears that the mere presence of these groups is not good enough for DisA inhibition. For example, ST003014 and ST003440 both contain thiohydantoin and haloarene/phenolic moiety yet they did not inhibit c-di-AMP synthesis by DisA (see Figure 2.2). Interestingly, ST028249, which also contains bromophenolic

fragment and a rhodanine moiety (which is similar to a thiohydantoin group), binds to DisA more tightly than bromophenol-TH ($K_d^{apparent}$ of 11 vs 21 μM, see Figure 2.5 and Table 2.1[17])[18] yet it is unable to inhibit c-di-AMP synthesis. Using α-^{32}P-ATP, we determined that the IC_{50} for inhibiting 5 μM of DisA by bromophenol-TH, when 50 μM of ATP is used as substrate is 56 μM (see Figure 2.6).

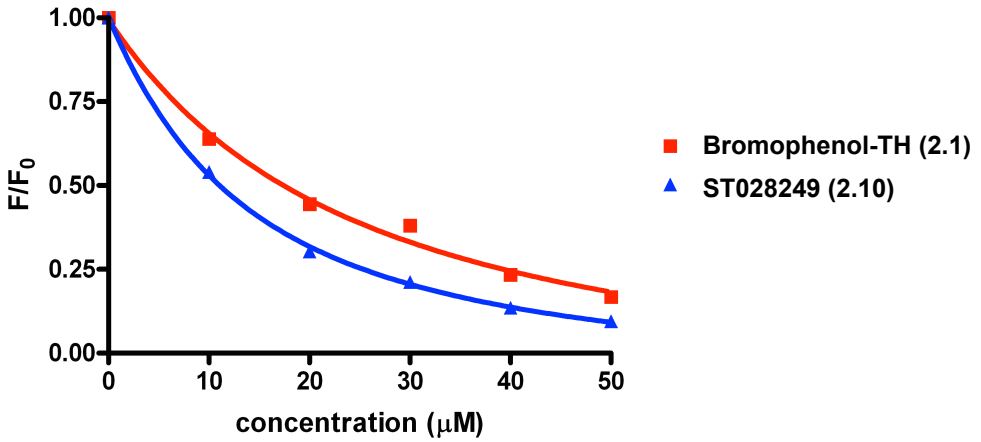

Figure 2.5. Binding affinity test. Addition of small molecules to protein causes reduction of protein intrinsic fluorescence. Normalized fluorescence of ST056083 (bromophenol-TH) and ST028249 binding to DisA at 340 nm.[2]

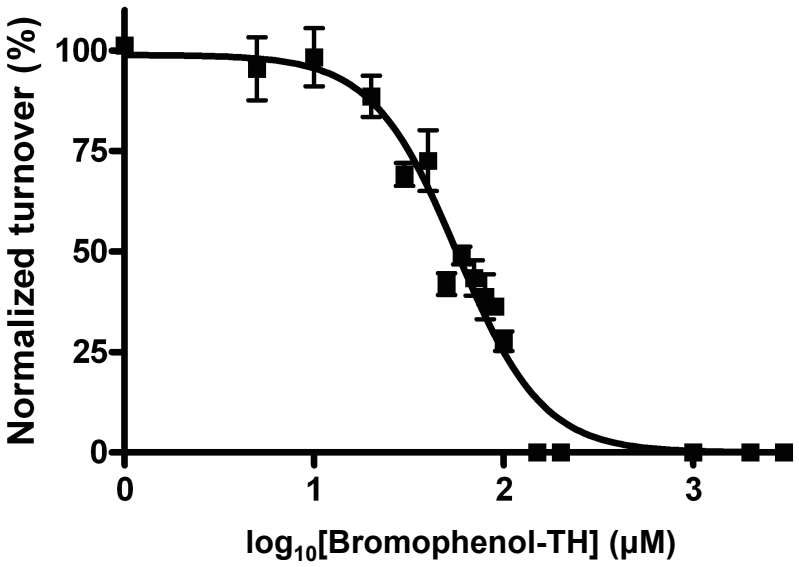

Figure 2.6. DisA inhibited by bromophenol-TH. Assay was performed using α-^{32}P-ATP and TLC to monitor reaction progress. Reactions were stopped after 5 min and percentage of c-di-AMP was calculated. DisA activity was normalized with respect to the percentage of c-di-AMP formation in the absence of bromophenol-TH. IC_{50} was measured as 56 μM.

To eliminate the possibility that the observed inhibition is due to non-specific aggregation, we also investigated the inhibition of DisA by bromophenol-TH in the presence of a surfactant, Triton X-100. Pleasingly, bromophenol-TH could still inhibit DisA in the presence of Triton X-100 (see Figure 2.7).

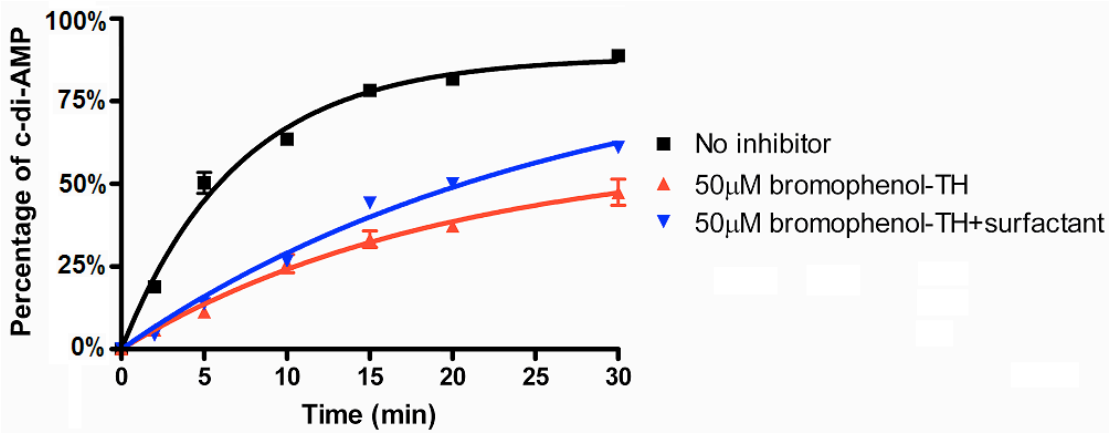

Figure 2.7. Effect of surfactant on bromophenol-TH inhibition. In the presence of 0.01% Triton X-100, 50 μM bromophenol-TH was still able to inhibit DisA. Assay was performed using α-^{32}P-ATP and TLC to monitor reaction progress.

Interestingly, bromophenol-TH does not bind to the same site as ATP because the addition of up to 1 mM ATP did not abrogate the binding of bromophenol-TH to DisA (see Figure 2.8).

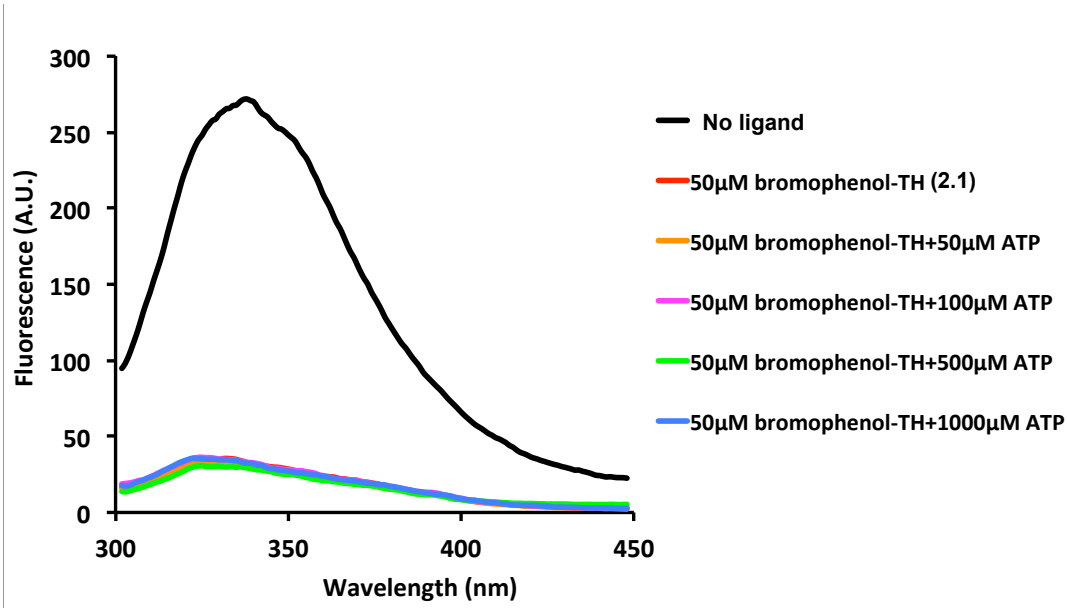

Figure 2.8. Bromophenol-TH (50 µM) when added to DisA (5 µM) caused the reduction of the protein intrinsic fluorescence. Adding ATP (up to 1 mM) did not restore fluorescence intensity, indicating that bromophenol-TH is an ATP-non-competitive inhibitor.

Bromophenol-TH contains a Michael acceptor and could potentially react with nucleophiles. To investigate if conjugate addition by nucleophiles would readily occur, we performed incubation with 1 mM cysteine and followed the reaction progress using UV absorbance. The UV intensity at 361 nm did not change after cysteine addition ad remained unchanged for 1 h (see Figure 2.9), implying that nucleophilic addition to bromophenol is not facile under the assay condition. Future structure-activity relationship studies are planned to optimize bromophenol-TH into a more potent inhibitor.

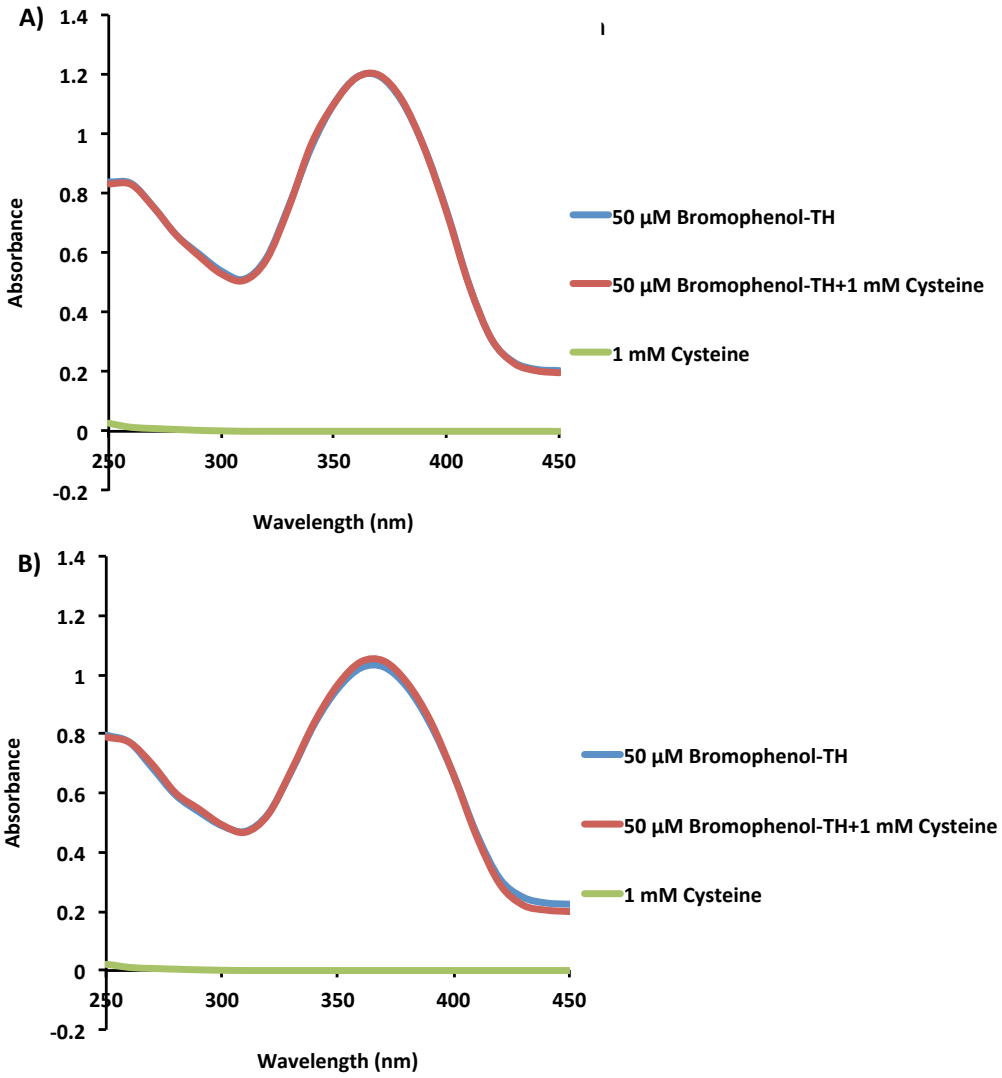

Figure 2.9. Stability of bromophenol-TH in the presence of cysteine, monitored via UV absorbance. 50 µM bromophenol-TH was incubated with 1 mM cysteine. UV absorbance of bromophenol-TH (250nm~450nm) was monitored over time. A) UV absorbance before incubation. B) UV absorbance after 1-hour incubation. The UV absorbance of cysteine-bromophenol-TH mixture was constant during 1-hour incubation period, implying that bromophenol did not react with cysteine.

To guide future SAR and optimization studies, we determined the binding

parameters for different fragments of bromophenol-TH, 3,5-dibromosalicylic acid, 3,5-dibromosalicylaldehyde and 2-thiohydantoine (see Figure 2.10). It appears that the bromophenol fragment is more important for binding to DisA than the thiohydantoine moiety (compare $K_d^{apparent}$ of 67 μM for 3,5-dibromosalicylaldehyde with >1 mM for 2-thiohydantoine, Table 2.1).

Table 2.1. $K_d^{apparent}$ of bromophenol-TH (ST056083), ST028249, 3,5-dibromosalicylic acid, 3,5-dibromosalicylaldehyde and 2-thiohydantoinebinding to 5 μM DisA measured by protein intrinsic fluorescence change.

Compound	**Bromophenol-TH (2.1)**	**ST028249 (2.10)**	**2-thiohydantoine (2.13)**
$K_d^{apparent}$	**21 μM**	**11 μM**	**> 1 mM**
Compound	**3,5-dibromosalicylic acid (2.11)**	**3,5-dibromosalicylaldehyde (2.12)**	
$K_d^{apparent}$	**125 μM**	**67 μM**	

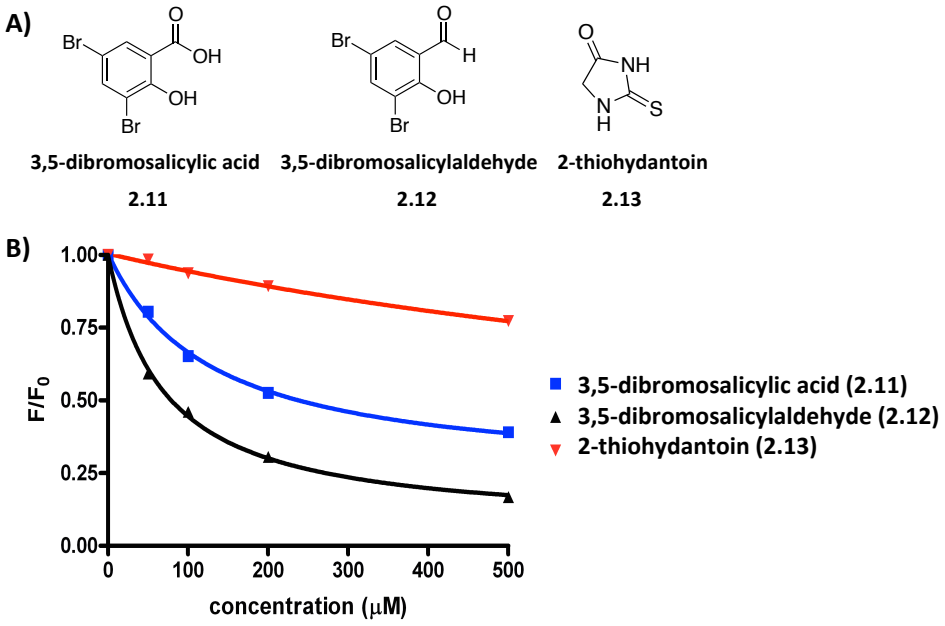

Figure 2.10. A) Structures of 3,5-dibromosalicylic acid, 3,5-dibromosalicylaldehyde and 2-thiohydantoine. B) Normalized fluorescence at 340 nm of 3,5-dibromosalicylic acid, 3,5-dibromosalicylaldehyde and 2-thiohydantoine binding to DisA.

2.1.3. Conclusion

In conclusion, we have demonstrated that the coralyne assay for c-di-AMP detection is a powerful assay to do high-throughput screening for discovering novel c-di-AMP synthesis inhibitors. Interestingly, although we initially selected TimTec's kinase inhibitor library set for screening, hoping to uncover an ATP-competitive inhibitor, the hit that we found does not compete with ATP for DisA binding. Hopefully this proof-of-concept paper would encourage others, especially those with access to large compound libraries, to utilize this cheap and commercially available reagent, coralyne, to discover nucleotide signalling inhibitors. Beyond the demonstrations that this is an enabling assay for inhibitor discovery, we also report

the first small molecule inhibitor of c-di-AMP synthesis. The inhibition of a diadenylate cyclase by a thiohydantoin adds to the impressive array of enzymes that this privilege compound structure inhibits.[19] Considering that c-di-AMP plays a crucial role in bacterial lifestyle, analogs of bromophenol-TH or other scaffolds, which could be discovered via the assay used in this paper, have great promise to be used as stand-alone antibacterial agents or be used in tandem with traditional antibiotics. We anticipate an explosion in c-di-AMP research and the design of small molecules that inhibit c-di-AMP.

2.1.4. Experimental

2.1.4.1. DisA purification

BL21(DE3) cells containing DisA plasmid were grown with 50 μg/mL Kanamycin at 37 °C and expression was induced by addition of 1 mM IPTG. After induction at 30 °C for 6 h, cells were harvested by centrifugation at 5,000 rpm for 15 min. Cells were resuspended in lysis buffer (50 mM sodium phosphate buffer, pH 8.0, 0.3 M NaCl) and lysed by sonication. After centrifuge at 22,000 rpm for 25 min, DisA was purified from supernatant using a GE Hitrap Nickel column and dialyzed into lysis buffer.

2.1.4.2. Real-time detection of c-di-AMP formation by coralyne and screening of ActiTarg-K 960 compound library and Sigma-Aldrich 40 compound library

ActiTarg-K 960 compound library compounds (Timtec) and Sigma-Aldrich 40 compound library were stored as 1 mM and 2 mM stock solutions in DMSO

respectively. 100 μM ATP, 10 μM coralyne, 3 mM KI and 50 μM compound from Timtec ActiTarg-K library or 100 μM compound from Sigma-Aldrich 40 compound library or 5% DMSO were mixed in reaction buffer (40 mM Tris-HCl, pH 8.0, 100 mM NaCl and 10 mM $MgCl_2$). Reaction was started by adding 10 μM DisA. Fluorescence measurements were performed on a Molecular devices SpectraMax M5e plate reader with λ_{ex} = 420 nm and λ_{em} = 475 nm. Reactions were monitored for 30 min (5 min interval).

2.1.4.3. Study of DisA-bromophenol-TH binding by intrinsic protein fluorescence

5 μM DisA was mixed with various concentrations of ligands and incubated at 25 °C for 1 hour. Protein intrinsic fluorescence was measured by Varian Cary Eclipse fluorescence spectrophotometer with λ_{ex} = 290 nm and λ_{em} = 300~450 nm. IC_{50} was calculated using fluorescence intensity at 340 nm.

The equation is as following:

$$L_t = IC_{50}\frac{F-F_0}{F_\infty-F} + P_t\frac{F-F_0}{F_\infty-F_0}$$

where F is the fluorescence intensity at 340 nm. F_0 is the fluorescence intensity at 340 nm in the absence of ligand. F_∞ is the fluorescence when all DisA are bound. IC_{50} is the IC_{50} of binding of ligand to DisA. P_t is the total protein concentration and L_t is the total ligand concentration.[2]

2.1.4.4. DisA inhibition by various concentrations of bromophenol-TH

50 μM ATP, 33 nM ^{32}P-ATP and various concentrations of bromophenol-TH or 10% DMSO were mixed in reaction buffer. 5 μM DisA was added to start reaction.

Reaction was stopped at 5 min and reaction mixture was spotted on a TLC plate (EMD Millipore TLC Cellulose). TLC running buffer was saturated $(NH_4)_2SO_4$: 1.5 M KH_2PO_4 = 1:1.5.

2.1.4.5. HPLC analysis

50 μM hints from Timtec ActiTarg-K 960 compound library and 100 μM hint from Sigma-Aldrich 40 compound library were mixed with 10 μM DisA and 100 μM ATP. Reactions were stopped by heating up to 95 °C for 5 min. Enzymes were removed by 10K filter and filtrate was separated by Purospher® STAR RP-18 (5 μm) LiChroCART® 250-10 column (buffer A: 0.1 M TEAA in water; buffer B: acetonitrile). Samples were eluted with 95%→80 % A at 0-16 min and 80%→10 % A at 16-18.5 min and kept 10% A at 18.5-22.5 min. Signals were detected at room temperature with a 254 nm UV detector.

2.1.4.6. DisA inhibition by 50 μM bromophenol-TH in the presence and absence of surfactant

50 μM ATP, 33 nM ^{32}P-ATP, 5 μM DisA and 50 μM bromophenol-TH or 5% DMSO were mixed in DisA reaction buffer. In samples with surfactant, 0.01% Triton X-100 was added to avoid non-specific aggregation.[142] These time course experiments were analyzed by TLC (EMD Millipore TLC Cellulose).

2.1.4.7. Bromophenol-TH stability in the presence of cysteine

50 μM bromophenol-TH was mixed with 1 mM cysteine and UV absorbance of bromophenol-TH at 361 nm was measured by Molecular devices SpectraMax M5e plate reader every 10 min for 1 hour.

2.2. Structure-activity relationship studies of c-di-AMP synthase inhibitor, bromophenol- thiohydantoin

This section (2.2.) was originally published as: Zheng Y.; Zhou J.; Cooper S.M.; Opoku-Temeng C.; Moreira De Brito, A.; Sintim H.O.; "Structure–activity relationship studies of c-di-AMP synthase inhibitor, bromophenol-thiohydantoin." *Tetrahedron*, 2015, in press.

2.2.1. Introduction

Multidrug-resistant bacteria continue to cause a threat to public health, despite decades of antibiotics development.[143] The US CDC in a report, emphasized the continuous need for new antibiotics to keep up with the ever evolving antibacterial resistance.[144] Efforts have been put into the discovery of new types of antibiotic targets. Enzymes that make or degrade bacterial cyclic dinucleotide (cdn) second messengers or proteins/RNA receptors of cdn have emerged as new antibacterial targets, because cyclic dinucleotides regulate various cellular processes in different bacterial species, including virulence, biofilms and cell wall synthesis.[5] Since its discovery in 2008,[80] c-di-AMP has been found in many Gram-positive bacteria and mycobacteria, including human pathogens *S. aureus,*[92] *M. tuberculosis,*[93] *L. monocytogenes,*[95] and other bacteria.[7] C-di-AMP is essential for bacterial survival.[7,9,10] In some bacteria, c-di-AMP has been shown to regulate DNA integrity scanning,[80] potassium ion transport,[11] bacterial cell wall homeostasis,[12] fatty acid synthesis[13] and host type I interferon response induction[14]. Attempts to delete c-di-AMP synthase, diadenylate cyclase (DAC), from the genome of important human

pathogens such as *S. aureus* have been unsuccessful,[15] implying that inhibitors of c-di-AMP synthase could have antibacterial properties.

Motivated by the potential utility of DAC inhibitors as important probes to study c-di-AMP signaling in bacteria or as new generation antibiotics we embarked on the development of a high throughput assay, using coralyne, to discover such inhibitors.[16] Using the coralyne assay, we identified the first c-di-AMP synthase inhibitor, 5-(3, 5-dibromo-2-hydroxylbenzylidene)-2-thioxoimidazolidin-4-one (referred to as bromophenol thiohydantoin or bromophenol-TH or BTH, see Figure 2.2 and 2.11 for structure).[17] BTH contains a halogen (Br), phenolic and 2-thiohydantoin (or 2-thioxoimidazolidin-4-one) moieties. To guide the development of BTH-based/inspired DAC inhibitors, we initiated a structure–activity relationship (SAR) study to tease out the salient features of BTH that are important for DisA inhibition. Herein, we present the synthesis of 19 BTH analogs, and investigate the importance of the various functionalities found on BTH for DAC inhibition.

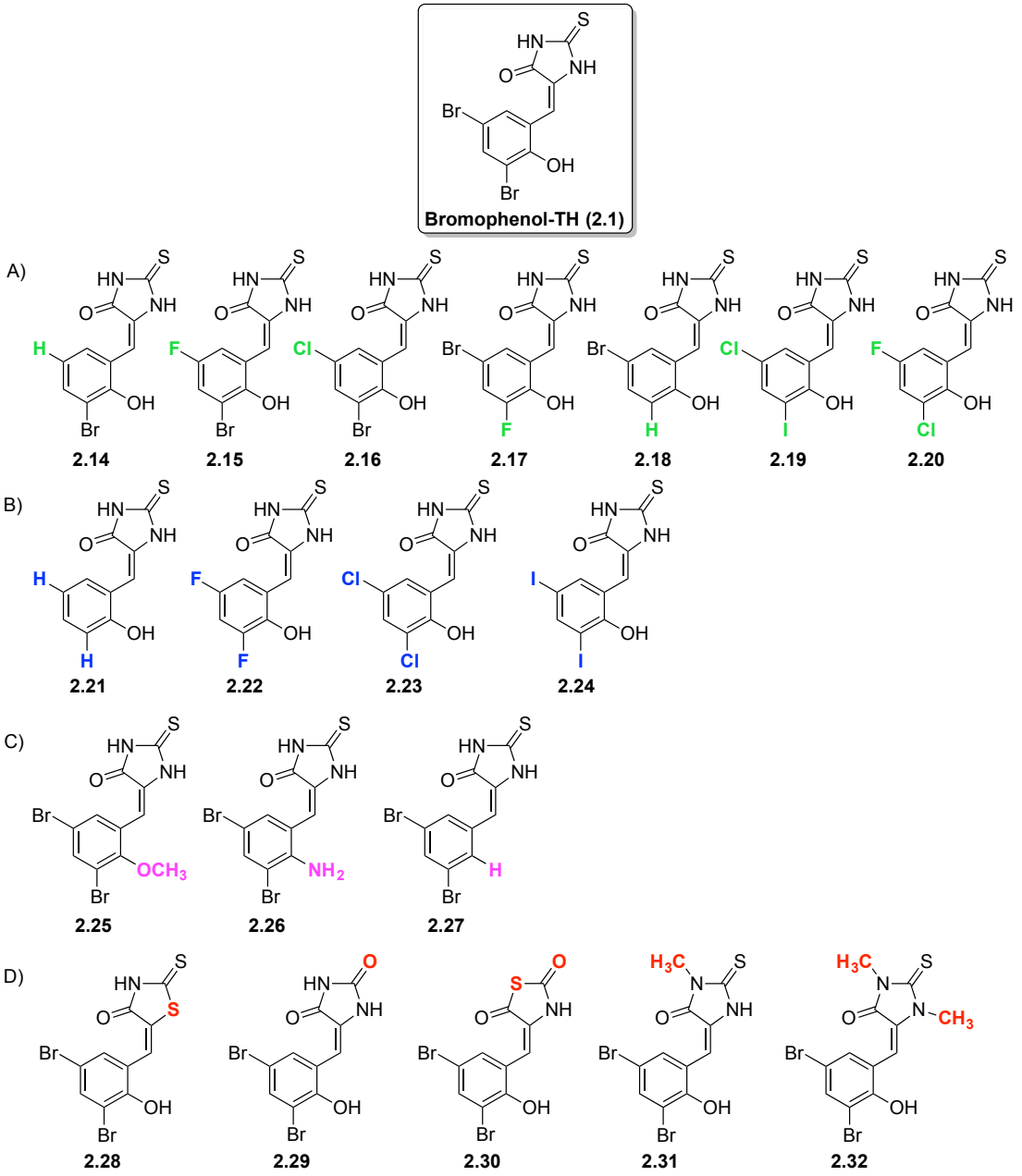

Figure 2.11. Structures of bromophenol-TH and analogs synthesized for this study. Ninteen BTH analogs are grouped into four categories, according to their substitution types.

2.2.2. Result and discussion

BTH, is easily prepared via the condensation of 3, 5-dibromosalicylic aldehyde and 2-thiohydantoin.[18-20] Conveniently, this ease of preparation allows for facile preparation of analogs *via* condensation reactions with various commercially available halo-substituted salicylic aldehydes and hydantoins, thiohydantoins or rhodanines. (Scheme 2.1). Electronic and steric derivations are possible by varying the halogens present on the aromatic ring.

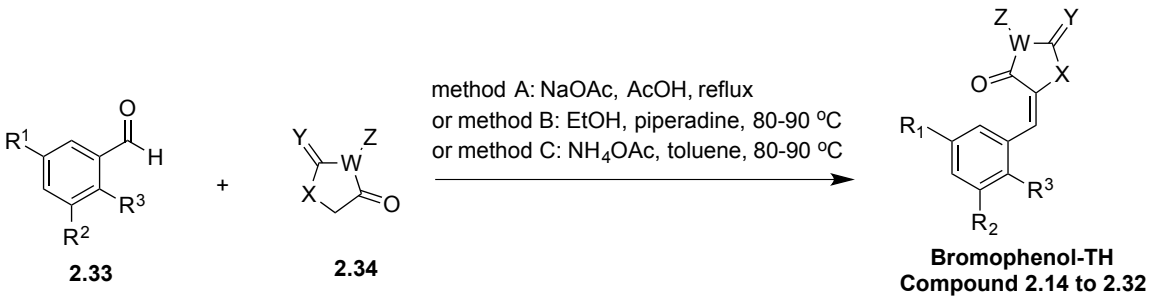

Scheme 2.1. Synthetic strategy for preparing BTH and analogs. Conditions for method A, B and C are listed above the arrow. The method that gave the best yield was chosen for each compound. Characterization of synthesized compounds see the published paper.[1]

Four types of BTH analogs (A, B, C, D, see Figure 2.12) were prepared. In type A, we synthesized analogs containing mixed halogens whereas type B consisted of only one type of halogens. In type C, we investigated the role of the phenolic group in BTH by replacing the OH with hydrogen, amino or methoxy groups. Type D explored how subtle changes to the heterocyclic ring of BTH would affect DisA inhibition.[21-23]

2.2.2.1. Inhibition of DisA by BTH analogs

The coralyne assay[16] (See Figure 2.12) was performed to identify the DisA inhibition effects of BTH analogs. In the absence of c-di-AMP, iodide quenches corlayne fluorescence. As DisA synthesizes c-di-AMP, the dinucleotide forms a complex with coralyne and protects coralyne from quenching effects. Coralyne fluorescence emission intensity correlates with c-di-AMP concentration. In the presence of inhibitors, the concentration of c-di-AMP would be lower and hence the fluorescence of coralyne would be reduced.[16] The coralyne assay indicated that BTH was the strongest inhibitor, followed by compound **2.28** in group D and compound **2.16** in group A. Other BTH analogs did not show significant inhibition of DisA. IC_{50} of BTH ($6.7 \pm 0.6 \times 10^{-5}$ M), compound **2.28** ($12.4 \pm 1.0 \times 10^{-5}$ M) and compound **2.16** ($17.9 \pm 1.7 \times 10^{-5}$ M) were obtained using radiolabeled ^{32}P-ATP (Figure 2.13). In group A, BTH, compound **2.14**, compound **2.15** and compound **2.16** have 3'-bromo and their inhibition effects increase as 5'-halogen size increases. It appears that the bromo substitution at the 3-position is important as deleting this substitution (compound **2.18**) resulted in loss of inhibition. Compound **2.19** or **2.20**, which replaced the dibromo with mixed halogens (Cl, F or I) were also inactive, highlighting the need for bromo substitution.

A)

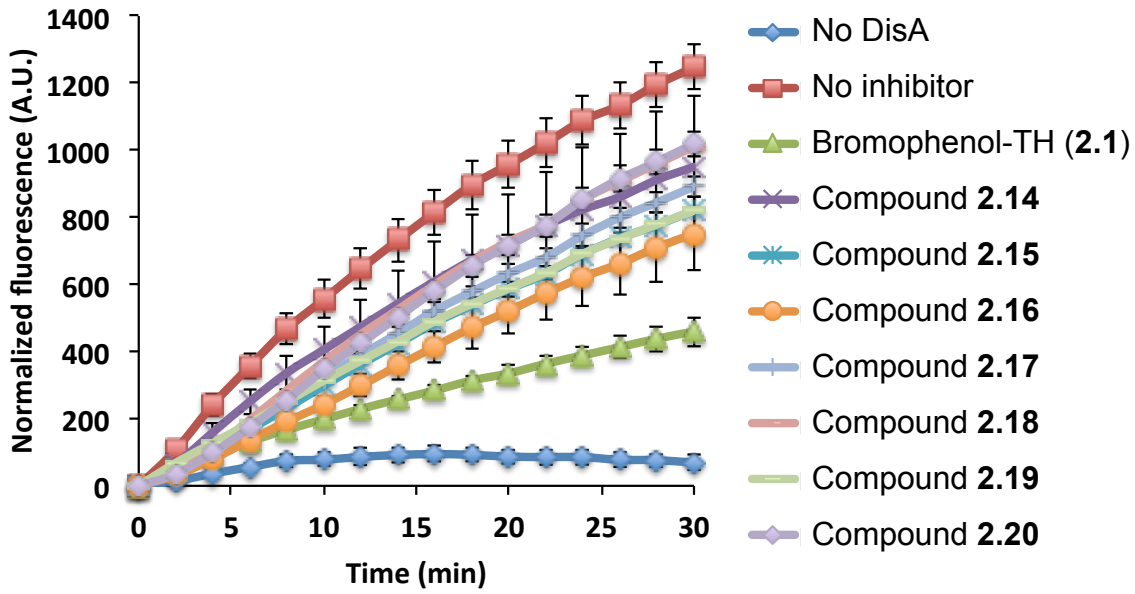
Normalized fluorescence (A.U.)
1400
1200
1000
800
600
400
200
0
0
5
10
15
20
25
30
Time (min)
No DisA
No inhibitor
Bromophenol-TH (2.1)
Compound 2.14
Compound 2.15
Compound 2.16
Compound 2.17
Compound 2.18
Compound 2.19
Compound 2.20

B)

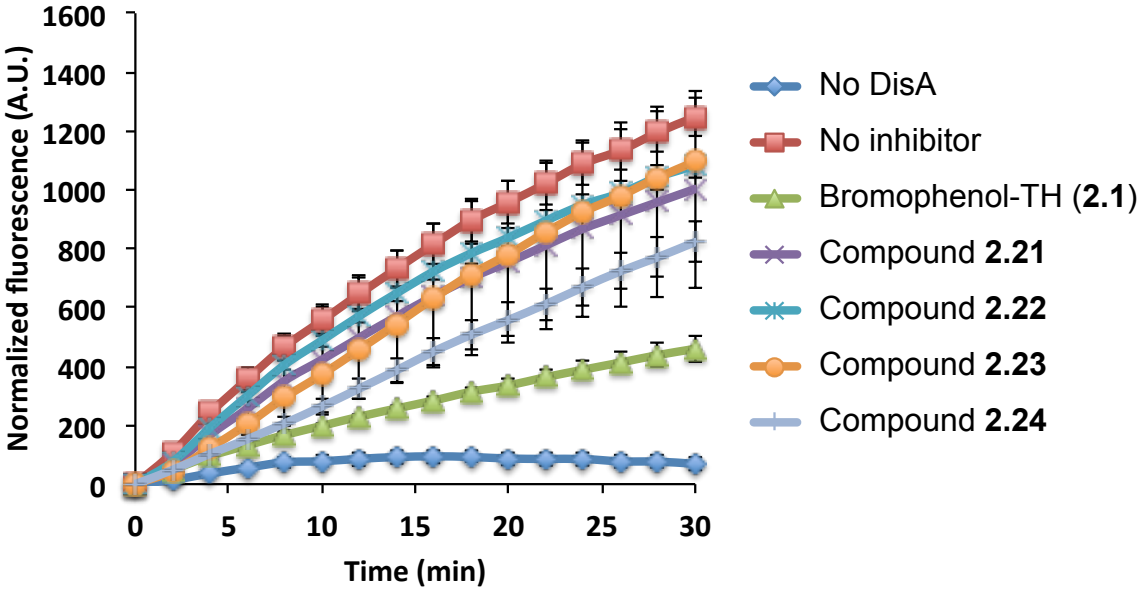
Normalized fluorescence (A.U.)
1600
1400
1200
1000
800
600
400
200
0
0
5
10
15
20
25
30
Time (min)
No DisA
No inhibitor
Bromophenol-TH (2.1)
Compound 2.21
Compound 2.22
Compound 2.23
Compound 2.24

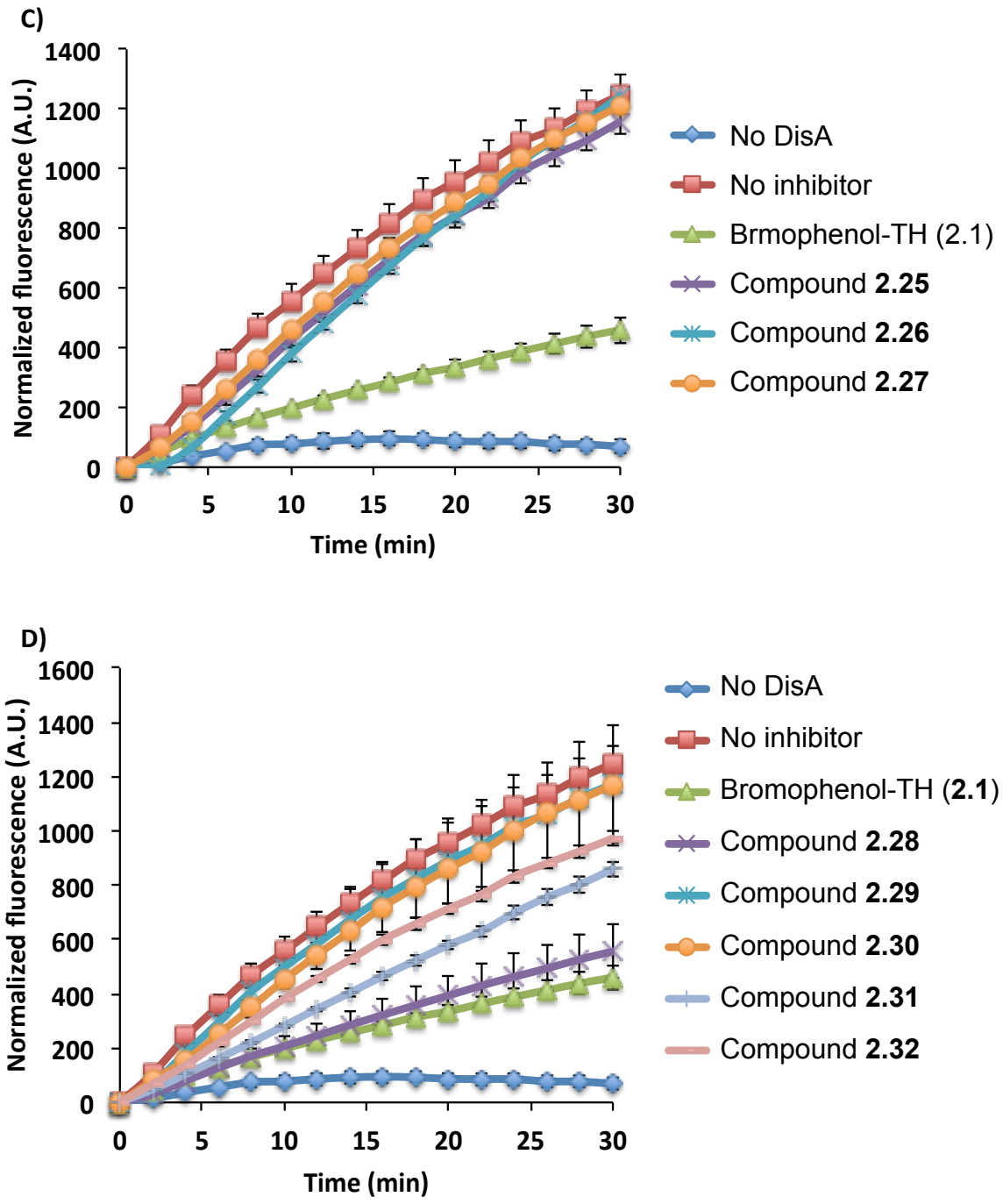

Figure 2.12. Graphs for the coralyne assay, showing DisA inhibition by BTH and the four groups of BTHAs. Only three molecules, BTH, compound **2.16** in group A and compound **2.28** in group D, showed significant inhibition.

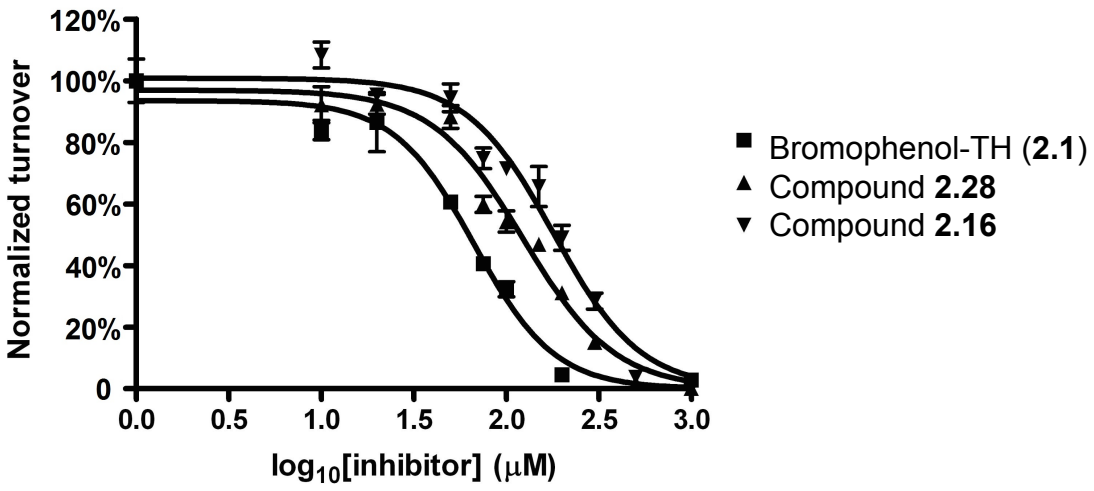

Figure 2.13. Enzymatic proficiency of DisA, 1 μM, (converting ^{32}P- ATP into ^{32}P-c-di-AMP) in the presence of increasing amounts of inhibitors BTH, compound **2.28** and compound **2.16**.

The diiodinated analog compound **2.24** of group B showed more inhibition than the non-halogenated analog compound **2.21**, difluorinated compound **2.22** and dichlorinated analog compound **2.23**, but it was still less active than BTH (see Supplementary Material, Figure S1). The hydroxyl group in BTH was replaced with a methoxy (compound **2.25**), amino (compound **2.26**) and hydrogen (compound **2.27**) to investigate if the phenolic moiety played a role in inhibition. In all of the three cases, replacement of the phenolic group with the aforementioned moieties completely diminished any inhibition effects. In group D, substitution of the nitrogen atom for sulfur atom at 1' position (2-thioxoimidazolidin-4-one to 2-thioxothiazolidin-4-one, compare compound **2.28** with BTH) has minor impact on inhibition, whereas replacement of the thiocarbonyl by carbonyl (2-thioxoimidazolidin-4-one to imidazolidine-2,4-dione, compare compound **2.29** with

BTH) strongly reduced the inhibition effects. Substitution of the N-3 of BTH is a non-covalent inhibitor

2.2.2.2. BTH is a non-covalent inhibitor

BTH is reported to be a non-competitive inhibitor[17], although the binding site for inhibitors within DisA is currently unknown. BTH contains an enone moiety and hence could act via covalent inhibition. To ascertain if covalent inhibition was operative, DisA was incubated with high concentration of BTH and then unbound BTH was removed by filtration. The remaining DisA was then washed three times with reaction buffer and then assayed for activity. The BTH-treated DisA retained enzymatic activity (similar to DMSO-treated DisA, see Figure 2.14), revealing that BTH is a non-covalent inhibitor.

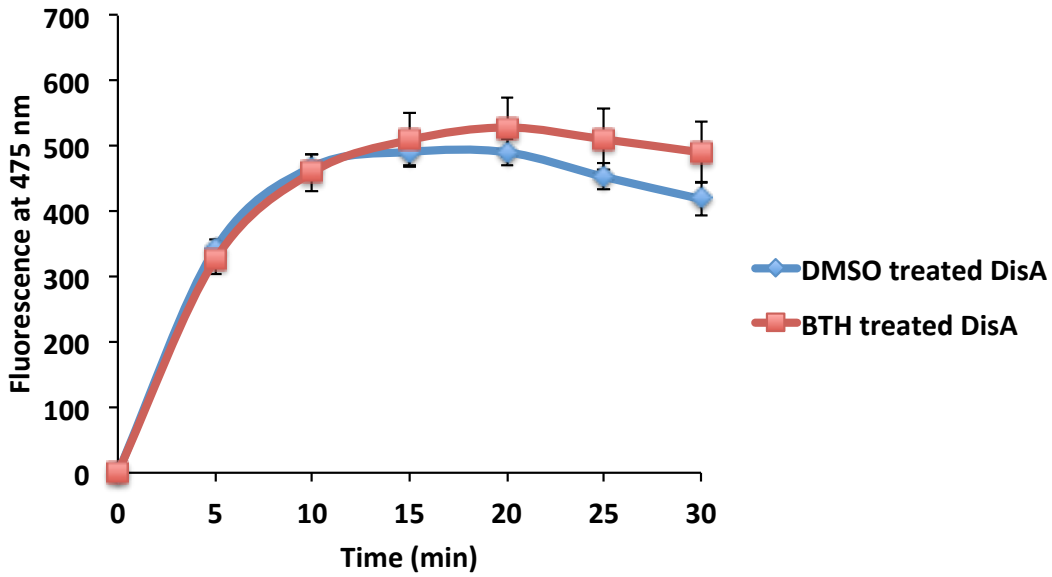

Figure 2.14. Enzymatic activities of DMSO- or BTH-treated DisA monitored by the coralyne assay.

2.2.2.3. BTH did not affect YybT, WspR D70E and RocR activity

We were curious to know the selectivity of BTH and analogs towards cyclic dinucleotide metabolism enzymes. We therefore tested BTH against a few cyclic dinucleotide-related enzymes, namely c-di-AMP PDE YybT from *B. subtilis*[24], c-di-GMP DGC WspR D70E[25] and c-di-GMP PDE RocR[26] from *P. aeruginosa*. Interestingly 100 μM of BTH did not affect any of these enzymes (See Figure 2.15), implying that BTH is indeed specific for c-di-AMP synthase, DisA.

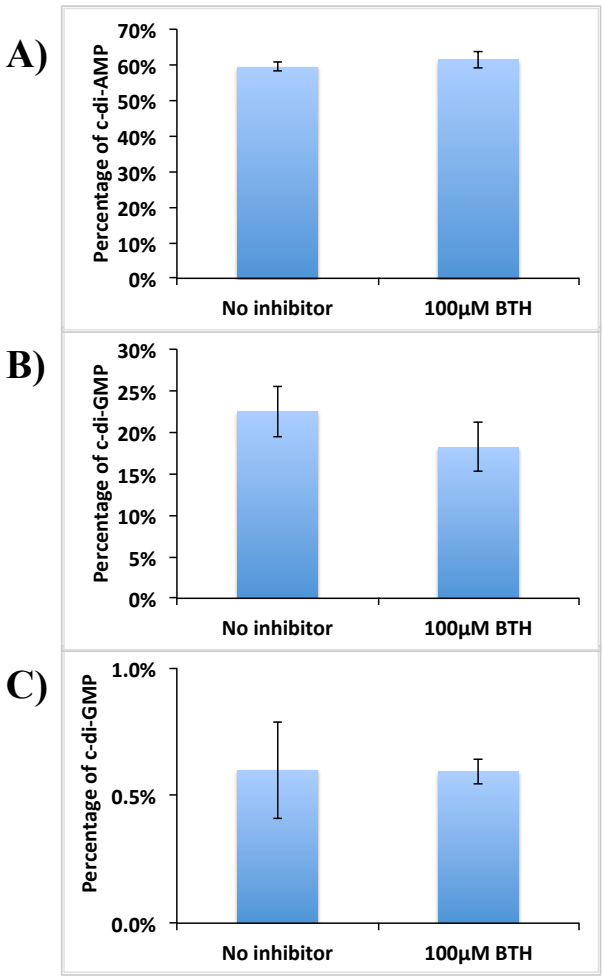

Figure 2.15. BTH did not affect YybT, WspR D70E and RocR activity. A) YybT cleavage. Percentages of remaining c-di-AMP after 30 min reaction were similar in the presence or absence of BTH. B) WspR D70E reaction. Percentages of synthesized

c-di-GMP after 2 hour reaction were similar in the presence or absence of BTH. C) RocR cleavage. Percentages of remaining c- di-GMP after 30 min reaction were similar in the presence or absence of BTH.

2.2.3. Conclusion

Cyclic dinucleotides have emerged as interesting second messengers in both prokaryotes and eukaryotes and there has been an explosion of research activities to unravel the intricacies of signaling regulated by these nucleotides. There is however a paucity of small molecules that inhibit the metabolic enzymes of cyclic dinucleotides and such molecules could have important roles in elucidating cdn signaling and/or become next generation antibacterial agents. In this paper, we have demonstrated that bromophenol TH, the first reported inhibitor of c-di-AMP synthase is sensitive to modifications and most changes to this inhibitor abrogated inhibition. Interestingly, seemingly minor changes (for example changing an aromatic bromo to a chloro or iodo substituent) resulted in drastic inhibition profile, highlighting that halogen substitution can be used to cause dramatic changes in enzyme affinity for a ligand. Despite the presence of an enone moiety, bromophenol TH is not a covalent inhibitor of DisA. Future work will involve the search of other heterocyclic groups, apart from hydantoin or rhodanines, which could be appended to the bromophenol moiety with the ultimate goal of discovering more potent inhibitors of DisA.

2.2.4. Experimental

2.2.4.1. Synthesis of BTH analogs

Three different synthetic protocols were explored for the synthesis of the analogs and the one that gave the best yield was chosen for making adequate amounts for characterization and biological evaluation.

General synthesis procedure **A**: A mixture of compound **20**, aldehyde (0.5 mmol, 1 equiv. **20**), compound **21** (1.2 equiv.), and NaOAc (3 equiv.) in glacial AcOH (4 mL) was stirred at reflux (12 h) until no starting material remained, assessed by TLC (SiO_2, hexane/ethyl acetate, 1:1, v/v). The reaction mixture was cooled down to room temperature, followed by the addition of iced water. The resulting precipitate was filtered and washed successively with water and Et_2O (10 mL). The product was subjected to column purification (hexane/ethyl acetate, 0→35%).

General synthesis procedure **B**: A mixture of aldehyde (0.5 mmol, 1 equiv. **20**), compound **21** (1.2 equiv.), and few drops of piperidine in EtOH (4 mL) was stirred at 80-90 ^oC (4-12 h) until no starting material remained, assessed by TLC (SiO_2, hexane/ethyl acetate, 1:1, v/v). The reaction mixture was cooled down to room temperature. The resulting precipitate was filtered and washed successively with water and Et_2O (10 mL).

General synthesis procedure **C**: A mixture of aldehyde (0.5 mmol, 1 equiv. **20**), compound **21** (1.1 equiv.), and NH_4OAc (1.5 equiv.) in toluene (4 mL) was stirred at 80-90 ^oC (12 h) until no starting material remained, assessed by TLC (SiO_2, hexane/ethyl acetate, 1:1, v/v). The reaction mixture was cooled down to room

temperature. The resulting precipitate was filtered and washed successively with water and Et_2O (10 mL).

Synthesis of BTH analogs were done by me colleagues Dr. Jie Zhou and Dr. Stefan M. Cooper. The characterization of these compounds can be found in the published paper[1].

2.2.4.2. Protein purification

BL21(DE3) cells with protein expression plasmids were cultured in LB medium with 100 μg/mL ampicillin or 50 μg/mL kanamycin at 37 °C. Expression was induced by addition of 1 mM IPTG. After induction at 30 °C for 6 hours (WspR D70E and YybT) or at 16 °C overnight (DisA and RocR), cells were harvested by centrifugation at 4,000 rpm for 15 min. Cells were resuspended in lysis buffer (10 mM Tris-HCl, pH 8.0, 100 mM NaCl for WspR D70E, RocR and YybT, and 50 mM sodium phosphate buffer, pH 8.0, 300 mM NaCl for DisA) and lysed by sonication. Proteins were purified by GE Hitrap Nickel columns using with the Bio-Rad NGC™ Chromatography System and dialyzed into lysis buffer.

2.2.4.3. The coralyne assay

BTH and analogs were stored as 100 mM stock solutions in DMSO. 300 μM ATP, 10 μM coralyne, 3 mM KI, 50 μM BTH/analogs and 1 μM DisA were mixed in reaction buffer, which contains 40 mM Tris-HCl, pH 7.5, 100 mM NaCl and 10 mM $MgCl_2$. Fluorescence measurements were performed on a Molecular Devices

SpectraMax M5e microplate reader (λ_{ex} = 420 nm and λ_{em} = 475 nm). Reactions were monitored for 30 min with 2 min interval.

2.2.4.4. IC50 measurements of BTH, compound **2.18** and compound **2.19**

300 μM ATP, 33 nM ^{32}P-ATP and various concentrations of BTH/analogs were mixed in reaction buffer. Reaction was initiated by addition of 1 μM DisA and performed at 30 °C for 1 hour. Aliquots of the reaction mixtures were spotted on a TLC plate (EMD Millipore TLC Cellulose). TLC running buffer was saturated $(NH_4)_2SO_4$: 1.5 M KH_2PO_4 = 1:1.5.

2.2.4.5. Assay to determine if BTH is a covalent inhibitor

10 μM DisA was incubated with 100 μM BTH or DMSO on ice for 90 min. BTH/DMSO was removed by filtration. DisA was washed by reaction buffer for three times. DisA was then incubated with 300 μM ATP, 10 μM coralyne and 3 mM KI. Reaction was monitored by fluorescence emission on a Molecular Devices SpectraMax M5e microplate reader (λ_{ex}=420 nm and λ_{em}=475 nm). The reaction was monitored for 30 min with 5 min interval.

2.2.4.6. Effect of BTH on YybT, WspR D70E and RocR activity

1.5 μM YybT reacted with 50 μM c-di-AMP and 16 nM ^{32}P-c-di-AMP in the presence or absence of 100 μM BTH in reaction buffer (100 mM Tris-HCl, pH 8.3, 20 mM KCl, 0.5 mM $MnCl_2$ and 1 mM DTT) at 37 °C. The reaction was stopped

after 30 min. 1 μM WspR D70E reacted with 300 μM GTP and 33 nM ^{32}P-GTP in the presence or absence of 100 μM BTH in reaction buffer (10 mM Tris-HCl, pH 8.0, 100 mM NaCl and 5 mM $MgCl_2$) at 37 °C. Reaction was stopped after 2 hours. 1.2 μM RocR reacted with 50 μM c-di-GMP and 16 nM ^{32}P-c-di-GMP in reaction buffer (100 mM Tris-HCl, pH 8.0, 20 mM KCl and 25 mM $MgCl_2$) at 37 °C. Reaction was stopped after 30 min. All the reactions were monitored by TLC.

Chapter 3 : Inhibition of Innate Immune Cytosolic Surveillance by a *Mycobacterium tuberculosis* Phosphodiesterase

This chapter has been submitted for publication. It is a collaboration work with William Bishai group in the Center for *Tuberculosis* Research at Johns Hopkins University. I performed biochemical enzymatic assays. Molecular biology, microbiological, cell culture, and animal based experiments were performed by Dr. Ruchi Jain Dey and Dr. Bappaditya Dey. Dr. Jie Zhou and David Sayre performed chemical synthesis of compounds. Laurene S. Cheung contributed to mass spectrometry experiments. Pankaj Kumar contributed to ITC experiments. Haidan Guo contributed to mouse experiments.

3.1. Introduction

The cytosolic surveillance pathway (CSP) plays an integral role in the detection and elimination of pathogens. Host cells utilize specialized receptor proteins and pattern recognition receptors (PRRs) that recognize pathogen associated molecular patterns (PAMPs) to mobilize the innate and adaptive arms of the immune system for clearance of pathogens. Bacterial cyclic dinucleotides (CDNs) such as cyclic diadenosine monophosphate (c-di-AMP) and cyclic diguanosine monophosphate (c-di-GMP) which have canonical 3'-5' phosphodiester linkages are known for their dual roles both as second messengers regulating bacterial physiology[145-147] and as PAMPs[148-151] that activate the host CSP during infection[1-4]. Bacterial CDNs are known to induce Type I interferons (IFN-α/β) in a stimulator of interferon genes (STING)-dependent manner.[125, 152] Recently, we reported that intoxication of macrophages with *M. tuberculosis*-derived c-di-AMP triggers a Type I IFN response via the STING-TBK1-IRF3 axis.[153] STING also recognizes host-derived, non-

canonical CDNs such as 2'3'-cyclic guanosine-adenosine monophosphate (2'3'-cGAMP)[9] produced by cytosolic DNA sensor cGAMP synthase (cGAS) in response to microbial or self-derived double-stranded DNA in the cytosol[154-162]. Diverse viral immune evasion strategies have been identified that inhibit cytosolic nucleic acid sensing pathways during infections; these include preventing DNA detection[163], degradation of certain DNA sensors such as IFI16[164], clamping of sensors (*e.g.* IFI16) thereby preventing DNA-dependent sensor activation[165]. Recent studies have also identified viral proteins such as HSV-1 ORF52 that bind directly to cGAS blocking its recognition of viral DNA substrates[166] and viral oncogenes that antagonize cGAS function[167]. However, bacterial mechanisms of immuno-evasion by targeting CDN-based CSP activation have not been reported. In this study, we identify a multi-functional mycobacterial PDE known as CdnP (Rv2837c), which inhibits the CSP through degradation of both bacterial-derived canonical CDNs and host-derived non-canonical CDNs.[93, 104, 168]

3.2. Result and Discussion

3.2.1. CdnP functions as a cyclic dinucleotide phosphodiesterase *in vitro* and *in vivo*

During our studies of the *M. tuberculosis* c-di-AMP biosynthetic cyclase, *disA* (*dacA*, Rv3586)[153], we identified an *M. tuberculosis* PDE homologue, Rv2837c, which encodes DHH-DHHA1 domains (DHH, Asp-His-His motif containing domain; DHHA1, DHH associated domain 1) associated with the ability to hydrolyze CDNs

with 3'-5' phosphodiester linkages as have been reported for *Streptococcus pneumoniae* (Pde2)[89], *Streptococcus pyogenes* and *Streptococcus suis* serotype 2 (GdpP)[134, 169], *Bacillus subtilis* (YybT)[170], *M. tuberculosis*[104], and *M. smegmatis*[171]. Subsequently, we confirmed that purified, recombinant *M. tuberculosis* CdnP hydrolyzes c-di-AMP efficiently and also possesses PDE activity for c-di-GMP (Figure 3.1).

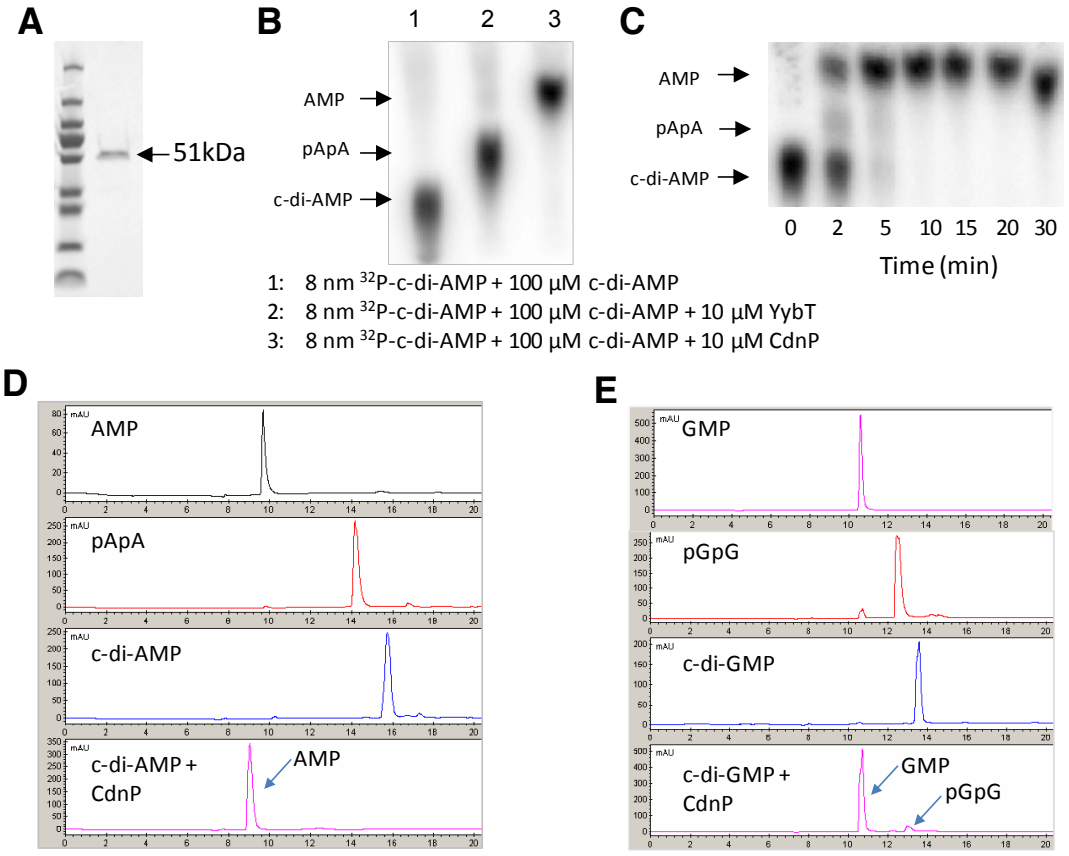

Figure 3.1. Purification of CdnP and PDE activity assays. A) Ni-NTA affinity purification of N-terminal, His-tagged CdnP (51 kDa). B) TLC depicting PDE activity of CdnP for ^{32}P-c-di-AMP. C) Time kinetics of ^{32}P-c-di-AMP cleavage by CdnP. D) and E) HPLC profiles for PDE activity of CdnP for c-di-AMP and c-di-GMP along with related standards.

Phosphodiesterase activity for cleavage of c-di-AMP was found to be optimal in the presence of Mn^{2+} and at a pH of ≥ 8.5 with a K_m of 1.2 ± 0.1 μM and a k_{cat} of 4.0 ± 0.1 min^{-1} (see Figure 3.2).

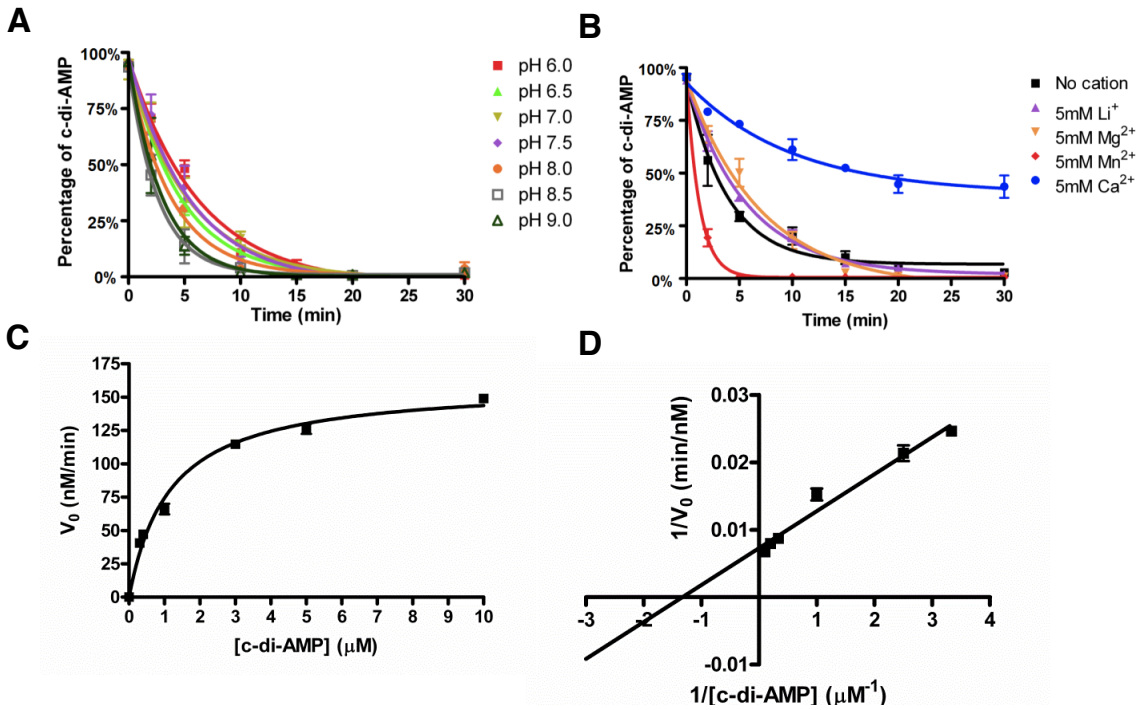

Figure 3.2. pH and cation activity profiles, and kinetics of c-di-AMP cleavage by CdnP. (A) pH profile of CdnP activity. Reactions were conducted at pH 6.0 to pH 9.0 using 2 μM of purified enzyme, 24 nM ^{32}P-c-di-AMP, and 1 mM Mn^{2+}. (B) Cation activity profiles of CdnP. Reactions were conducted at pH 9.0 in the presence of 5 mM Li^{+}, Mg^{2+}, Mn^{2+} or Ca^{2+}. Data are mean ± SD (n = 3). (C) Michaelis-Menten kinetic analysis for c-di-AMP cleavage by CdnP. (D) Lineweaver-Burk plot for c-di-AMP cleavage by CdnP.

To confirm the effect of CdnP on intra-bacterial CDN levels, we measured the levels of c-di-AMP and c-di-GMP in recombinant *M. tuberculosis* strains grown in

culture by an LC-MS/MS MRM method and found that intra-bacterial c-di-AMP levels in an *M. tuberculosis cdnP* disrupted mutant (*Mtb-cdnP*::Tn, an *M. tuberculosis* strain with a transposon insertion disrupting the C-terminus DHH domain of *Rv2837c*[172]) were ~535-fold higher than in wild-type *M. tuberculosis* CDC1551 (*Mtb*-WT) (see Figure 3.3A). We also observed an increase in c-di-GMP levels in the *Mtb-cdnP*::Tn compared to the wild-type strain (Table 3.1). Modified expression of the CdnP protein in these recombinant strains compared to WT was confirmed by Western blotting (Figure 3.4).

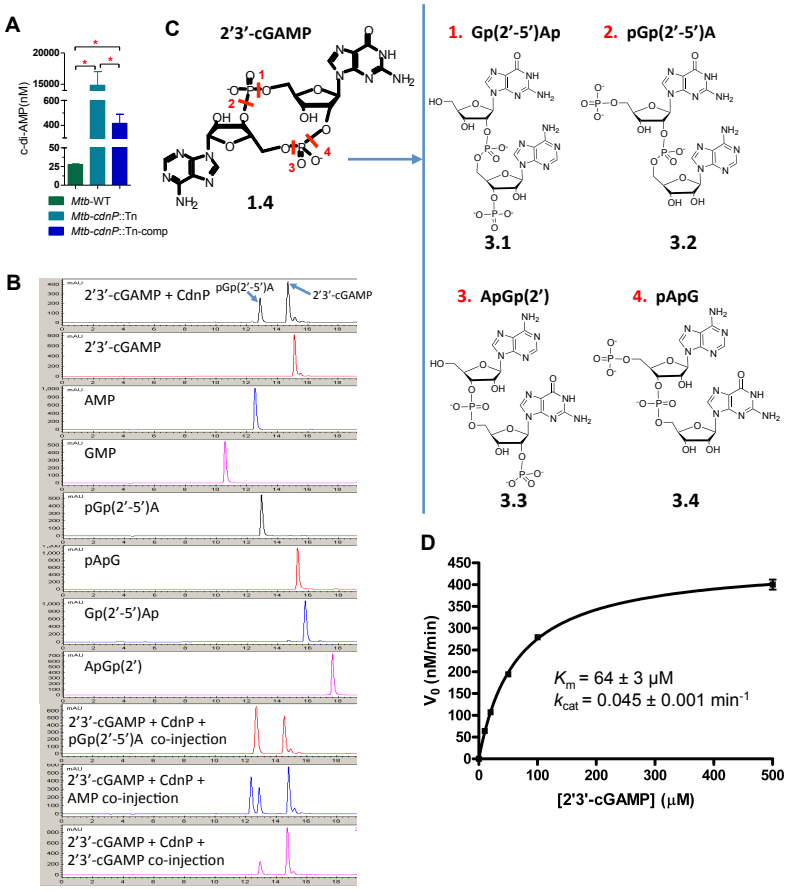

Figure 3.3. *M. tuberculosis* CdnP hydrolyzes both bacterial and host CDNs. (A) Influence of *M. tuberculosis* CdnP activity on intra-bacterial levels of c-di-AMP.

Nucleotides extracted from 4 x 10^8 bacilli were analyzed by LC-MS/MS MRM for quantification of c-di-AMP. Data are means ± SD of duplicate samples and a representative of two experiments.*, $p < 0.05$ by Student's t-test (two-tailed). (B) HPLC profiles of 2'3'-cGAMP (100 μM) cleavage by CdnP and nucleotide standards. (C) Possible cleavage products from 2'3'-cGAMP on incubation with CdnP. (D) Time kinetics of 2'3'-cGAMP cleavage by CdnP.

Table 0.1. Influence of *M. tuberculosis* CdnP activity on intra-bacterial levels of c-di-GMP. Nucleotides extracted from 4 x 10^8 bacilli were analyzed by LC-MS/MS MRM for quantitation of c-di-GMP. Data are means ± SD (n = 2) and are representative of two experiments. *ND: non-detectable or under our limit of detection (2 nM).

Intra bacterial c-di-GMP levels			
Mtb-WT	*Mtb-cdnP*::Tn (nM)	*Mtb-cdnP::Tn*-comp (nM)	*Mtb-cdnP*-OE
ND*	11.251 ± 2.637	6.129 ± 0.544	ND
Data are Mean ± SD of duplicate samples and representative of two experiments. *ND, Not detected			

1. *Mtb*-WT
2. *Mtb-cdnP*::Tn
3. *Mtb-cdnP*::Tn-comp
4. *Mtb-cdnP*-OE

Figure 3.4. Expression of CdnP protein in *M. tuberculosis*. Total membrane proteins of *M. tuberculosis* were extracted, followed by SDS-PAGE and western blotting

using rabbit polyclonal antibody against *M. tuberculosis* CdnP. No CdnP expression was detected in *Mtb-cdnP*::Tn mutant while markedly greater expression was observed in *Mtb-cdnP*-OE strain.

3.2.2. *M. tuberculosis* CdnP hydrolyzes 2'3'-cGAMP *in vitro*

To date, bacterial enzymes with 2'3'-cGAMP phosphodiesterase activity have not been reported. We hypothesized that *M. tuberculosis* CdnP may possess hydrolytic activity for 2'3'-cGAMP enabling the pathogen to subvert host cGAS-mediated CSP signaling. Since 2'3'-cGAMP contains one canonical 3'-5' phosphodiester bond, and mycobacterial CdnP is capable of cleaving this linkage in CDNs, we reasoned that 2'3'-cGAMP was a plausible additional substrate of mycobacterial CdnP. To test this, we investigated the cleavage of 2'3'-cGAMP by purified CdnP *in vitro* using HPLC detection of the reaction products. As may be seen in Figure 3.3, on exposure to purified CdnP, a new, shorter retention-time peak appears in addition to the 2'3'-cGAMP peak in the chromatograms demonstrating that 2'3'-cGAMP is a substrate for CdnP.

We next sought to identify the hydrolysis products of CdnP-mediated cleavage of 2'3'-cGAMP. Assuming cleavage might occur at any of the four phosphoester bonds of 2'3'-cGAMP (Fig. 3.3C), HPLC analysis for the reaction products was carried out by co-injection with chemically synthesized standards [Gp(2'-5')Ap, pGp(2'-5')A, ApGp(2'), pApG, 2'3'-cGAMP, GMP and AMP] as may be seen in Figure 3.3B. From the co-injection HPLC traces, we identified the cleavage product as a linear pGp(2'-5')A molecule (Figure 3.3B). Kinetic analysis of 2'3'-cGAMP cleavage by CdnP revealed a K_m of 64.0 ± 3.0 μM and a k_{cat} of 0.045 ± 0.001 min^{-1} (Figure 3.3D).

Further determination of binding affinity by isothermal titration calorimetry (ITC) showed the K_d of CdnP for cGAMP to be 1.08 x 10^{-4} M (Figure 3.5A). We also investigated if the capacity of *M. tuberculosis* CdnP to cleave 2'3'-cGAMP is unique, or whether other microbial phosphodiesterases with DHH/DHHA1 or EAL domains such as *Bacillus subtilis* YybT[170], *Staphylococcus aureus* GdpP[173] or *Pseudomonas aeruginosa* RocR[79], also possess this activity (Figure 3.6). Interestingly, while the PDE from each these other bacteria showed PDE activity towards bacterial CDNs (Figure 3.6A, C, E), none exhibited cleavage of 2'3'-cGAMP (Figure 3.6B, D, F). Together, these results establish that *M. tuberculosis* CdnP is uniquely capable of cleaving the 3'-5' phosphodiester linkage of host-derived 2'3'-cGAMP to produce a linear dinucleotide molecule, pGp(2'-5')A.

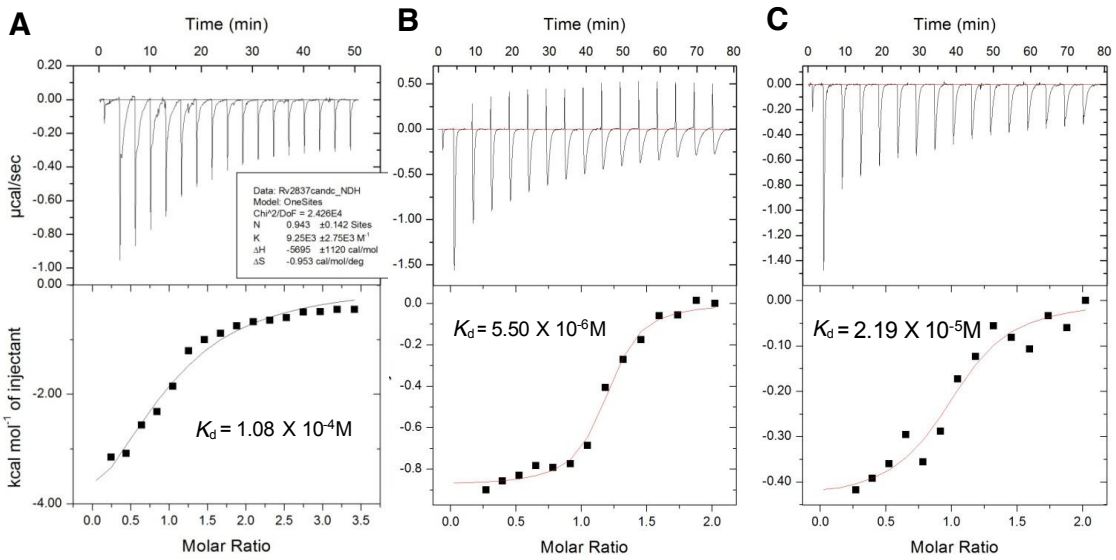

Figure 3.5. Isothermal Titration Calorimetry (ITC) profiles for binding of CdnP with 2'3'-cGAMP, c-di-AMP and pApA. (A-C) Figures depict raw thermograms and the binding isotherms from the integrated thermogram fit using the one-site model in the Origin software package. (A) 2'3'-cGAMP, (B) c-di-AMP and (C) pApA exhibited

dissociation constants (K_d) of 1.08 x 10^{-4} M, 5.50 x 10^{-6} M, and 2.19 x 10^{-4} M, respectively. Binding of each ligand was thermodynamically driven. Additional parameters were as follows. For 2'3'-cGAMP: N = 0.94 ± 0.14 sites, K_a = 9.25 ± 2.75 x 10^3 M^{-1}, ΔH = -5795 ± 1120 cal/mol, and ΔS = -0.953 cal/mol/deg. For c-di-AMP: N = 1.15 ± 0.04 sites, K_a = 1.80 ± 0.27 x 10^5 M^{-1}, ΔH = -876.9 ± 105 cal/mol, and ΔS = 21.1 cal/mol/deg. For pApA: N = 1.00 ± 0.17 sites, K_a = 4.56 ± 0.27 x 10^4 M^{-1}, ΔH = -439.8 ± 122 cal/mol, and ΔS = 19.8 cal/mol/deg.

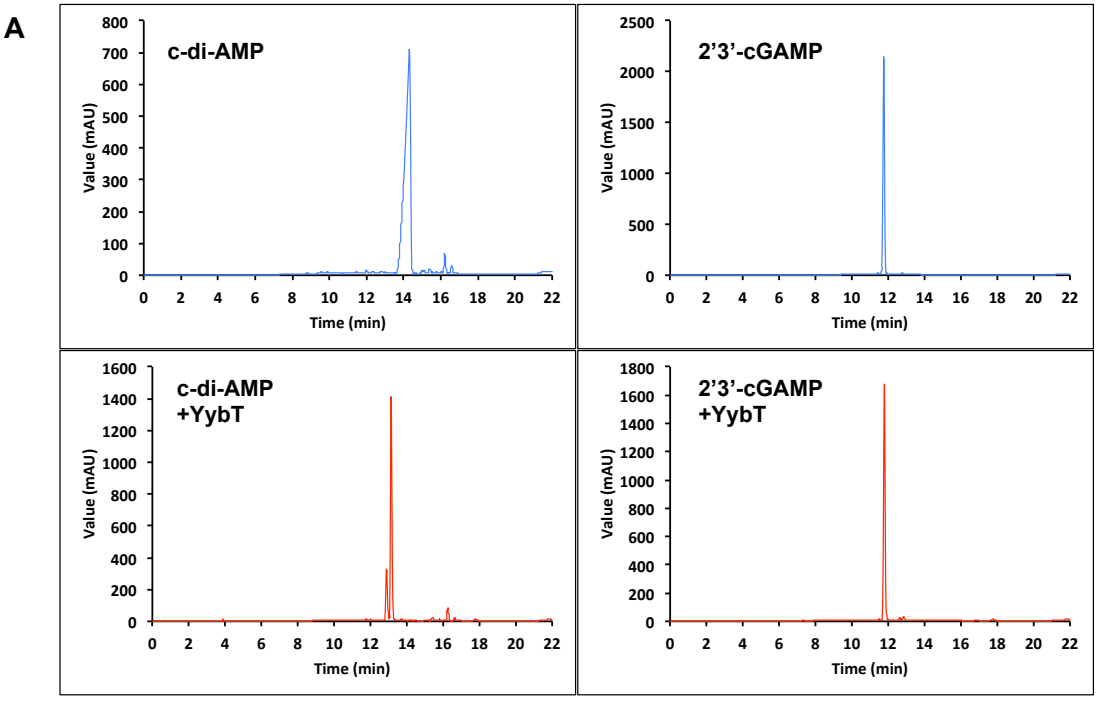

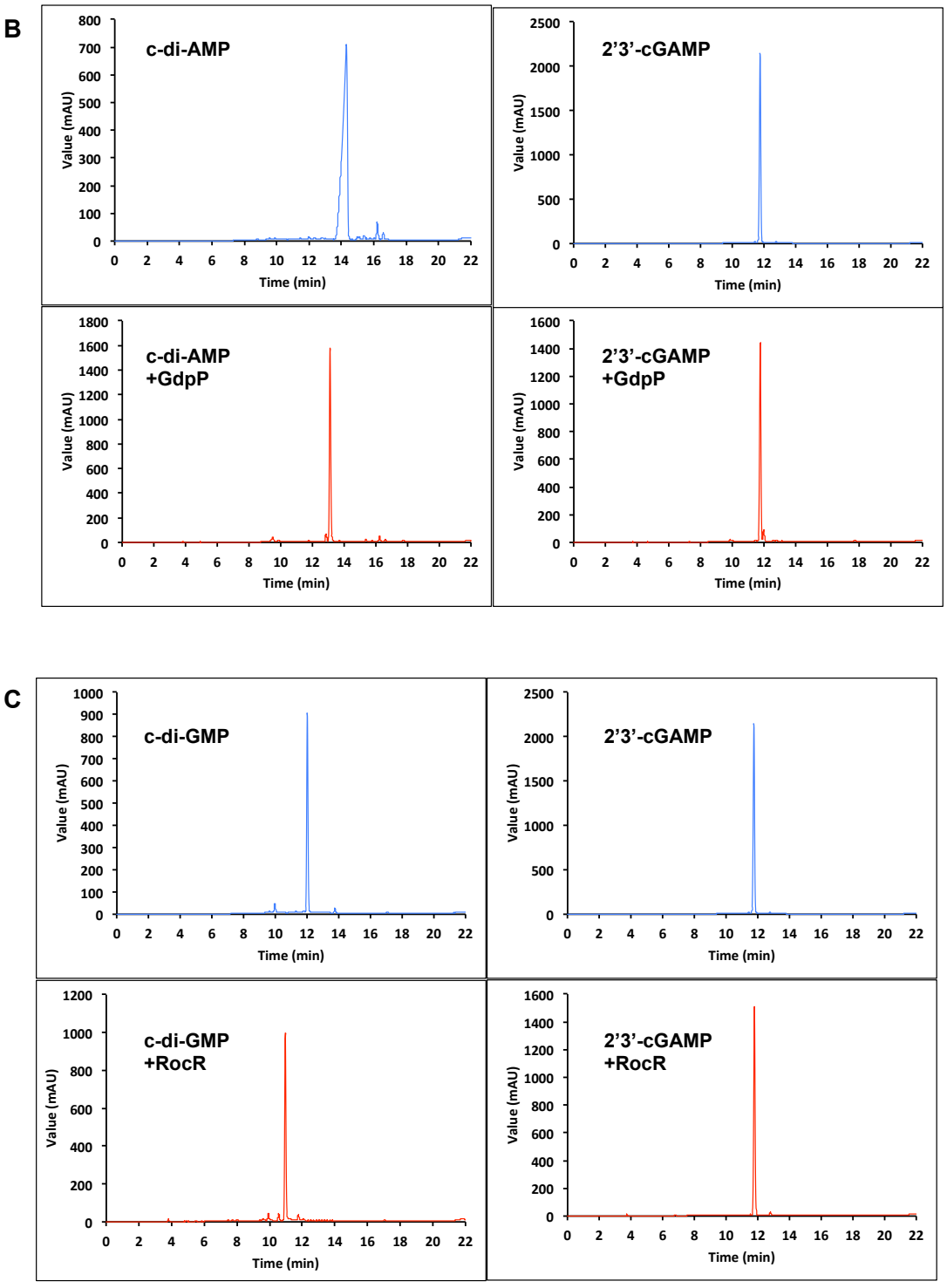

Figure 3.6. Cleavage of bacterial CDNs and 2'3'-cGAMP by CDN phosphodiesterases from different pathogenic bacteria. (A-B) HPLC profile showing

in vitro phosphodiesterase activity of YybT (*Bacillus subtilis*) for (A) c-di-AMP and (B) 2'3'-cGAMP. (C-D) HPLC profile showing *in vitro* phosphodiesterase activity of GdpP (*Staphylococcus aureus*) for (C) c-di-AMP and (D) 2'3'-cGAMP. (E-F) HPLC profile showing *in vitro* phosphodiesterase activity of RocR (*Pseudomonas aeruginosa*) for (E) c-di-GMP and (F) 2'3'-cGAMP.

3.2.3. CdnP is required for *M. tuberculosis* virulence in the mouse model

To evaluate the role of CdnP in disease pathogenesis, we infected groups of mice with the *Mtb-cdnP*::Tn mutant, the complemented mutant (*Mtb-cdnP*::Tn-comp), and the *Mtb*-WT strain using an aerosol infection model. Despite an *in vitro* growth profile identical to *Mtb*-WT in broth culture, we observed significant virulence attenuation of the *Mtb-cdnP*::Tn strain with a median time to death (MTD) of 86.5 days compared to 33.5 and 41.5 days for *Mtb*-WT and *Mtb-cdnP*::Tn-comp, respectively (Figure 3.7A). In addition to enhanced survival, *Mtb-cdnP*::Tn infected mice exhibited an ~0.8 $\log_{10}$ reduction in pulmonary bacillary load and pathology at 4 weeks post-infection (Figure 3.7B, C). Thus, loss of CdnP leads to reduced virulence and pathogenicity. This finding corresponds well with our earlier observation that overexpression of the bacterial c-di-AMP biosynthesis gene *disA* produces a similar reduced virulence phenotype[153] and with reports in several other intracellular bacterial infections including *M. tuberculosis* demonstrating reduced virulence consequent to mutation in c-di-AMP PDE activity [89, 104, 169, 174].

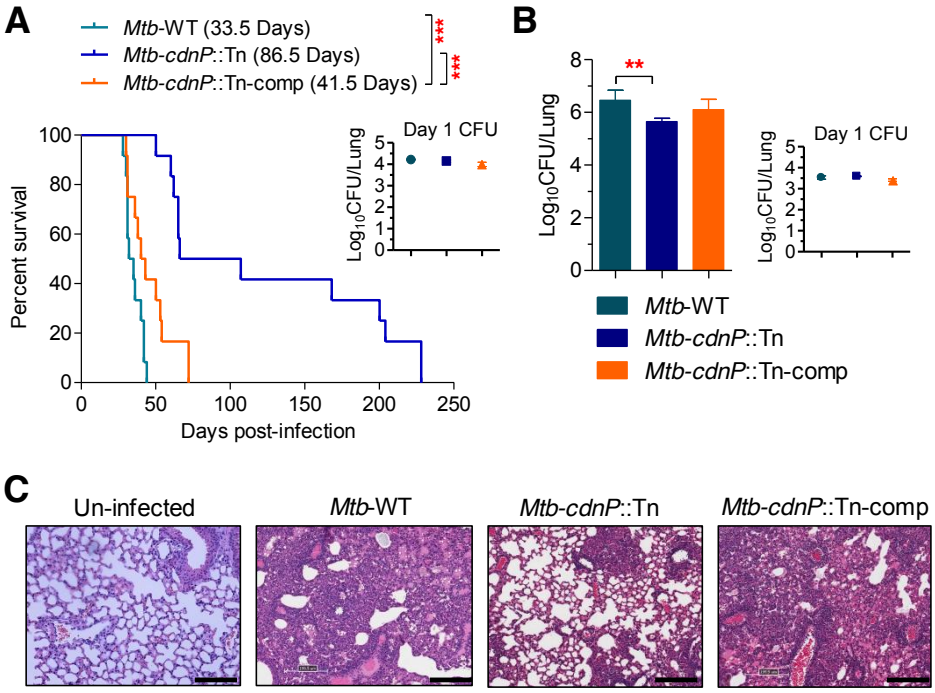

Figure 3.7. Disruption of CdnP activity leads to virulence attenuation of *M. tuberculosis*. (A) Survival of mice (n = 12) following infection with various *M. tuberculosis* strains. ***, $p < 0.001$ by Log-rank (Mantel-Cox) test. Inset graph depicts day 1 CFU/lung. Data are means ± range (n = 3). (B) Bacillary load of various *M. tuberculosis* strains in mouse lungs at 4 weeks post-infection. Data are means ± SD (n = 4). Inset graph depicts day 1 CFU/lung. Data are means ± range (n = 3). **, $p < 0.01$ by Student's t-test (two-tailed). (C) Histopathological features of lungs of representative mouse from each group and in uninfected controls. Scale bar is 200 µm.

3.2.4. CdnP activity reduces macrophage Type I IFN responses during infection in a STING-IRF3-dependent manner

As both bacterial- and host-derived CDNs are known to induce Type I IFN responses, we next assessed whether perturbation of CdnP expression in *M. tuberculosis* influences induction of the Type I IFN response. We infected murine RAW- Blue^{TM} ISG indicator macrophage cells (InvivoGen) with *Mtb-cdpP*::Tn, *Mtb*-WT, *Mtb-cdpP*::Tn-comp, and a CdnP overexpressing strain (*Mtb-cdnP*-OE). While the *Mtb-cdnP*-OE strain resulted in an ~3.2 fold and ~3.0 fold reduction of IRF3 activation and IFN-β secretion, respectively, compared with *Mtb*-WT infection, the *Mtb-cdnP*::Tn strain resulted in an ~3.6 and ~2.5 fold elevation of these same two markers of CSP activation (Figure 3.8A). These findings were also confirmed in murine primary bone marrow derived macrophages (BMDMs) and dendritic cells (BMDCs) (Figure 3.8B). In addition, we also observed increased production of IL-1α, TNF-α, and IL-6 in response to infection with the *Mtb-cdnP*::Tn strain in both BMDMs and BMDCs (Figure 3.8C-E). These findings indicate that during infection loss of bacterial CdnP expression leads to increased macrophage and dendritic cell Type I IFN responses as well as pro-inflammatory cytokine responses, while over expression of *cdnP* gives the inverse phenotypes.

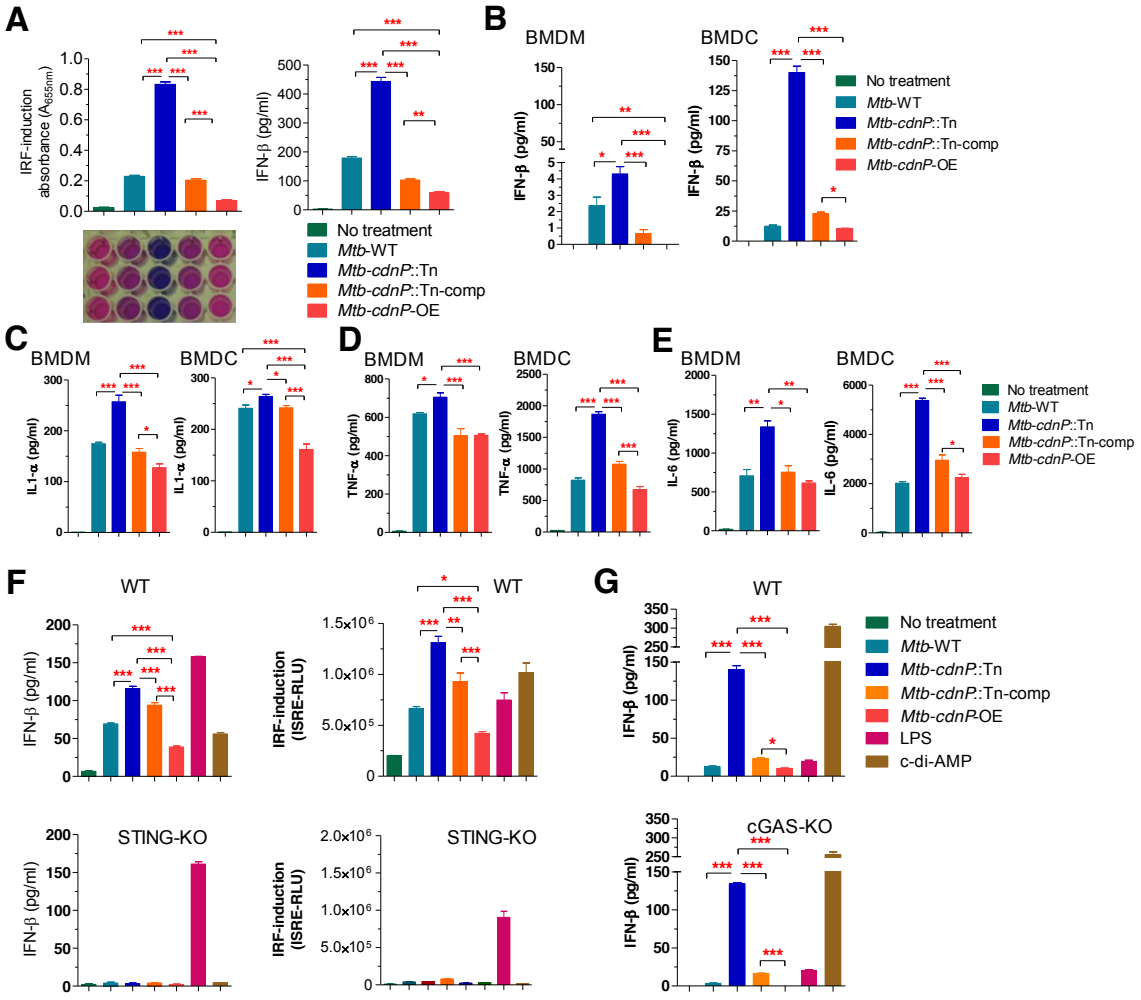

Figure 3.8. CdnP activity regulates host CSP activation and Type-I IFN responses. (A) IRF pathway activation as measured by IRF-SEAP™ QUANTI Blue™ reporter assay and IFN-β levels at 24 h post-infection in the culture supernatants of RAW-Blue™ ISG cells infected with different *M. tuberculosis* strains (MOI = 1:5). (B-E) ELISA of (B) IFN-β, (C) IL-1α, (D) TNF-α and (E) IL-6 in culture media at 24 h post-infection from BMDM and BMDC cells infected with various *M. tuberculosis* strains at an MOI of 1:10. (F) STING-dependent induction of the Type I interferon response. ELISA of IFN-β and ISRE-RLU (as a measure of IRF induction, RLU = relative light units) in the 18 h post-infection (MOI = 1:5) culture supernatants of

RAW-Lucia™ ISG cells derived from STING-ablated [STING-KO] and control [WT] macrophage IRF reporter cells. (G) ELISA of IFN-β in the culture supernatants of BMDCs from control [WT] and cGAS ablated [cGAS-KO] mice infected with various *M. tuberculosis* strains (MOI = 1:5). Data (A-G) are means ± SE (n = 3) and are representative of at least three experiments.*, $p < 0.05$; **, $p < 0.01$ and ***, $p < 0.001$. one-way ANOVA with Tukey's post-test.

To determine whether the alterations in the Type I IFN response originate from the CDN-STING-IRF3 signaling axis, we tested these same strains in murine RAW264.7-derived STING ablated [STING-KO] IRF reporter cells (RAW-Lucia™ ISG-KO-STING Cells, InvivoGen). Infection of $STING^{-/-}$ cells resulted in a complete loss of Type I IFN induction in all *M. tuberculosis* strains irrespective of the *cdnP* genotype (Figure. 3.8F), while the same assay in control [WT] IRF reporter macrophage cells (Figure. 3.8F) gave patterns nearly identical to those seen in the murine RAW- Blue™ ISG indicator macrophage cells (Figure. 3.8A). A similar response pattern was observed when the strains were tested in human THP-1 STING sufficient (WT) and knocked-down cells (STING-KD) (Figure 3.9). These results confirm that macrophage inflammatory signaling influenced by the bacterial phosphodiesterase CdnP is dependent on the STING-IRF3 pathway.

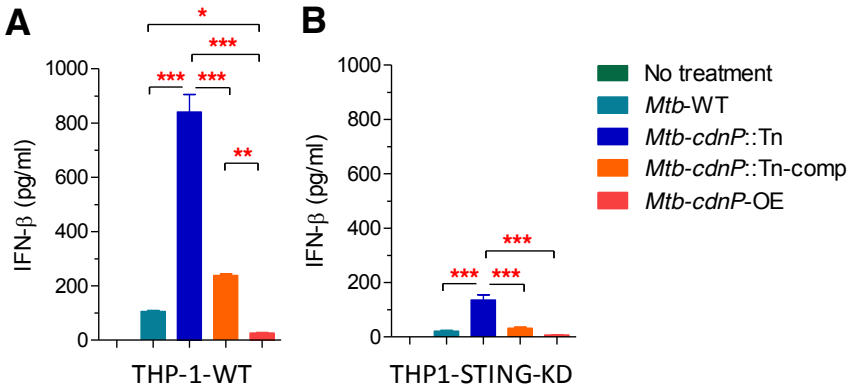

Figure 3.9. Reduced IFN-β response following *M. tuberculosis* infection in human THP-1 monocytes harboring a stable knock-down (KD) of STING. (A-B) ELISA of IFN-β in culture media of (A) THP1-WT and (B) THP1-STING-KD cells (Invivogen) at 18 h after infection with various *M. tuberculosis* strains at MOI of 1:10 as measured by ELISA. Data are means ± SE (n = 3) of at the least three experiments. *, $p < 0.05$, **, $p < 0.01$ and ***, $p < 0.001$ by one-way ANOVA with Tukey's post-test.

We next assessed the influence of STING mutation on the *in vivo* virulence of the *Mtb*-CdnP mutant. Compared to wild type mice infection (Figure 3.7B), in the absence of STING the *Mtb*-WT and *Mtb*-CdnP mutant strains showed comparable bacillary lung burdens indicating that upon loss of STING the attenuated virulence of the *Mtb*-CdnP mutant is no longer detectable (Figure 3.10A). Similarly in BMDMs from STING$^{+/+}$ and STING$^{-/-}$ animals, the growth rates of the *Mtb*-WT and *Mtb*-CdnP mutant strains were similar (Figure 3.10B). Our finding that an intact STING protein is required to detect a virulence difference between the *Mtb*-WT and *Mtb*-CdnP mutant strains was further corroborated by an another experiment showing that the

median survival times of mice lacking IFNαβ-R [IFNαβ-R (-/-)] infected with *Mtb*-WT and *Mtb*-CdnP mutant were nearly identical (Figure 3.10C). These results indicate elevated STING-signaling leading to a more robust Type I IFN response accounts for the virulence defect of the *Mtb*-CdnP mutant and that other potential changes in microbial physiology that stem from loss of CdnP do not compromise its pathogenicity.

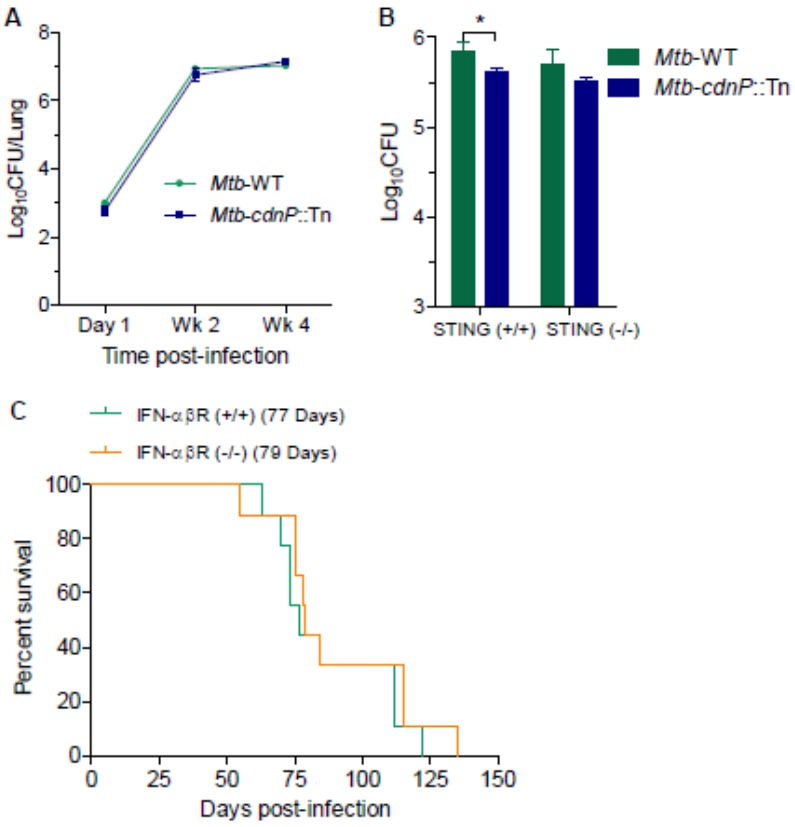

Figure 3.10. Influence of STING and IFN-aβR mutation on *in vivo* virulence of *Mtb-cdnP*::Tn mutant. (A) Bacillary load of various *M. tuberculosis* strains in lungs at 4 weeks post-infection of WT [STING (+/+)] and STING ablated [STING (-/-)] mice. Data are means ± SD (n = 4). Student's t-test (two-tailed). (B) *ex vivo* bacterial growth in BMDMs derived from WT [STING (+/+)] and STING ablated [STING (-/-

)] mice (C) Survival of WT [IFN-aβR (+/+)] and IFN-aβR ablated [IFN-aβR (-/-)] mice (n = 9) following infection with *Mtb-cdnP*::Tn mutant.

3.2.5. Interplay of CdnP-mediated CDN hydrolysis and cGAS-mediated cytosolic surveillance

To determine whether the Type I IFN response differences observed with the *Mtb-cdpP*::Tn strain originate from phosphodiesterase-mediated reduction of bacterial-derived CDN levels or host-derived 2'3'-cGAMP, we infected BMDCs derived from cGAS-KO mice with our *cdnP* recombinant strains. Compared with cGAS-sufficient cells (WT), we observed a 73% drop in IFN-β levels following *Mtb*-WT infection in cGAS-KO BMDCs (Figure 3.8G) indicating that during WT infection cGAS plays an important role in triggering the STING-IRF3 axis. Moreover, with the same cGAS-KO BMDCs, IFN-β secretion dropped even further with *Mtb-cdnP*-OE infection rendering it undetectable. However, in stark contrast to *Mtb*-WT and *Mtb-cdnP*-OE, infection with the *M. tuberculosis* strain lacking CdnP led to high level of Type I IFN expression in cGAS-KO BMDCs. Indeed, with the *Mtb-cdpP*::Tn infection the IFN-β levels (134.5 pg/mL) were nearly as high in cGAS-KO BMDCs as those observed from cGAS-sufficient control cells (140.1 pg/mL) (Figure 3.8G). This shows that in the absence of the bacterial CdnP, the resulting accumulation of bacterial CDNs (Figure 3.3A) may bypass the requirement for bDNA-stimulation of cGAS and host-generated 2'3'-cGAMP for induction of Type I IFN responses.

3.2.6. *M. tuberculosis* CdnP modulates levels of host-derived 2'3'-cGAMP in macrophages

Based on our *in vitro* finding that 2'3'-cGAMP is a substrate of CdnP, we next investigated whether CdnP modulates host-derived cyclic dinucleotide levels *ex vivo*. To investigate this, we measured intra-macrophage 2'3'-cGAMP levels following infection with the *M. tuberculosis* CdnP recombinant strains. These studies revealed significantly higher 2'3'-cGAMP levels following infection with *Mtb-cdpP*::Tn compared with the *Mtb*-WT strain (Figure 3.11A). We also observed a significant reduction in 2'3'-cGAMP levels in cells infected with *Mtb-cdnP*-OE strain. These results strongly suggest that during infection *M. tuberculosis* CdnP accesses host-derived 2'3'-cGAMP and hydrolyzes it. Lysis of *M. tuberculosis* cells, which can occur after phagosomal escape, releases bacterial content into the host's cytosol. Bacterial DNA, which is released during cell lysis, is known to activate the cytosolic surveillance pathway (CSP). Analogously, bacterial cell lysis after phagosomal escape would release bacterial-derived CdnP into the host's cytosol and facilitate the hydrolysis of 2'3'-cGAMP. Thus, bacterial CdnP is capable of manipulating the host cytosolic surveillance system (CSP) by modulating both host 2'3'-cGAMP levels as well as bacterial CDN levels.

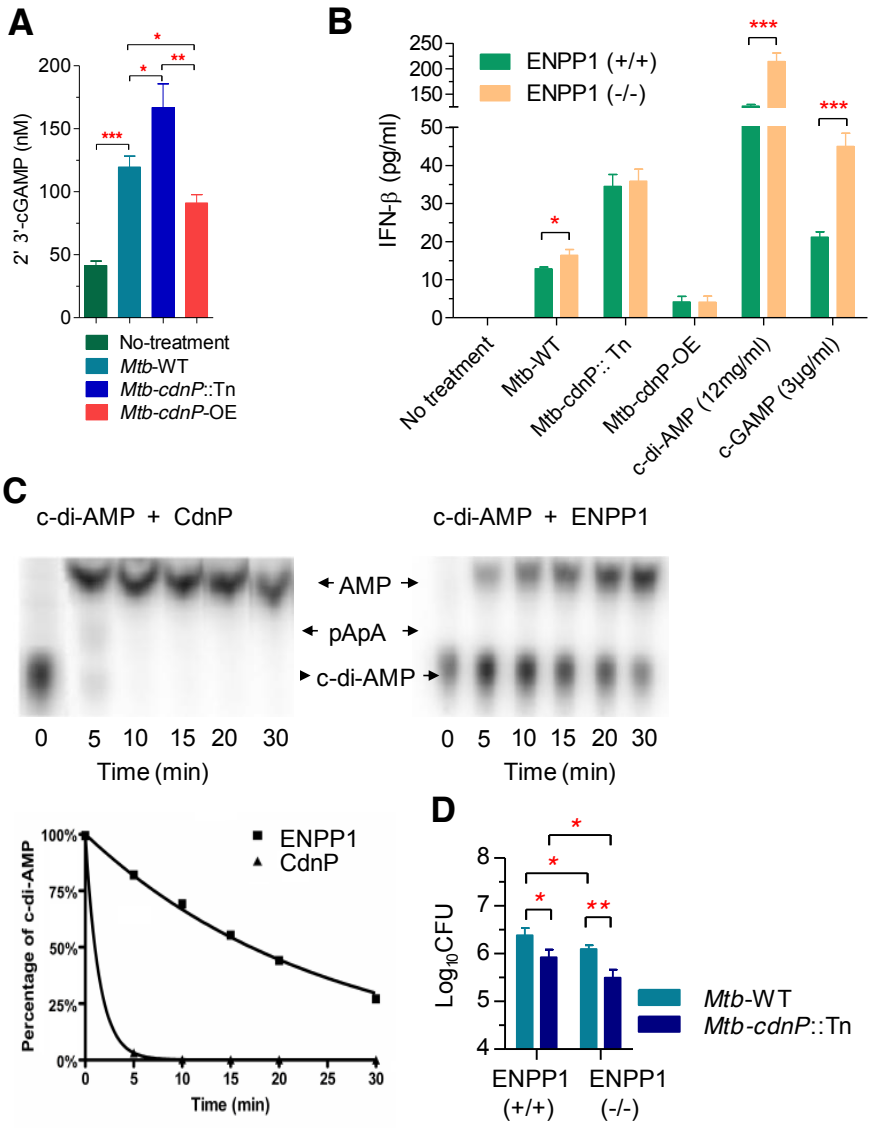

Figure 3.11. Regulation of intra-macrophage CDN homeostasis by bacterial CdnP and host ENPP1. (A) Nucleotides extracted from infected macrophages were analyzed by LC-MS/MS MRM for quantification of 2'3'-cGAMP. Data are means ± SD (n=3) and representative of two experiments.*, $p < 0.05$, **, $p < 0.01$ and ***, $p < 0.001$ by Student's t-test (two-tailed). (B) Levels of IFN-β in the culture supernatants of BMDCs from WT [ENPP1 (+/+)] and ENPP1 ablated [ENPP1 (-/-)] mice infected with various *M. tuberculosis* strains (MOI = 1:5) measured by ELISA. Data are

means ± SD (n=4).*, $p < 0.05$ and ***, $p < 0.001$. Student's t-test (two-tailed). (C) Comparative TLC profile of c-di-AMP cleavage by CdnP (*M. tuberculosis*) and ENPP1 (human). (D) Intracellular growth of *Mtb*-WT and *Mtb-cdnP*::Tn in BMDMs from WT [ENPP1 (+/+)] and ENPP1 ablated [ENPP1 (-/-)] mice at day 5 post-infection (MOI = 1:10). Data are means ± SD (n=3).*, $p < 0.05$ and **, $p < 0.01$,Student's t-test (two-tailed).

3.2.7. Biological effects of CdnP-mediated cGAMP linearization on the Type I IFN response

We next sought to investigate if modulation of Type I IFN levels is a direct effect of *M. tuberculosis* CdnP or if host PDEs are also involved. For this we employed cells lacking the host PDE known as ectonucleotide pyrophosphatase/phosphodiesterase 1 (ENPP1) which is capable of hydrolyzing 2'3'-cGAMP[175]. We observed that in BMDCs from ENPP1 (-/-) mice Type I IFN levels were significantly increased the response to exogenous synthetic cGAMP and c-di-AMP stimulation compared with ENPP1 (+/+) cells (Figure 3.11B). However, on comparing ENPP1 knockout versus ENPP1 proficient BMDCs following infection with our *M. tuberculosis* CdpP recombinant strains, the differences in Type I IFN expression levels were negligible whether the infecting strains was *Mtb*-WT, *Mtb-cdnP*::Tn, or *Mtb-cdnP*-OE (Figure 3.11B). These results signify that despite the presence of a host PDE, which is capable of modulating the CSP through CDN hydrolysis, the bacterial enzyme CdnP plays a major role in influencing the Type I IFN response.

Our finding that CdnP hydrolyzes 2'3'-cGAMP into linear pGp(2'-5')A and that elevated CdnP expression inhibits induction of Type I IFN response suggested that the linear byproducts have little to no activity. To test this possibility directly we evaluated chemically synthesized linear dinucleotides pGp(2'-5')A and pApA along with c-di-AMP and 2'3'-cGAMP for activation of Type I interferon responses in RAW-Blue^{TM} ISG indicator cells (InvivoGen). While 2'3'-cGAMP and c-di-AMP were found to be highly potent signal inducers, the linear pApA and pGpA molecules failed to trigger Type I IFN responses, even at concentrations of 0.125 μM or higher (Figure 3.12).

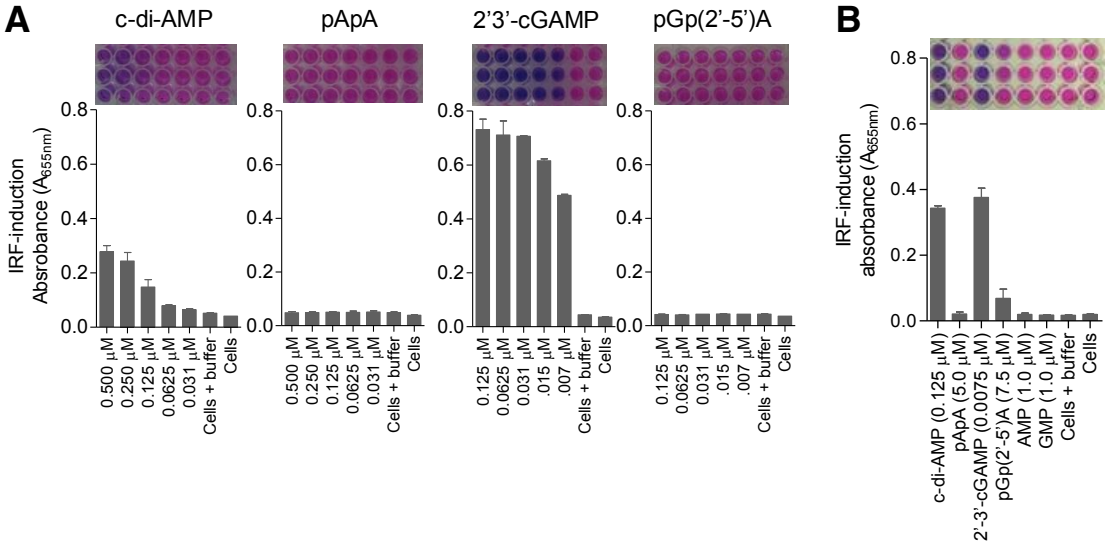

Figure 3.12. IRF pathway activation as measured by IRF-SEAP^{TM} QUANTI Blue^{TM} reporter assay in the culture supernatants of RAW-BlueTM ISG cells stimulated with c-di-AMP, linear pApA, 2'3'-cGAMP, and linear pGp(2'-5')A following reversible digitonin permeabilization. Data are means ± SD (n = 3) and representative of two experiments.

3.2.8. Role of host PDEs in CDN metabolism and *M. tuberculosis* virulence

Considering the enhanced Type I IFN response to c-di-AMP in cells lacking host ENPP1 (Figure 3.11B) and the ability of ENPP1 to hydrolyze the 3'-5' as well as 2'-5' phosphodiester bonds in 2'3'-cGAMP[175] (Figure 3.13), we next investigated whether bacterial c-di-AMP is a potential substrate of ENPP1. We found that while ENPP1 does hydrolyze c-di-AMP to AMP, the reaction is considerably slower than CdnP-mediated hydrolysis. At equal enzyme concentrations with c-di-AMP as the substrate, ENPP1 achieved only ~75% cleavage after 30 min compared with CdnP which cleaved 100% of the c-di-AMP within 5 min **(**Figure 3.11C**)**.

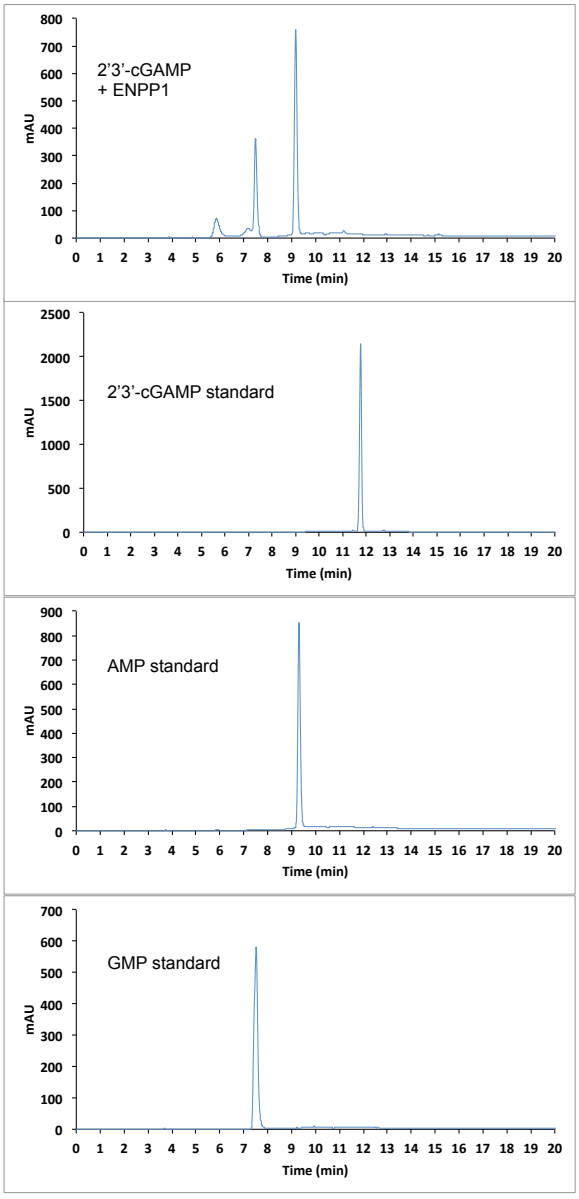

Figure 3.13. HPLC profiles for cleavage of 2'3'-cGAMP (100 µM) by human ENPP1 (2 µM). Figure depicts products obtained following enzymatic reaction at 37°C for 2 hours.

Our finding that the host PDE, ENPP1, is capable of degrading bacterial c-di-AMP suggests that host cell activity levels of ENPP1 may influence *M. tuberculosis*

virulence. We hypothesized that disruption of ENPP1 might enhance the susceptibility of *M. tuberculosis* to CDN-mediated host immunity. To address this question we performed a comparative analysis of intracellular growth of *Mtb*-WT and *Mtb-cdnP*::Tn mutant in BMDMs derived from ENPP1 (-/-) and ENPP1 (+/+) wild type mice. As may be seen, bacterial growth was significant inhibited in ENPP1 (-/-) cells compared with ENPP1-WT cells at day 5 post-infection (Figure 3.11D). Additionally, in the absence of both ENPP1 and CdnP, intracellular growth is even further inhibited with an ~1 $\log_{10}$ CFU difference at day 5 (comparison of *Mtb*-WT in ENPP1-WT cells with *Mtb-cdnP*::Tn in ENPP1 (-/-) cells, Figure 3.11D).

As *M. tuberculosis* CdnP is unable to hydrolyze the linear pGp(2'-5')A dinucleotide further into the mononucleotides AMP and GMP, we sought to determine the cellular fate of the linear pGp(2'-5')A dinucleotide. We reasoned that linear pGp(2'-5')A molecules would not be re-cyclized back to 2'3'-cGAMP by cGAS or any other cyclases, since known CDN cyclases require a triphosphate at the 5'-end.[176, 177] Consequently, we hypothesized that host 2'-5' phosphodiesterase activity may be responsible for further hydrolysis of the linear dinucleotide. To address this hypothesis, we evaluated PDE12, a human 2'-PDE enzyme reported to degrade the 2'-5'-linked oligoadenylates (2-5As) generated by vertebrate 2'-5' oligoadenylate synthetases upon sensing viral RNA during infection.[178, 179] Following incubation of pGp(2'-5')A with purified PDE12 *in vitro*, reaction products were analyzed by HPLC (Figure 3.14). Incubation of PDE12 with pGp(2'-5')A resulted in two product species corresponding to peaks of AMP and GMP, indicating that PDE12 hydrolyzes linear pGp(2'-5')A into the corresponding mononucleotides. We

observed that PDE12 can also cleave linear pApA into AMP (Figure 3.14A). However, PDE12 is incapable of hydrolyzing intact 2'3'-cGAMP or c-di-AMP (Figure 3.14B and C), a finding consistent with recent studies of human PDEs with CDN activity[175]. We also tested the human enzyme oligoribonuclease REXO2 (Sfn) which is an oligoribonuclease involved in mitochondrial RNA degradation and homeostasis and is an orthologue of bacterial nanoRNase (Nrn) [180]. Our studies demonstrate that REXO2 does not hydrolyze 2'3'-cGAMP (Figure 3.14B) or c-di-AMP (Figure 3.14D and E).

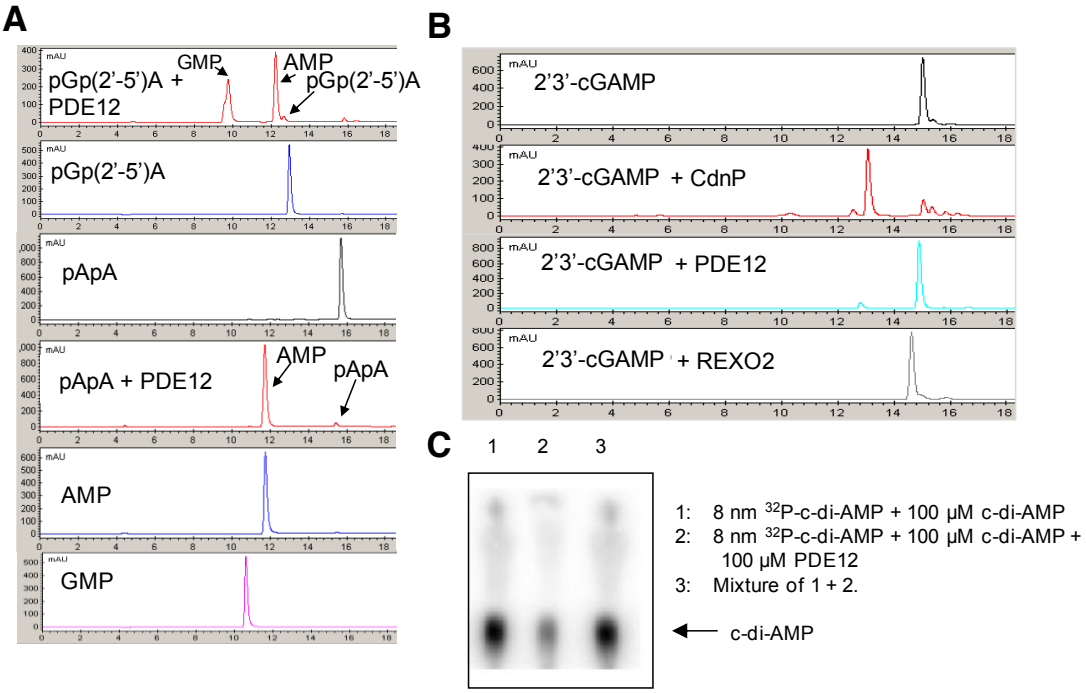

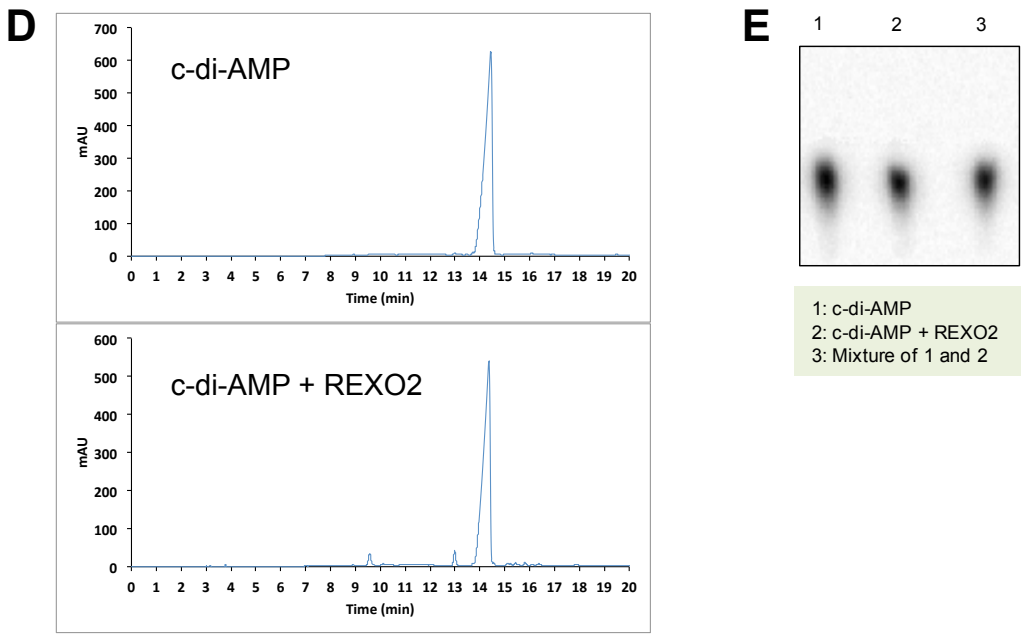

Figure 3.14. (A) HPLC profiles for cleavage of pGp(2'-5')A and pApA by host PDE12 and related standards. (B) HPLC profiles showing PDE activity of CdnP (*M. tuberculosis*), PDE12 (human), REXO2 (human) for 2'3'-cGAMP. (C) TLC depicting PDE activity of PDE12 for ^{32}P-c-di-AMP. (D) HPLC profiles showing PDE activity of REXO2 (human) for c-di-AMP (E) TLC depicting PDE activity of REXO2 (human) for ^{32}P-c-di-AMP.

3.2.9. FDA-approved PDE-inhibitors have activity against CdnP

Our findings that *M. tuberculosis* CdnP modulates both bacterial and host CDN levels and that mutation of the *cdnP* gene leads to *in vivo* attenuation of *M. tuberculosis* virulence suggest that small molecule inhibitors of CdnP may sensitize bacteria to host-mediated destruction. To test this hypothesis, we assessed a number of commercially available PDE inhibitors for their activity against *M. tuberculosis* CdnP *in vitro* (Table 3.2). We also included four FDA-approved PDE inhibitors

(PDE-Is) in this analysis: cilostazol (PDE3-I), cilomilast (PDE4-I), sildenafil (PDE5-I), and tadalafil (PDE5-I).

Table 3.2. List of commercially available inhibitors used in the study

	Inhibitor	**Systematic (IUPAC) name**	**Target PDE/ Source**
1	Calbiochem-454202. (from Calbiochem PDE Inhibitor Set I)	8-Methoxymethyl-3-isobutyl-1-methylxanthine	PDE-1 (cAMP and cGMP) (EMD Millipore)
2	Cilostazol*	6-[4-(1-cyclohexyl-1*H*-tetrazol-5-yl)butoxy]-3,4-dihydro-2(1*H*)-quinolinone	PDE-3 (cAMP) (Sigma)
3	Trequinsin-HCl (from Calbiochem PDE Inhibitor Set I. #382425)	9,10-Dimethoxy-3-methyl-2-(2,4,6-trimethylphenyl)imino-6,7-dihydropyrimido[6,1-*a*]isoquinolin-4-one	PDE-3(cGMP) (EMD Millipore)
4	Cilomilast*	4-cyano-4-(3-cyclopentyloxy-4-methoxyphenyl)cyclohexane-1-carboxylic acid	PDE-4 (cAMP) (Sigma)
5	Rolipram (from Calbiochem PDE Inhibitor Set I. #557330)	4-[3-(Cyclopentyloxy)-4-methoxyphenyl]-2-pyrrolidinone	PDE-4 (cAMP) (EMD Millipore)
6	Calbiochem-475250	4-{[3',4'-(Methylenedioxy)benzyl]amino}-6-methoxyquinazoline	PDE-5(cGMP) (EMD Millipore)
7	Tadalafil*	methyl-pyrazino [1', 2':1,6] pyrido[3,4-*b*]indole-1,4-dione	PDE-5(cGMP) (Sigma)
8	Sildenafil*	7-oxo-3-propyl-1*H*-pyrazolo[4,3-*d*]pyrimidin-5-yl)	PDE-5 (cGMP) (Sigma)
* FDA approved PDE inhibitors.			

As may be seen in Figure 3.15A the four FDA-approved PDE-inhibitors were active against CdnP albeit at a high inhibitor concentrations (250 μM). These results indicate that CdnP is a druggable target.

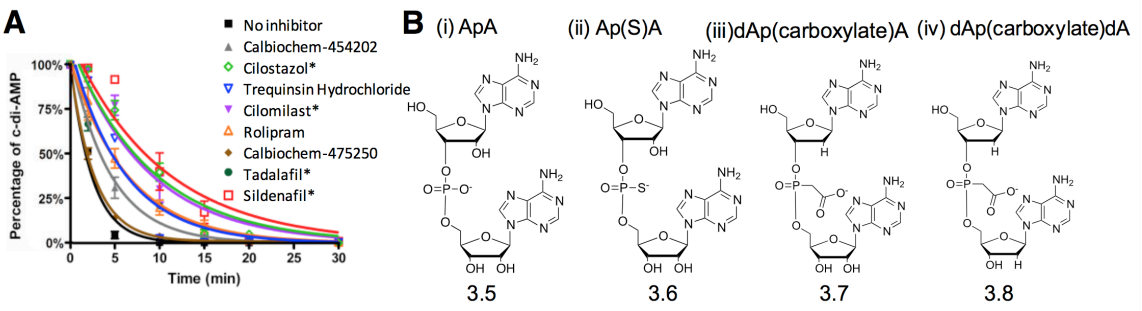

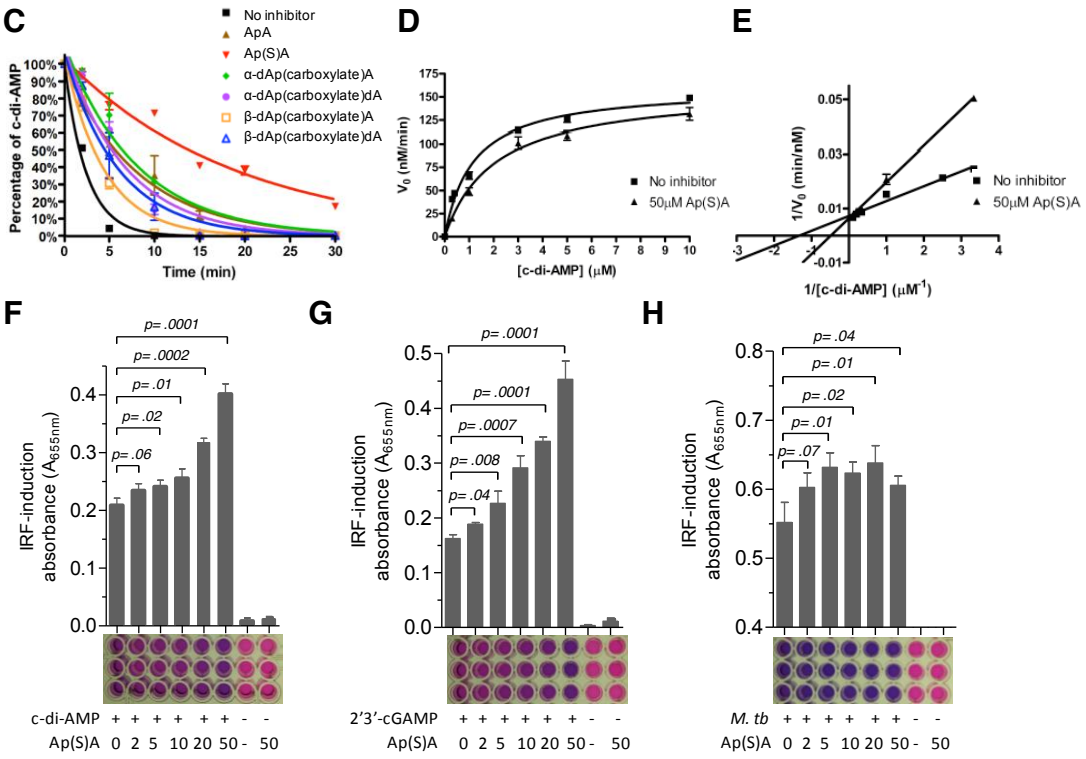

Figure 3.15. Inhibition of CdnP by PDE inhibitors and ApA analogs. (A) Commercially available PDE inhibitors (250 μM) were tested for their ability to inhibit CdnP activity with ^{32}P-c-di-AMP as the substrate. Reaction products were analyzed using TLC. The figure depicts percentage ^{32}P-c-di-AMP present over time during CdnP hydrolysis in the presence of various inhibitors. Data are means ± SD (n = 3). *, FDA approved drugs. (B) Structures of ApA analogs. (C, D) Inhibition of CdnP activity by ApA analogs (250 μM), (C) graphical representation of percentage ^{32}P-c-di-AMP present over time during CdnP hydrolysis in the presence of various inhibitors. Data are means ± SD (n = 3). (D) Michaelis–Menten kinetics of c-di-AMP cleavage by CdnP with or without the inhibitor Ap(S)A. (E) Lineweaver–Burk plot showing that Ap(S)A is a competitive inhibitor. (F - H) Biological effect of Ap(S)A (0 – 50 μM) analog on IRF induction following stimulation with (F) c-di-AMP (8.4

μM), (G) 2'3'-cGAMP (1.04 μM) (H) M. tuberculosis infection (MOI = 1:10) in RAW-BlueTM ISG cells. Data are means ± SD (n = 3), Student's t-test (two-tailed).

3.2.10. Design and evaluation of CdnP inhibitors

Next we designed inhibitors to interfere specifically with the enzymatic activity of *M. tuberculosis* CdnP. We designed six linear analogs of pApA, which lacked a 5'-phosphate and some which contained modifications of the phosphodiester linkage: ApA, Ap(S)A, α-dAp(carboxylate)A, α-dAp(carboxylate)dA, β-dAp(carboxylate)A and β-dAp(carboxylate)dA (Figure 3.15B). We tested the six analogs for inhibition of CdnP activity against c-di-AMP (Figure 3.15C and Figure 3.16). Among the inhibitors tested, the sulfur analog Ap(S)A demonstrated maximal inhibitory activity (K_i = 65 ± 23 μM) (Figure 3.15C). Kinetic analysis revealed that Ap(S)A gives classic substrate inhibition and acts as a competitive inhibitor (Figure 3.15D and E). In addition, all linear pApA analogs, aside from ApA, were found to be resistant to hydrolysis by CdnP (Figure 3.17). We also conducted *in vitro* inhibition studies of ENPP1 hydrolysis of 2'3'-cGAMP in the presence of Ap(S)A and found that the inhibitor has modest activity (Figure 3.18).

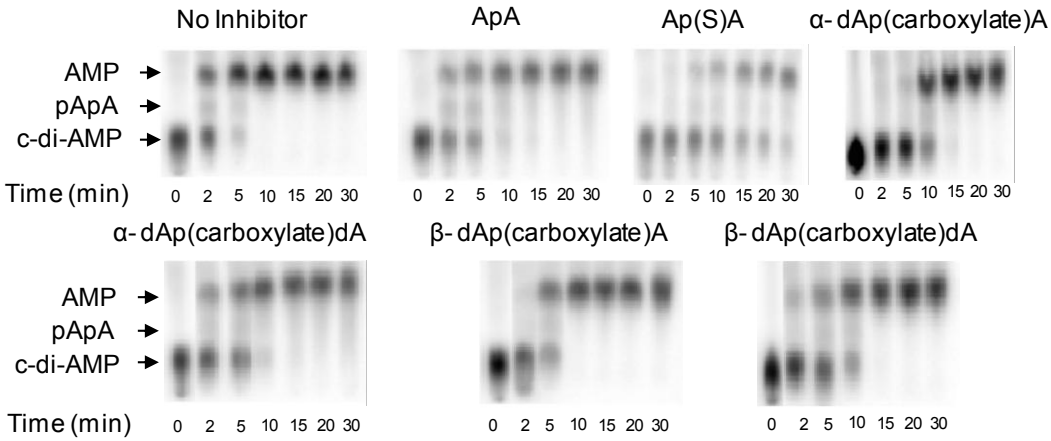

Figure 3.16. Inhibition of CdnP by PDE inhibitors and ApA analogs. Commercially available PDE inhibitors (250 μM) were tested for their ability to inhibit CdnP activity with ^{32}P-c-di-AMP as the substrate. Reaction products were analyzed using TLC. The figure depicts representative TLC images showing ^{32}P-c-di-AMP present over time during CdnP hydrolysis in the presence of various inhibitors.

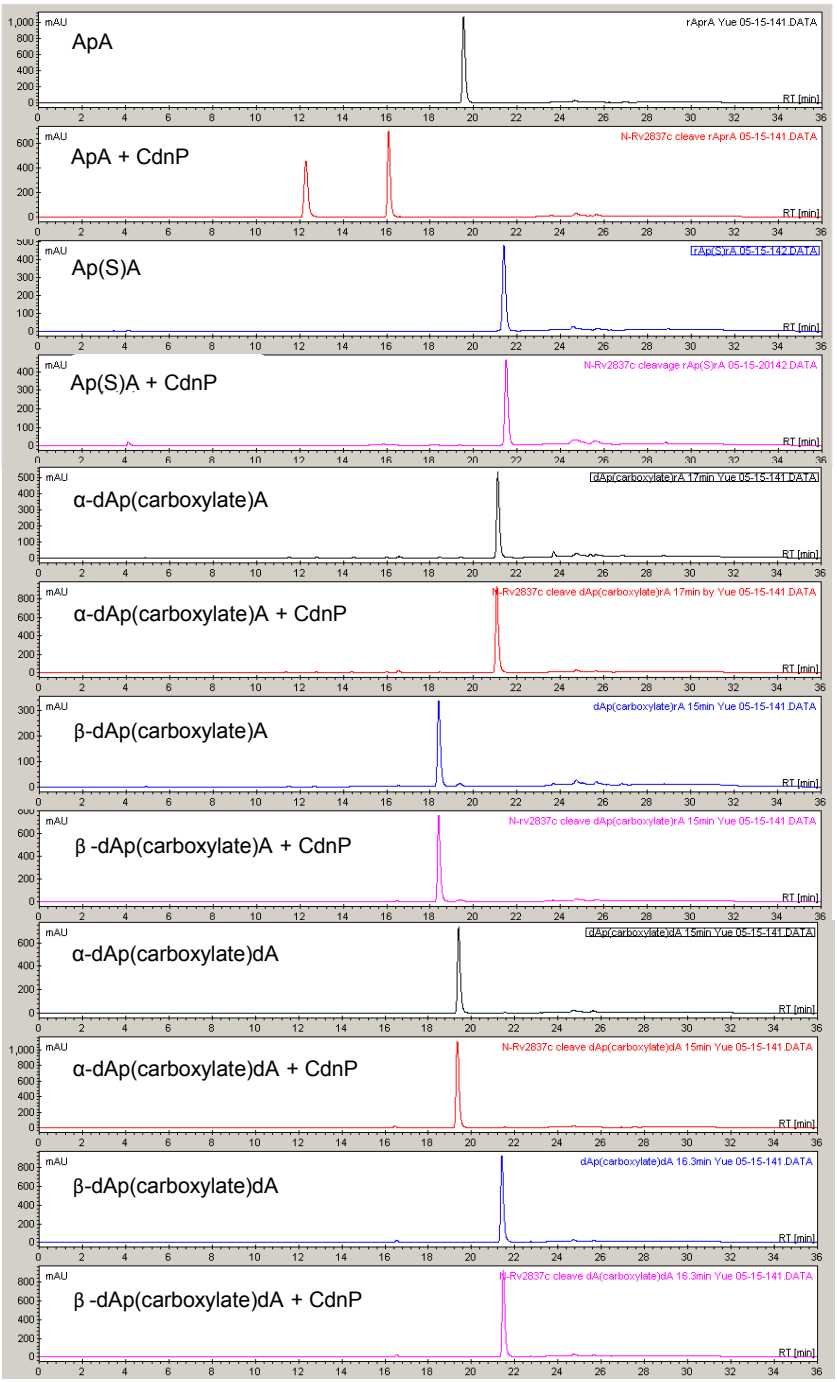

Figure 3.17. Phosphodiesterase activity of CdnP for ApA analogs. HPLC profiles showing PDE activity of CdnP for six different analogs: ApA, Ap(S)A, α- and β-dAp(carboxylate)A and α- and β-dAp(carboxylate)dA. Assay conditions are as described in the Experimental section.

A

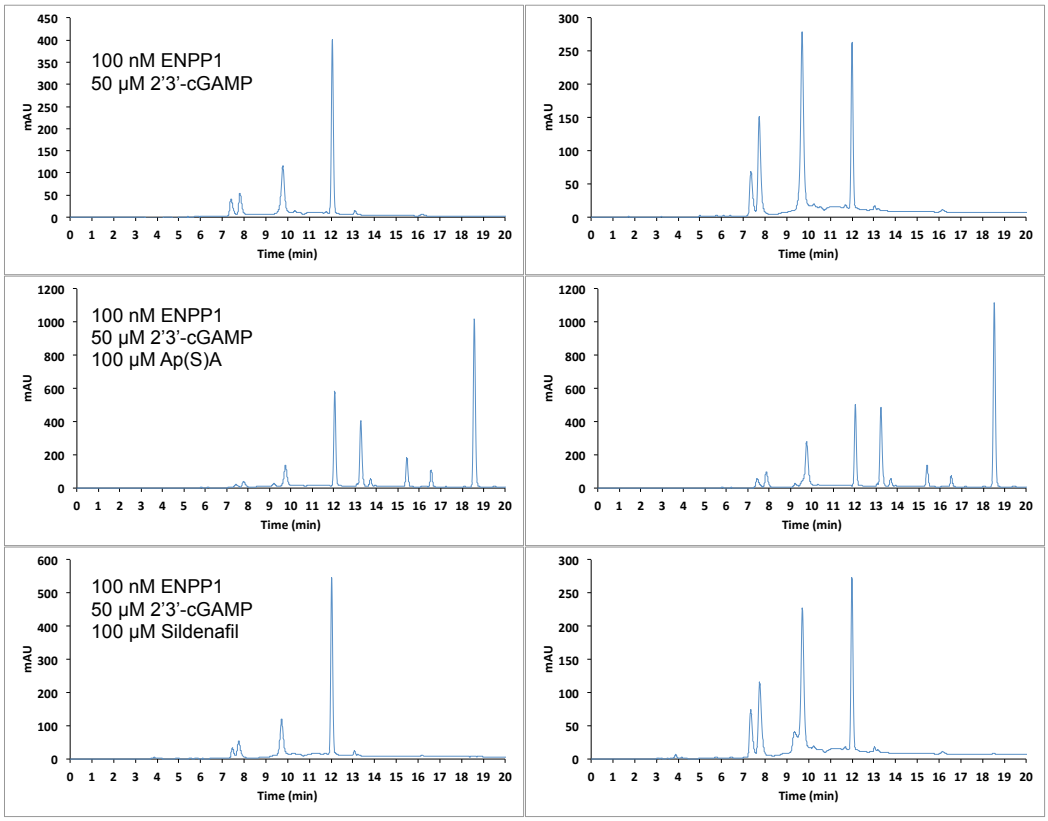

B

2'3'-cGAMP + ENPP1	GMP peak area	AMP peak area	2'3'-cGAMP peak area	Remaining 2'3'-cGAMP (%)
10 min	14.2099	16.8001	41.2387	57
Ap(S)A + 10 min	10.3995	19.7239	60.8550	67
Sildenafil + 10 min	13.8761	18.4486	55.1234	63
30 min	33.8650	41.2361	26.2149	26
Ap(S)A + 30 min	24.6771	47.8381	50.9488	41
Sildenafil + 30 min	31.0765	37.6025	28.2303	29

Figure 3.18. Inhibition of PDE activity of ENPP1 towards 2'3'-cGAMP by Ap(S)A and Sildenafil. Ap(S)A and commercially available PDE inhibitor Sildenafil (100 μM) were tested for their ability to inhibit PDE activity of ENPP1 towards 2'3'-cGAMP. Reaction products were analyzed using HPLC. (A) The figure depicts representative chromatograms showing 2'3'-cGAMP present over time during

ENPP1 hydrolysis in the presence of various inhibitors. (B) Table depicting quantitative statistics of HPLC profiles.

To evaluate the activity of Ap(S)A *in vivo*, we tested its ability to potentiate CDN signaling as measured with RAW-Blue^{TM} ISG indicator cells. Exposure to the inhibitor Ap(S)A resulted a marked enhancement in IRF induction in uninfected cells whose CSP was triggered by addition of exogenous c-di-AMP or cGAMP (Figure 3.15F and G and Figure 3.19). The inhibitory activity of Ap(S)A was also evident in context of *M. tuberculosis* cellular infection (Figure 3.15H and Figure 3.20). Using RAW- Blue^{TM} ISG indicator cells we observed an ~20% increase in IRF induction in the presence of 5 mM Ap(S)A (Figure 3.15H). These observations reveal that inhibition of *M. tuberculosis* CdnP is achievable and that CdnP inhibition during *M. tuberculosis* results in detectable potentiation of the CSP, an event that is associated with reduced bacterial pathogenicity.

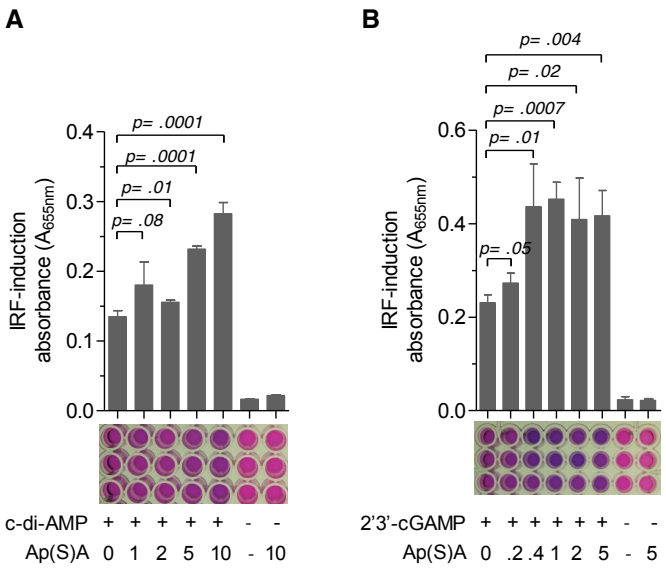

Figure 3.19. Influence of Ap(S)A on CDN mediated IRF induction. The figure depicts the biological effect of Ap(S)A analog (0 - 10 μM) on IRF induction in RAW-Blue™ ISG cells following stimulation with (A) c-di-AMP (0.5 μM) and (B) 2'3'-cGAMP (0.1 μM) in the presence of transfection reagent X-tremeGENE (Roche) following manufacturer's recommendation.

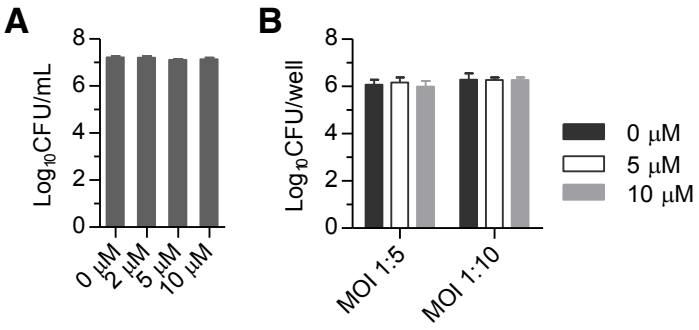

Figure 3.20. Influence of Ap(S)A on *in vitro* and *ex vivo* growth of *M. tuberculosis*. (A) The figure depicts the effect of Ap(S)A analog (0 - 10 μM) on growth of *M. tuberculosis* in 7H9 broth. *M. tuberculosis* was cultured in the presence of Ap(S)A for 7 days in 7H9 broth and CFU was enumerated. (B) Growth of *M. tuberculosis* in

RAW-Blue^{TM} ISG cells 2 days following infection at the indicated MOIs in the presence of Ap(S)A (0 - 10 μM).

3.3. Conclusion

As a highly successful human pathogen, *M. tuberculosis* has evolved extensive mechanisms to evade the immune system at multiple levels[181]. While some of the virulence mechanisms rely on factors released by *M. tuberculosis*, others depend on host components that are either hijacked or co-opted to prevent generation of an effective immune response. In this study we reveal a multi-level immune evasion strategy of *M. tuberculosis* whereby it inhibits the host cell's CSP by deploying the CdnP phosphodiesterase. CdnP activity benefits microbial pathogenicity through hydrolysis of two important categories of innate immune signaling molecules. First, CdnP action reduces immune detection of bacterial-derived c-di-AMP and c-di-GMP--which are known PAMPs--by degrading them into non-immunogenic nucleotides. And second, it also degrades host-derived 2'3'-cGAMP--a danger associated molecular pattern (DAMP) generated on detection of bDNA--thereby muting the cell's ability to signal detection of foreign nucleic acid (schematic model shown in Figure 3.21).

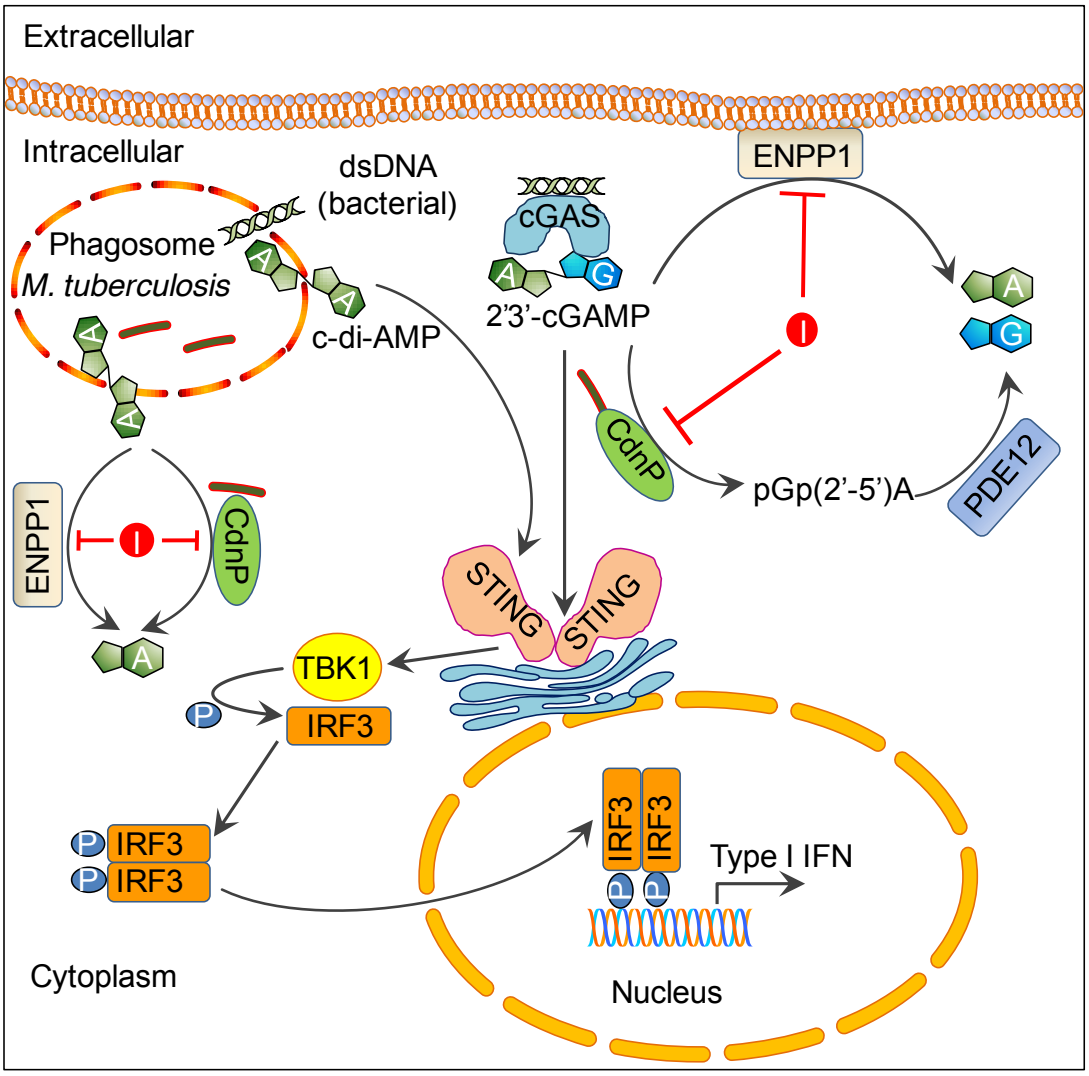

Figure 3.21. A schematic model for regulation of CDN signaling and inhibition of cGAS-mediated innate surveillance by *M. tuberculosis* CdnP. Cyclic-di-nucleotides (CDNs) such as c-di-AMP, secreted by either phagosomal or cytoplasmic *M. tuberculosis* are detected by host cytoplasmic receptors such as STING. Activated STING activates kinase TBK1 leading to phosphorylation and dimerization of IRF3 which translocates into the nucleus and stimulates transcription of Type-I IFN response genes. Access of bacterial DNA to the cytosolic compartment is sensed by the dsDNA receptor, cGAS, which synthesizes 2'3'-cGAMP. Host-produced 2'3'-

cGAMP binds to STING and stimulates a signaling cascade similar to that induced by bacterial CDNs. *M. tuberculosis*-derived CdnP hydrolyzes both bacterial-derived c-di-AMP and host-derived 2'3'-cGAMP during infection. CdnP hydrolysis of 2'3'-cGAMP yields the linearized, non-immunostimulatory molecule pGp(2'-5')A which is further degraded into AMP and GMP by the action of the host 2'-5' linear nuclease, PDE12. Alternatively, the host PDE, ENPP1, degrades host 2'3'-cGAMP into AMP and GMP and also may act on bacterial c-di-AMP cleaving it into two AMP molecules. Linear dinucleotide mimetics designed in this study interferes with the CDN PDE activity of bacterial CdnP and host ENPP1.

Our observation that CdnP may work in concert with the host-derived nuclease PDE12 to hydrolyze 2'3'-cGAMP into non-immunogenic mononucleotides suggests that *M. tuberculosis* co-opts a host enzyme to fully inhibit host 2'3'-cGAMP signaling. Importantly, previous studies have shown up-regulation of both host PDE12[182] and bacterial *cdnP* (*Rv2837c*) [168, 183] in human TB granulomas suggesting that CdnP-mediated subversion of the CSP is a biologically relevant virulence mechanism of *M. tuberculosis*. Further direct evidence for the biological significance of *M. tuberculosis* CdnP comes from our observation that the magnitude of the Type I IFN response in infected cells was governed by the *cdnP* genotype of the infecting strain and was independent of the presence or absence of the host PDE, ENPP1 (Figure 3.11D).

Among the various control mechanisms employed by the host to regulate the cGAS-cGAMP-STING pathway[184, 185], direct degradation of 2'3'-cGAMP via host

ENPP1 represents a key pathway to prevent self-damage from prolonged immune activation in the face of infection or exposure to self-DNA[175]. We observed that host ENPP1 also has the ability to cleave bacterial CDNs in addition to its natural substrate, 2'3'-cGAMP, and that host cells lacking ENPP1 display enhanced clearance of *M. tuberculosis*. This indicates that in addition to the PDE activity of bacterial CdnP lowering cytosolic CDN levels and leading to enhanced virulence, the host enzyme ENPP1 also exerts biologically relevant downregulation of CSP activation during infection which is deleterious to host defense. Since a non-hydrolyzable dinucleotide mimetic Ap(S)A which inhibits CdnP was capable of potentiating the CSP response, it is possible that dual inhibition of both *M. tuberculosis* CdnP and host ENPP1 action would further enhance CSP signaling to achieve improved host anti-bacterial responses.

While our study clearly reveals CdnP-mediated hydrolysis of host-derived 2'3'-cGAMP, how this mycobacterial enzyme gains excess to 2'3'-cGAMP and other substrates remains uncertain. The observations that CdnP is localized in the mycobacterial membrane[186], CDNs traverse the eukaryotic lipid bilayer without transfection[155, 175] and 2'3'-cGAMP can enter adjacent cells via gap junctions [187], suggest that CdnP may gain access to host cyclic dinucleotides during phases of infection when *M. tuberculosis* resides either in the cytosol or a permeable phagosomal compartment.

This mechanism of immune evasion by *M. tuberculosis* as elucidated in our study shows important parallels to observations in viral infections, wherein viruses have been shown to counteract or block innate immunity by interfering with IFN-inducible

2’5’- oligoadenylate (2-5A) synthetases (OASs) and ribonuclease (RNase) L, which constitute important components of the host antiviral pathway.[188, 189] Recent studies have also demonstrated cGAS to be an important innate sensor of retroviral nucleic acid as well, such that infection with human immunodeficiency virus (HIV), simian immunodeficiency virus (SIV) or murine leukemia virus (MLV) activates cGAS to produce 2’3’-cGAMP, thus stimulating the cGAMP/STING/IFN axis.[156] Recently, while viruses have been shown to manipulate cGAS signaling at the level of production, whether they possess mechanisms to degrade 2’3’-cGAMP is yet to be determined.[189, 190]

In summary our study provides evidence for bacterial interference and subversion of eukaryotic CDN signaling and concomitant antimicrobial defenses. The *M. tuberculosis*-derived phosphodiesterase CdnP promotes virulence via direct degradation of intracellular c-di-AMP (a bacterial PAMP) and 2’3’-cGAMP and thus inhibition of the STING/IRF/IFN signaling pathway. These data underscore the important role of CDN homeostasis in governing the outcome of *M. tuberculosis* infection. Moreover, the ability of small molecule CdnP inhibitors to increase intracellular CDN levels and potentiate CSP activation suggests that inhibition of this class of phosphodiesterases may offer an attractive pharmacologic, anti-virulence strategy against TB and other related intracellular infections.

3.4. Experimental

3.4.1 Synthesis of ^{32}P -c-di-AMP

^{32}P-c-di-AMP synthesis: 333 nM ^{32}P-ATP and 5 μM DisA (*Bacillus subtilis*) were mixed in reaction buffer (40 mM Tris-HCl, pH 8.0, 100 mM NaCl and 10 mM $MgCl_2$). After overnight incubation, reaction were stopped by heating up to 95°C for 5 min.

3.4.2. CdnP Cleavage of c-di-AMP

24 nM ^{32}P-c-di-AMP, 2 μM CdnP and various concentrations of c-di-AMP were mixed in reaction buffer (50 mM Tris-HCl, pH 9.0 and 1mM Mn^{2+}). At different time points, reaction mixture was spotted on a TLC plate (EMD Millipore TLC Cellulose). The mobile phase used for the TLC was saturated $(NH_4)_2SO_4$: 1.5 M KH_2PO_4 = 1:1.5.

3.4.3. CdnP Cleavage of c-di-AMP at Different pHs

24 nM ^{32}P-c-di-AMP and 2 μM CdnP were used in 50 mM Tris-HCl buffers with different pHs (pH 6.0, 6.5, 7.0, 7.5, 8.0, 8.5 and 9.0) containing 1 mM Mn^{2+}. At different time points, reaction mixture was spotted on a TLC plate (EMD Millipore TLC Cellulose). The mobile phase used for the TLC was saturated $(NH_4)_2SO_4$: 1.5 M KH_2PO_4 = 1:1.5.

3.4.4. CdnP Cleavage of c-di-AMP in the presence of different cations

24 nM ^{32}P-c-di-AMP and 2 μM CdnP were used in 50 mM Tris-HCl, pH 9.0. Different cations (Li^+, Mg^{2+}, Mn^{2+} and Ca^{2+}) were added at a concentration of 5 mM to the reaction mixture to test the effect of these cations on enzymatic activity.

3.4.5. Cleavage of c-di-AMP with inhibitors

^{32}P-c-di-AMP was generated from ^{32}P-ATP by DisA. 24 nM ^{32}P-c-di-AMP, 2.5 μM c-di-AMP, 2 μM CdnP and 250 μM inhibitors were mixed and incubated at 37°C. The reaction progress was analyzed using polyethyleneimine cellulose TLC plate (EMD). Mobile phase used for the TLC was a mixture of 4 mL saturated $(NH_4)_2SO_4$ and 6 mL 1.5 M KH_2PO_4.

The following equations were used to calculate percent of c-di-AMP and percent inhibition:

$$\text{Percentage of c-di-AMP} = \frac{I_{\text{c-di-AMP}}}{I_{\text{c-di-AMP}} + I_{\text{pApA}} + I_{\text{AMP}}} \times 100\%$$

$$\text{Percentage cleaved c-di-AMP} = \frac{\text{Percentage of c-di-AMP}_{t=0} - \text{Percentage of c-di-AMP}_{t}}{\text{Percentage of c-di-AMP}_{t=0}} \times 100\%$$

$$\text{Percentage inhibition} = \frac{\text{Percentage cleaved c-di-AMP}_{\text{no inhibitor}} - \text{Percentage cleaved c-di-AMP}_{\text{inhibitor}}}{\text{Percentage cleaved c-di-AMP}_{\text{no inhibitor}}} \times 100\%$$

Where I = intensity of radioactive spot on the TLC plate.

3.4.6. CdnP cleavage of c-di-AMP and c-di-GMP analyzed by HPLC

2 μM CdnP and 100 μM c-di-AMP or c-di-GMP were incubated overnight in 50 mM Tris-HCl, pH 7.5 and 1mM Mn^{2+}. Separation was performed on Varian ProStar HPLC using Purospher® STAR RP-18 (5 μm) LiChroCART® 250-10 column. The mobile phases are buffer A: 0.1 M TEAA in water and buffer B: acetonitrile. Samples were eluted with 95%→80 % A at 0-16 min and 80%→10 % A at 16-18.5 min and kept 10% A at 18.5-22 min. Signals were detected at room temperature with a 254 nm UV detector.

3.4.7. Cleavage of 2'3'-cGAMP

10 μM CdnP or 10 μM RocR (*Pseudomonas aeruginosa*) or 10 μM YybT (*Bacillus subtilis*) or 10 μM GdpP (*Staphylococcus aureus*) or 1.7 μM hPDE12 (Origene) or 2.8 μM hREXO2 (Origene) were incubated over-night with 100 μM 2'3'-cGAMP (Invivogen) in reaction buffers. RocR reaction buffer is 10 mM Tris-HCl, pH 8.0, 100 mM NaCl and 5 mM $MgCl_2$. YybT buffer is 100 mM Tris-HCl, pH 8.3, 10 mM KCl and 500 μM $MnCl_2$. GdpP buffer is 50 mM Tris-HCl pH 8.5, 10 mM KCl and 100 μM $MnCl_2$. hPDE12 buffer is 100 mM Tris-HCl, pH7.5 and 10 mM $MgCl_2$. hREXO2 buffer is 50 mM HEPES-KOH, pH 7.4, 50mM KCl, 2% glycerol, 0.01% Triton X-100 and 10 mM $MnCl_2$. Separation was performed on Varian ProStar HPLC using Cosmosil C18-MS-II column. The mobile phases are buffer A: 0.1 M TEAA in water and buffer B: acetonitrile. Samples were eluted with 99%→87 % A at 0-16 min and 87%→10 % A at 16-25.5 min, kept 10% A at 18.5-22 min and washed back to 1% A at 25.5-36 min. Signals were detected by a 254 nm UV detector.

3.4.8. Cleavage of pGp(2'-5')A

1.7 μM PDE12 was incubated overnight with 100 μM pGp(2'-5')A in 100 mM Tris-HCl, pH7.5 and 10 mM $MgCl_2$. Separation was performed on Varian ProStar HPLC using Cosmosil C18-MS-II column. The mobile phases are buffer A: 0.1 M TEAA in water and buffer B: acetonitrile. Samples were eluted with 99%→87 % A at 0-16 min and 87%→10 % A at 16-25.5 min, kept 10% A at 18.5-22 min and washed back to 1% A at 25.5-36 min. Signals were detected by a 254 nm UV detector.

3.4.9. Cleavage of c-di-AMP by ENPP1

24 nM ^{32}P-c-di-AMP and 2.5 μM cold c-di-AMP was cleaved by 2 μM ENPP1. Aliquots of the reactions were taken at various time points and analyzed by TLC. ENPP1 reaction was carried out in a buffer containing 20 mM Tris-HCl, pH 9.0, 2 mM $CaCl_2$, 0.2 mM $ZnCl_2$ and 0.01% Triton X-100.

3.4.10. Kinetics of c-di-AMP Cleavage by CdnP with or without Inhibitor

40 nM CdnP was incubated with 24 nM ^{32}P-c-di-AMP plus different concentrations of cold c-di-AMP. For the inhibition studies, 50 μM Ap(S)A was added. The reaction progress was analyzed by TLC. Initial reactions velocities were calculated and fit with Michaelis–Menten kinetics equation.

3.4.11. Kinetics of 2'3'-cGAMP Cleavage by CdnP

10 μM CdnP was incubated with different concentrations of 2'3'-cGAMP. At various time points, aliquots of the reactions were stopped by heating up to 95 °C for 5 min and enzymes were removed by filteration. After HPLC analysis, initial reactions velocities were calculated and fit with Michaelis–Menten kinetics equation.

3.4.12. Other experiments

The details of plasmids, *M. tuberculosis* strains, cell lines and animals used in this study is included in the laboratory notebook of Ruchi Jain Dey and Bappaditya Dey in the Center for Tuberculosis Research at Johns Hopkins University, as well as CdnP expression and purification, macrophage and mice infection with *M. tuberculosis*. Extraction of nucleotides from *M. tuberculosis* and macrophage cytoplasm is discribed in the laboratory notebook of Laurene S. Cheung in the Center for

Tuberculosis Research at Johns Hopkins University. The details of ITC experiment is included in the laboratory notebook of Pankaj Kumar in the Center for Tuberculosis Research at Johns Hopkins University. Chemical synthesis of nucleotides is discribed in the laboratory notebook of Jie Zhou and David A. Sayre in the Department of Chemistry and Biochemistry at University of Maryland, College Park.

Chapter 4: Inhibition of *P. aeruginosa* Swarming Motility with a Benzoisothiazolinone Derivative, an Inhibitor of c-di-GMP Phosphodiesterase RocR

This work has been submitted for publication.

4.1. Introduction

Cyclic dinucleotides are now acknowledged as important second messengers in bacteria.[1] These second messengers also elicit innate immune response in mammalian cells.[5] The first cyclic dinucleotide bis-(3'-5')-cyclic dimeric GMP (c-di-GMP) was discovered in *G. xylinum* by Benziman in 1987.[10] At that time c-di-GMP was recognized as a regulator of cellulose synthesis. Following Benziman's seminal discovery, the field of cyclic dinucleotides went into a hiatus, only to be resurrected in the last decade, where the key roles played by c-di-GMP in signal transduction systems have been uncovered.[11, 14, 125, 191] In the majority of bacteria studied so far, the intracellular concentrations of c-di-GMP determine whether a bacterium chooses the mobile planktonic or the sedentary biofilm lifestyles (Figure 1.2). At high intracellular concentrations, c-di-GMP promotes the production of exopolysaccharides and other adhesion factors to facilitate biofilm formation.[192] On the other hand, c-di-GMP retards the expression of flagella and impedes bacterial swimming and swarming activities.[193] C-di-GMP also represses the expression of the acute virulence genes.[194] It is emerging however that there are nuances to c-di-GMP system in that gross intracellular concentration of the dinucleotide alone is not the

sole determinant of a phenotype but rather the micro-concentrations of c-di-GMP and the relative localizations of c-di-GMP regulatory enzymes or adaptor proteins and/or binding RNAs dictate the phenotypic outcome.[40, 195, 196] The intracellular concentration of c-di-GMP is controlled by its metabolic enzymes: diguanylate cyclase (DGC) and phosphodiesterase (PDE). DGCs dimerize two GTP into pppGpG, which is subsequently cyclized into c-di-GMP.[18] PDEs hydrolyze c-di-GMP to ether linear pGpG or two molecules of GMP, depending on the key residues in their active sites.[197, 198] The major product of EAL domain phosphodiesterase is pGpG and these enzymes only slowly hydrolyze pGpG to GMP.[199] HD-GYP domain phosphodiesterase hydrolyzes c-di-GMP directly to GMP efficiently.[30] Some c-di-GMP metabolism enzymes (both DGC and PDE) also contain sensory domains that sense various signals, such as oxygen[200, 201], light[202, 203], NO[204, 205] etc, to modulate enzymatic activity. Given that c-di-GMP binds to a plethora of downstream protein receptors[35] and RNA riboswitches[15] and regulates important bacterial behaviours, the roles of its metabolic enzymes are clearly worthy of attention.

Perplexingly, for most bacteria more than one c-di-GMP metabolism enzyme (DGC and PDE) exist and it is unclear if these metabolism enzymes exist for synergistic and/or redundancy purposes. An important study by Römling showed mutation of the major DGC AdrA in *Salmonella* dramatically reduced total c-di-GMP concentration, but the downstream CsgD expression was not affected, because two other DGCs STM2123 and STM3388 could keep c-di-GMP level in a localized pool.[206] The nuanced roles played by different c-di-GMP metabolism enzymes is illustrated in *P. aeruginosa*, which harbors 33 GGDEF domain proteins, 21 EAL

domain proteins and 3 HD-GYP domain proteins (see Table S1 for the roles of some PDEs in *P. aeruginosa*).[29] This begs the question why 33 different c-di-GMP synthases and 24 phosphodiesterases are needed for making or hydrolyzing one metabolite.[29] A seminal study by Hengge and co-workers provided some insights into why some c-di-GMP metabolism enzymes do not change the intracellular concentrations of c-di-GMP, yet affect bacterial phenotype (a case of global versus localized signaling). In this study, the authors showed that in *Salmonella* CsgD expression is not only regulated by total c-di-GMP concentration, but also the local DGC-PDE interactions; EAL domain YciR could act as trigger enzyme that inhibits csgD expression via direct contact with YdaM (a DGC) and MlrA (a transcription factor).[196] Thus it is now clear that the cellular functions of c-di-GMP PDE are not only achieved by decreasing global c-di-GMP concentration. The ability to specifically inhibit each of these PDE enzymes in a specific bacteria, without affecting others of similar function, will help identify the cellular processes that are directly or indirectly regulated by these enzymes. Thus far, there have not been many reports of cell permeable inhibitors of c-di-GMP PDEs and the lack of such probes obviously impedes efforts to delineate the intricacies of c-di-GMP signalling.

In our efforts to illuminate cyclic dinucleotide signalling with chemical probes, we have identified a *P. aeruginosa* RocR inhibitor and herein demonstrate that this inhibitor of RocR can affect swarming (but not swimming). Also, we disclose an interesting finding that the RocR inhibitor promotes the production of pyoverdine and pyocyanin, virulence factors. Gene expression analysis by Hancock *et al.* revealed that virulence factors and antibiotic resistance genes are expressed more in swarming

cells than in swimming cells.[207] So the identification of a small molecule that can inhibit swarming yet facilitate the production of virulence factors is intriguing. Our data provides a cautionary tale for medicinal chemists who desire to develop anti-virulence strategies to be aware that the inhibition of one virulence factor could inadvertently promote the expression of other virulent factors in a manner that is complex and not easily predicted *a priori*.

4.2. Result and Discussion

4.2.1. Identification of a RocR inhibitor

We utilized high throughput docking to identify potential inhibitors of cyclic dinucleotide metabolic enzymes. Our ultimate goal was to find inhibitors against RocR, a *P. aeruginosa* PDE that has been shown to be important for virulence but the crystal structure of RocR reported to date did not have a bound ligand[26] so this presented a challenge. On the other hand the crystal structure YahA (also named PdeL), an EAL domain phosphodiesterase from *E. coli,*[199] in complex with its substrate, c-di-GMP, has been solved (PDB: 4LJ3)[28] so we decided to use this PDE for our docking experiment. Using the structures of 250,000 commercially available compounds, we performed the docking experiment against YahA and identified a handful of putative PDE binders. We then tested the ligands, which were identified as binders of PDE *in silico*, for inhibition of c-di-GMP cleavage by RocR[208] and YahA. Only one compound (a benzisothiazolone derivative, compound **4.1**, see Figure 4.1) could inhibit the cleavage of c-di-GMP by RocR (Figure 4.1). Paradoxically this

compound did not inhibit the cleavage of c-di-GMP by YahA from *E. coli* (Figure 4.2), although YahA was the protein that was used for the docking experiment. Nonetheless we were still excited about the ability of the "hit" compound to inhibit RocR since *P. aeruginosa* is an important human pathogen, which causes respiratory tract, urinary tract, wound and burns infections.[209] *P. aeruginosa* also colonizes medical devices and causes hospital-acquired infections. Cystic fibrosis (CF) patients are especially susceptible to this opportunistic pathogen. Thus small molecules that perturb any signaling system in *P. aeruginosa* could be useful for illuminating *P. aeruginosa* biology and in some cases could even have therapeutic value. C-di-GMP regulates some phenotypes of *P. aeruginosa* and RocR has been shown to be a major c-di-GMP PDE in this pathogen.[208] Mutation of the *rocR* gene abolished the virulence of *P. aeruginosa* in mouse infection model.[194]

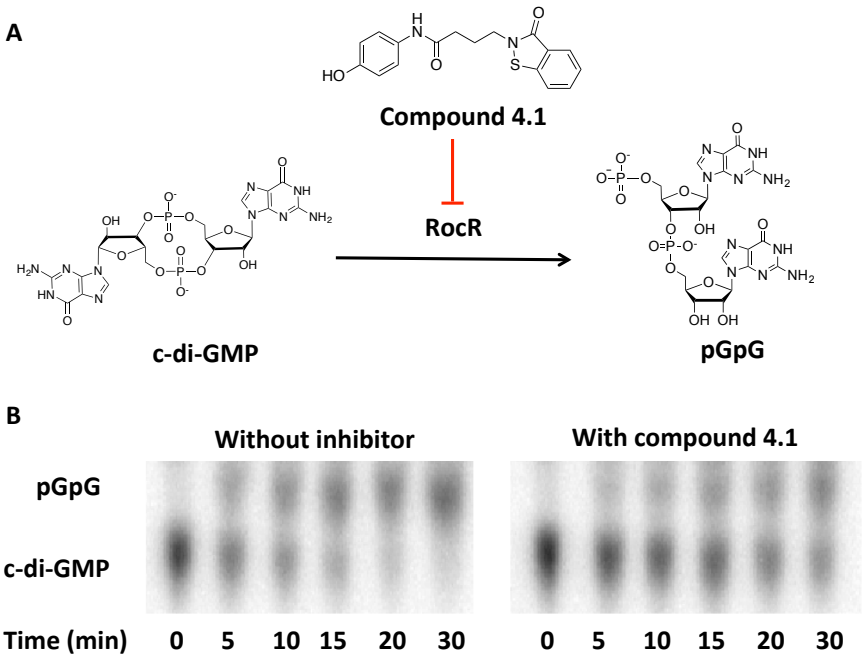

Figure 4.1. (A) The structure of compound **4.1**. Compound **4.1** inhibits the cleavage of ^{32}P-c-di-GMP to ^{32}P-pGpG by RocR. (B) The image of TLC plates of RocR cleavage with or without compound **4.1**. 50 μM c-di-GMP and 16 nM ^{32}P--c-di-GMP were cleaved by 0.6 μM RocR in the presence or absence of 100 μM compound **4.1** at 37 °C for 30 min. Compound **4.1** significantly slowed down RocR cleavage.

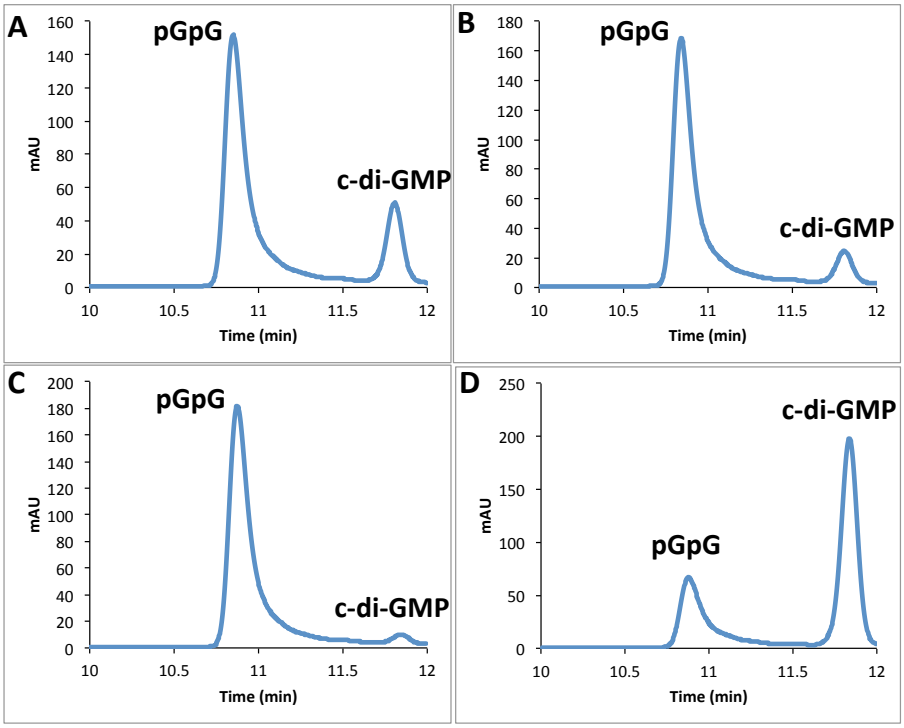

Figure 4.2. Compound **4.1** affects YahA and RocR cleavage analysed by HPLC. (A) 0.7 μM YahA cleaves 50 μM c-di-GMP in the absence of compound **4.1**. (B) 0.7 μM YahA cleaves 50 μM c-di-GMP with 100 μM compound **4.1**. (C) 0.6 μM RocR cleaves 50 μM c-di-GMP in the absence of compound **4.1**. (D) 0.6 μM RocR cleaves

50 μM c-di-GMP with 100 μM compound **4.1**. The reactions were conducted at 37 °C for 30 min.

To ascertain if the benzoisothiazolone core was important for the inhibition of RocR, we synthesized two structurally similar compounds **4.2** and **4.3** (Figure 4.3) and tested them for RocR inhibition. Compound **4.2** was not as potent as compound **4.1**, whereas **4.3** was not active (see Figure 4.4), confirming the essentiality of the benzoisothiazolone moiety for RocR inhibition. The benzoisothiazolone unit is found in several biologically active molecules,[210-216] including orally active drug leads against metabotropic glutamate subtype 2 receptor[33] and phosphomannose isomerase[34]; the PDE RocR adds to the growing list of enzymes that this pharmacophore inhibits.

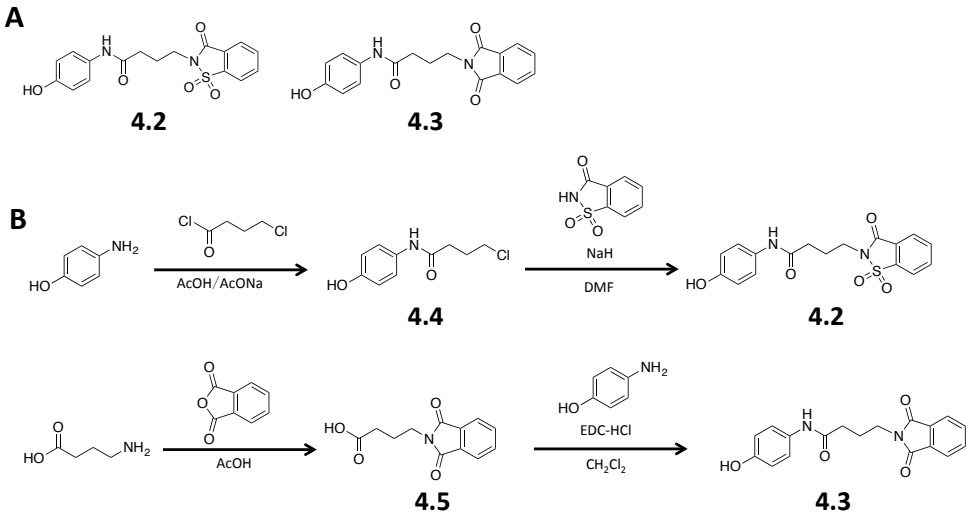

Figure 4.3. (A) The structures of compound **4.2** and **4.3**. (B) Synthesis scheme of compound **4.2** and **4.3**. Details of synthesis see the laboratory notebook of Genichiro

Tsuji in the Department of Chemistry and Biochemistry at University of Maryland, College Park.

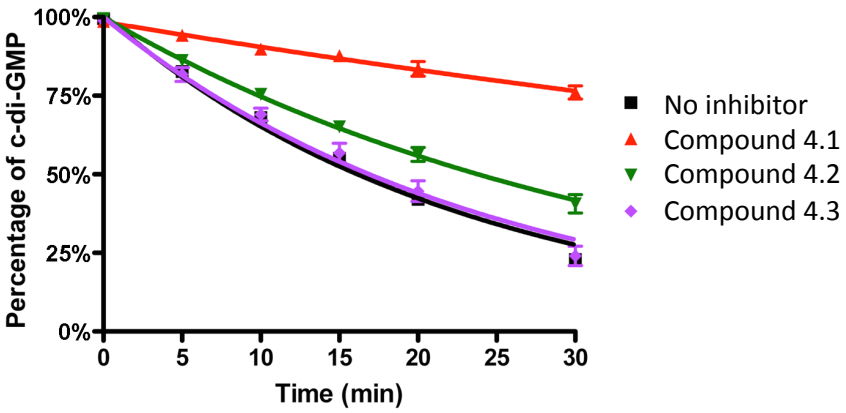

Figure 4.4. Inhibition of RocR reaction by compound **4.1**, **4.2** and **4.3**. 50 μM c-di-GMP and 16 nM ^{32}P-c-di-GMP were cleaved by 0.4 μM RocR in the presence or absence of 100 μM small molecules at 37 °C for 30 min. Compared with compound **4.1**, compound **4.2** has a much weaker inhibition and compound **4.3** completely lost RocR inhibition activity.

4.2.2. Thermodynamic and kinetic parameters

We performed kinetic and thermodynamic experiments to determine binding and inhibition parameters of compound **4.1**. A Lineweaver-Burk plot of the inverse of initial reaction speed against the inverse of c-di-GMP concentration at fixed concentration of compound **4.1** gave an inhibition constant (K_i) of 83 ± 7 μM (Figure 4.5A). According to the Lineweaver–Burk plot, compound **4.1** is a non-competitive inhibitor (Figure 4.5B). An apparent dissociation constant, $K_d^{apparent}$, of 15 μM (average from two different analytic methods, see Figure 4.6) was obtained by

measuring the change of RocR intrinsic fluorescence in the presence of different concentrations of compound **4.1**.

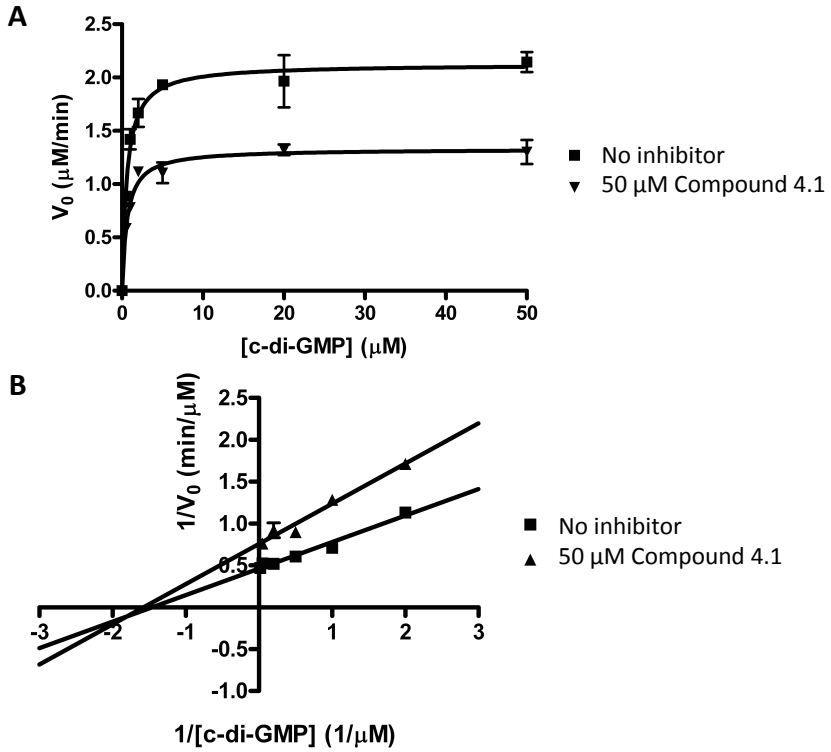

Figure 4.5. Kinetics of inhibition of RocR by compound **4.1**. (A) Michaelis–Menten kinetics. (B) Lineweaver–Burk plot showed that compound **4.1** is a non-competitive inhibitor.

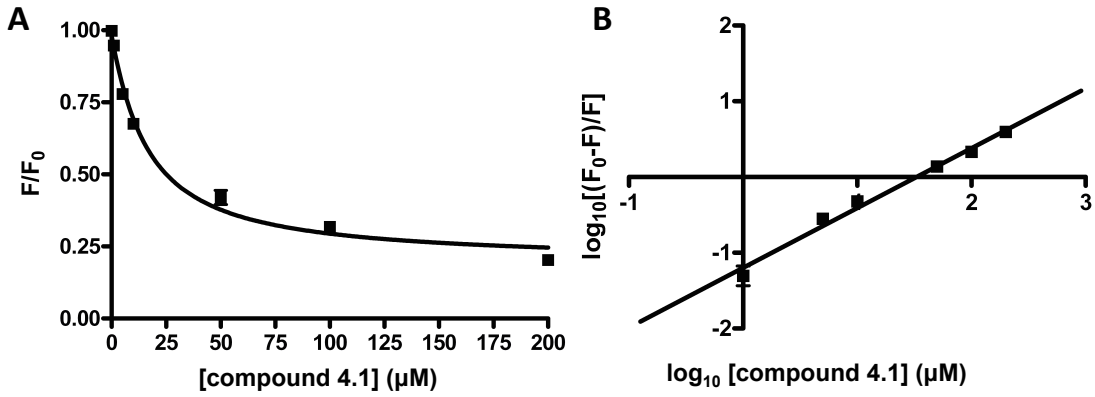

Figure 4.6. Binding of compound **4.1** to RocR. (A) Normalized RocR intrinsic fluorescence change with different concentrations of compound **4.1**, indicating a dissociation constant K_d of 14 ± 2 μM (Equation (4.1)[35]. (B) Stern–Volmer plot of the RocR intrinsic fluorescence. K_d was calculated as 16 ± 2 μM using Equation (4.2)[36], see methods section.

4.2.3. Intracellular concentrations of c-di-GMP and pGpG.

The intracellular concentration of c-di-GMP depends on the cooperation of multiple DGCs and PDEs. Mutation of some PDE genes lead to the global change of c-di-GMP concentration, such as DipA[197] and BifA[217]. (See Table 4.1). However, some PDEs do not change the overall c-di-GMP level, yet they affect bacterial phenotype (this phenomenon is thought to occur via micro-domain regulation). In PAO1, mutation of PDE gene Δ*nbdA* did not change intracellular c-di-GMP levels.[198] Interestingly, Δ*nbdA* strain abolished NO-induced biofilm dispersion compared with WT PAO1.[198] Mutation of another PDE gene *mucR* increased c-di-GMP level in the biofilm cells, but decreased c-di-GMP level the planktonic cells.[198] The effect of *rocR* on the global c-di-GMP level is unknown. Treatment of PAO1 with compound **4.1**

did not change the intracellular concentration of c-di-GMP and pGpG (see Figure 4.7). We proceeded to investigate if compound **4.1** could affect any PAO1 phenotype, *vide infra*.

Table 4.1. Information of selected PDEs from *P. aeruginosa*

Name	Intracellular c-di-GMP level	*In vitro* activity	Phenotype
NbdA[198]	Δ*nbdA* did not alter c-di-GMP levels but overexpression of *nbdA* reduced c-di-GMP level.	Yes	Biofilm dispersal
MucR[198]	Δ*mucR* increased c-di-GMP level in the biofilm cells, but decreased c-di-GMP level the planktonic cells	Yes	Biofilm dispersal
BifA[217]	Δ*bifA* increased c-di-GMP level	Yes	Δ*bifA* reduced swarming motility and increased biofilm formation
RocR[27]	N/A	Yes	*rocR* mutant reduced virulence
DipA[197]	Δ*dipA* increased c-di-GMP level	Yes	Biofilm dispersal, Δ*dipA* reduced swarming motility
PvrR[218, 219]	*pvrR* overexpression reduced c-di-GMP level	Yes	*pvrR* overexpression reduced biofilm formation, *pvrR* mutant reduced virulence
PA4108[220]	PA4108 mutant increased c-di-GMP level	Yes	PA4108 mutant reduced swarming motility and pyocyanin production
PA4781[220]	PA4781 mutant increased c-di-GMP level	Yes	PA4781 mutant reduced swarming motility and increased pyoverdin production

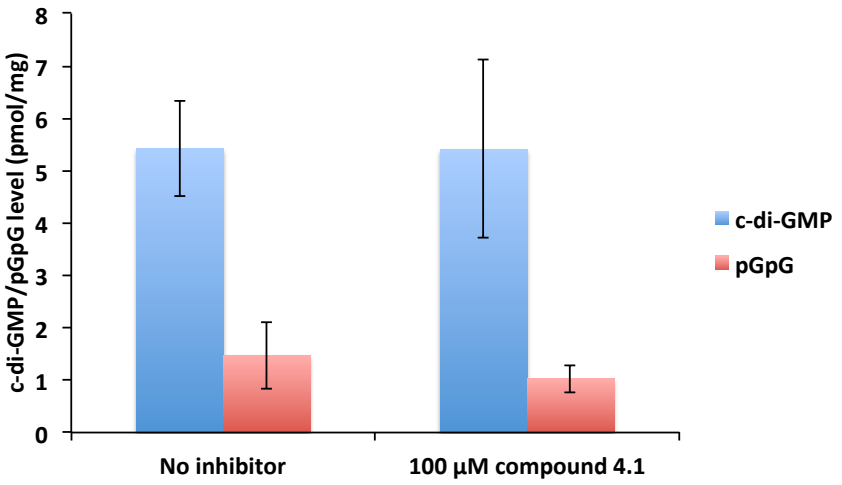

Figure 4.7. PAO1 intracellular concentrations of c-di-GMP and pGpG in the presence or absence of compound **4.1**. C-di-GMP and pGpG concentration was quantified by LC-MS/MS. The details of extraction and quantification see Methods.

4.2.4. Effects of compound **4.1** on bacterial behaviors

There are about 21 EAL domain PDE in *P. aeruginosa* and 3 HD-GYP domain PDE.[29] Many of these PDEs remain uncharacterized. RocR (PA3947) is one of the most well-studied and most active phosphodiesterases found in *P. aeruginosa*.[208] RocR is essential for *P. aeruginosa* acute infection; infection with *rocR* mutant *P. aeruginosa* did not have fatal effects on mice.[194] In another catheter-associated urinary tract infection (CAUTI) model, *P. aeruginosa* strain that overexpressed RocR was observed to have less CFU in the bladders and kidneys of infected mice than wild type strain.[221] Because in *P. aeruginosa* c-di-GMP phosphodiesterase mutants were viable (but avirulent) it is likely that PDE inhibitors will not be used for growth inhibition per se but rather could be used to attenuate bacterial virulence. Indeed, even at high concentrations (100 µM) compound **4.1** did not kill *P. aeruginosa*

(Figure 4.8).

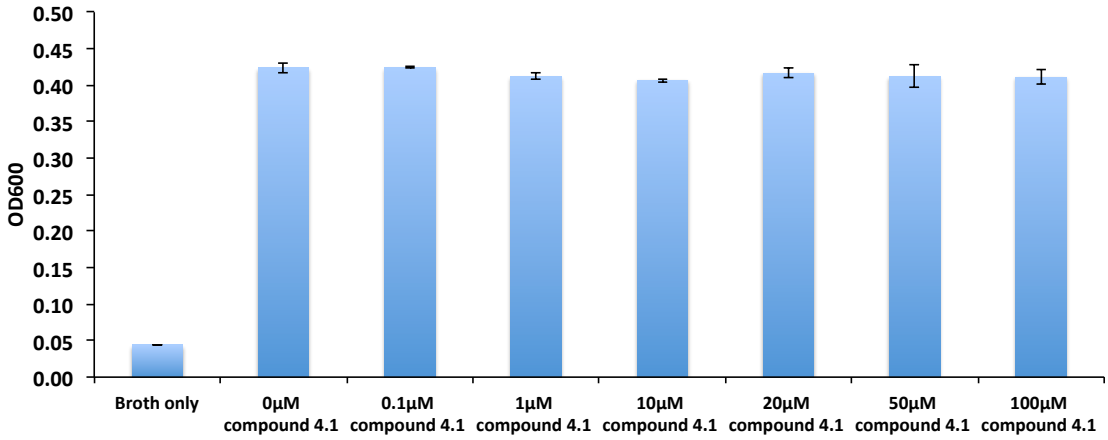

Figure 4.8. Viability tests of compound **4.1** on PAO1. PAO1 was treated with different concentrations of compound **4.1**. Compound 4.1 did not kill PAO1 cells.

4.2.5. Motility

The ability to move on surfaces (swarming) or in a viscous mucous (swimming) is critical for the invasive virulence of *P. aeruginosa*. Bacterial motility apparatus, such as flagella, are considered as virulence factors; in a mice burn wound model, non-motile *P. aeruginosa* were able to proliferate in the burn wound but were unable to cause bacteraemia or systemic invasion, and therefore the infection was localized to the skin wound.[222] Small molecules that inhibit bacterial motilities are of interest due to the potential to use such molecules in reduce bacterial virulence.[223, 224] Chan and co-workers found that caffeine inhibited PAO1 swarming at 0.3 mg/mL, probably via inhibition of quorum sensing.[225] Fukui and co-workers showed that anteiso-C15:0, which is a branched-chain fatty acid completely abolished PAO1 swarming at 5 μg/mL.[226]

P. aeruginosa swimming and swarming motilities are powered by a single polar flagellum[227], although others have proposed that swarmer cells might have two flagella.[228, 229] C-di-GMP mediates flagella biosynthetic gene repression via binding to a key transcription factor, FleQ.[67] *P. aeruginosa* encodes two stator complexes, MotAB (PA4954/4953) and MotCD (PA1460/1461).[68] These stators are cytoplasmic membrane channels that generate flagella rotation torque by proton conduction[69]. The numbers of MotAB and MotCD in a motor is dynamic and both MotAB and MotCD stators can provide energy for swimming motility. Disabling one stator did not completely abolish swimming.[68] However MotAB and MotCD have opposite functions in swarmer cells.[69] MotCD generates torque for swarming, but MotAB impedes it. Via an unknown mechanism, c-di-GMP downregulates the proportion of MotCD in a motor and slows down swarming.[70] From the foregoing, an inhibitor of PDE should inhibit swarming. At high concentration (100 μM), compound **4.1**, a PDE inhibitor, swarming was completely inhibited but global c-di-GMP was not affected; a perplexing finding. The swarming inhibition was dose dependent (see Figure 4.9), confirming that it is due to the direct action of compound **4.1**. Interestingly compound **4.1** did not impede bacterial swimming motility (Figure 4.10), in line with our observation that compound **4.1** did not change global c-di-GMP concentration. These opposite observations validate earlier findings by others, who have shown that although swimming and swarming utilize some common apparatus, there are some differences between these two.[207] Swarming is a group behavior, whereas swimming is not.[230] As the population of *P. aeruginosa* increases, so does the concentration of quorum sensing autoinducers, which promote the production of the surfactant

rhamnolipid[228] to aid swarming.[48] Rhamnolipid is also a potent virulence factor, which is associated with ventilator-associated pneumonia[231], resistance to macrophage phagocytosis[232], respiratory epithelium invasion[233], host cell membrane disruption[233], etc. Therefore, we tested the rhamnolipid production of PAO1 in the presence or absence of compound **4.1** (Figure 4.11). 100 μM compound **4.1** reduced the production of rhamnolipid, which is critical for PAO1 swarming motility.

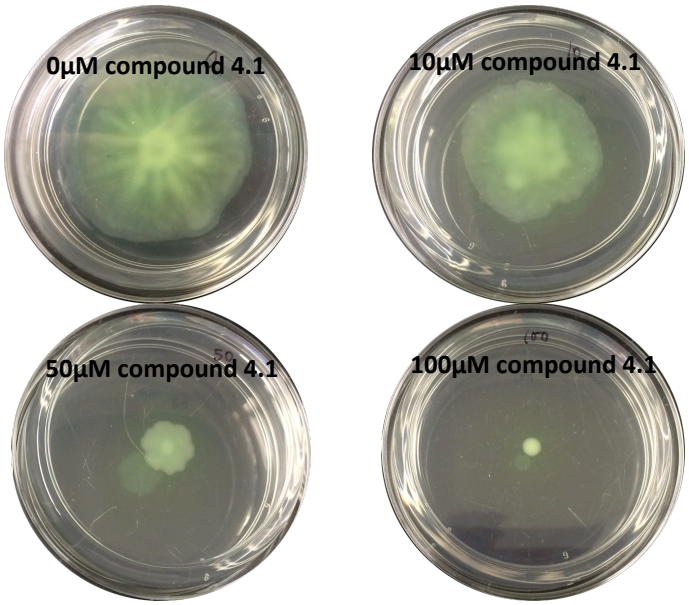

Figure 4.9. Swarming assay. Different concentrations of compound **4.1** (concentration indicated in the graph) were added to the swarming agar. 1 μl of PAO1 overnight culture was inoculated in the middle of the agar surface. Pictures were taken after 48 h incubation. The swarming mobility of PAO1 was restricted by 50 μM and 100 μM compound **4.1**.

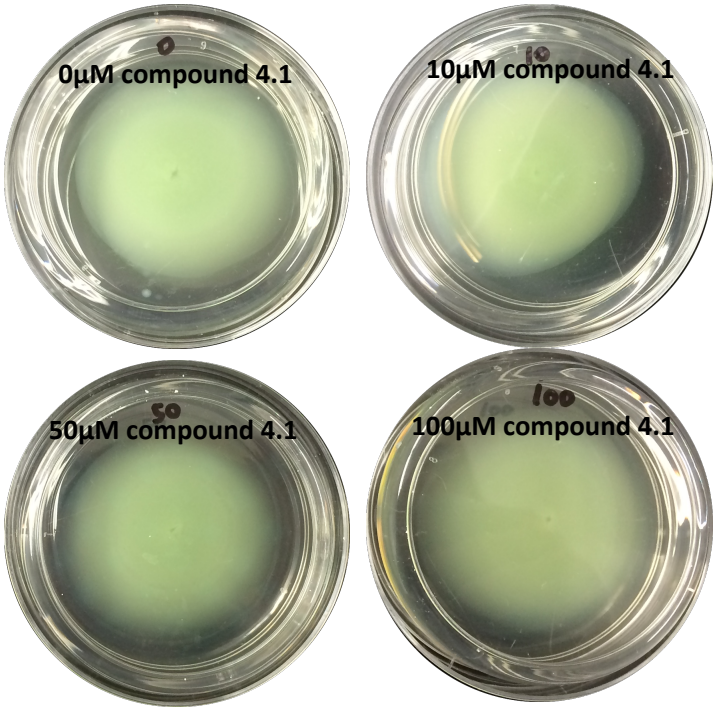

Figure 4.10. Swimming assay. Different concentrations of compound **4.1** (concentration indicated in the graph) were added to the swimming agar. PAO1 overnight culture was inoculated into the agar by a needle. Pictures were taken after 24 h incubation. Compound **4.1** did not inhibit PAO1 swimming motility.

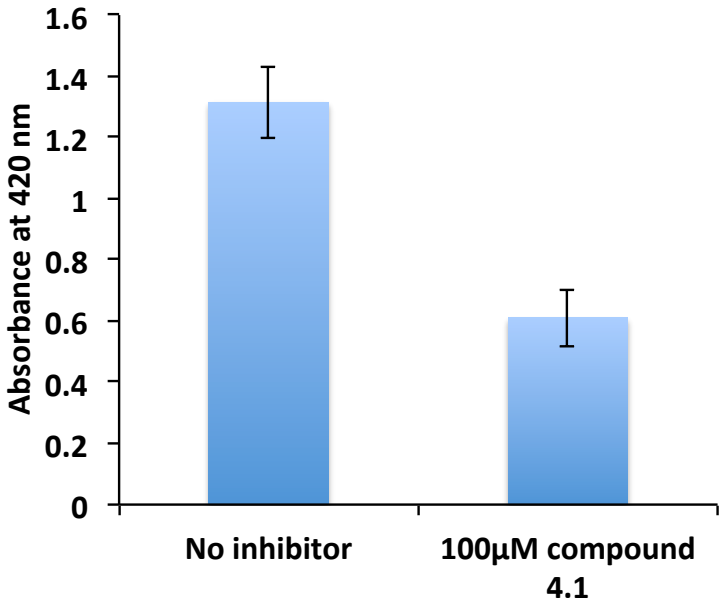

Figure 4.11. Rhamnolipid production. PAO1 was cultured with or without 100 µM compound **4.1**. Rhamnolipid was extracted with diethyl ether and evaporated to dryness. The extracted rhamnolipid was reacted with 0.19% (w/v) orcinol in 50% (v/v) concentrated H_2SO_4 at 80 °C for 30 min. The production of rhamnolipid was quantified by measuring absorbance at 421 nm.

4.2.6. Quorum sensing

Several studies have documented an overlap between c-di-GMP and quorum sensing signaling.[5, 234] In a seminal study, Woods and Ueda revealed that the transcription factor LasR when complexed with the quorum sensing signal, 3-oxo-C12-HSL, facilitated the transcription of the *tpbA* gene.[234] TpbA is a phosphatase, which dephosphorylates TpbB (a GGDEF-containing c-di-GMP synthase) to reduce intracellular concentration of c-di-GMP. The foregoing and other studies have shown a regulation of c-di-GMP synthesis or degradation by quorum sensing but the

opposite regulation whereby c-di-GMP modulates quorum sensing has not been extensively studied. We were therefore curious to know if the RocR inhibitor, compound **4.1**, could inhibit phenotypes (such as pyocyanin and pyoverdine, see Figure 4.12) that are regulated by quorum sensing.[235]

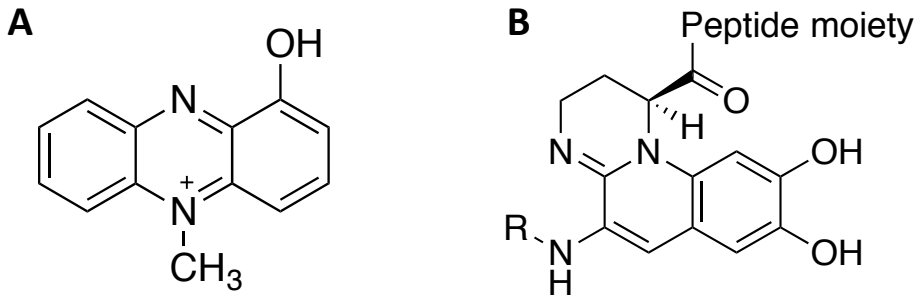

Figure 4.12. Structures of (A) pyocyanin and (B) pyoverdine.

Pyocyanin, a redox-active secondary metabolite, is a blue-green pigment.[236] It is produced by *P. aeruginosa* to kill competing bacteria cells, damage host cells and repress host immune system.[237, 238] One study showed that pyocyanin could slow down host nasal ciliary beat frequency and disrupt the epithelium.[239] Pyocyanin also inhibits cellular respiration, cell cycle, vacuolar ATPase and retards epidermal cell growth.[240] Pyoverdines (also named fluorescins, pseudobactins) are a group of siderophores produced by *P. aeruginosa* to sequester iron.[241] Pyoverdine structures are diverse but they all consist of a dihydroquinoline-type chromophore and a peptide. Pyoverdines are synthesized in the cytoplasm, mature in the periplasm and then secreted to outside environment to acquire iron.[242] Iron is important for *P. aeruginosa* growth and biofilm formation.[243] In addition to iron sequestration, pyoverdine has also been reported to up-regulate the production of other virulence factors, such as

exotoxin A and endoprotease.[244]

Compound **4.1** was added to King agar A[245], used to detect pyocyanin production, and PAO1 was grown on the agar. After 24 h incubation, the agar plate became bluer (see Figure 4.13), indicative of enhanced production of pyocyanin in the presence of compound **4.1**. A liquid culture also showed enhancement of pyocyanin production upon the addition of compound **4.1**, although at higher concentration the enhancement effect became negligible (see Figure 4.14).

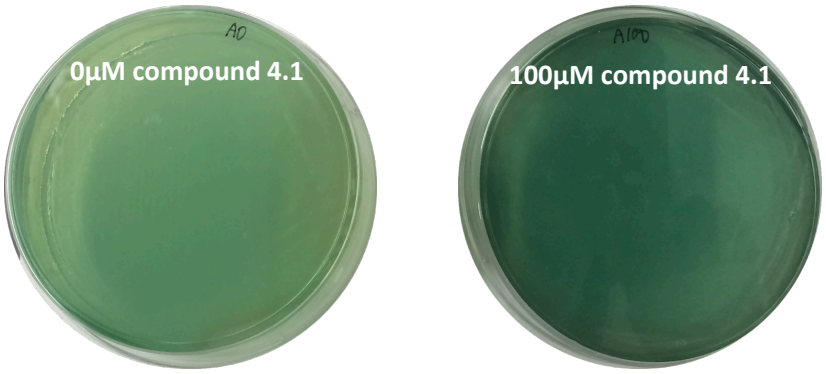

Figure 4.13. Pyocyanin assay. 0 or 100 μM compound **4.1** was added to King agar A. Diluted PAO1 culture was spread evenly on the agar surface. After 24 h incubation, 100 μM compound **4.1** significantly increased pyocyanin production.

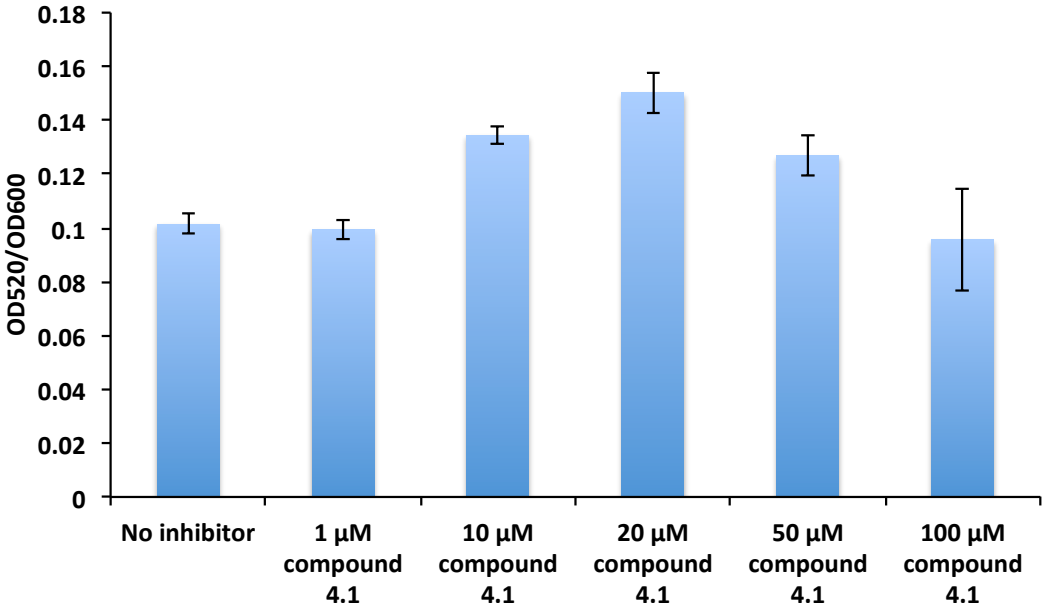

Figure 4.14. Pyocyanin test. PAO1 was treated with different concentrations of compound **4.1**. After 2 days, pyocyanin was extracted from culture supernatant by chloroform and quantified by OD_{520} and normalized to OD_{600}.

Similarly when *P. aeruginosa* was grown on King agar B[245], used to detect pyoverdine production, the plate became greener (see Figure 4.15), indicating that compound **4.1** also increases pyoverdine synthesis. Here too, a liquid culture also showed enhancement of pyoverdine production upon the addition of compound **4.1** (see Figure 4.16) Both pyocyanin and pyoverdine synthesis are regulated by quorum sensing autoinducers (see Figure 1.4) but other studies have indicated that there might be other non-QS modulation of these virulence factors. For example Liang and co-workers have demonstrated that pyocyanin synthesis could be modulated by AlgR in a non-QS mechanism.[246] It turns out that AlgR also modulates c-di-GMP synthesis and hence there is a link (albeit ill defined) between pyocyanin synthesis and c-di-

GMP regulation. Semmelhack and co-workers also revealed that small molecule inhibitors that attenuated pyocyanin synthesis acted via a non-QS mechanism.[247] This work hints at the possibility of c-di-GMP directly regulating the synthesis of pyocyanin and/or pyoverdine. Cautious must however be in order, since the link could be an indirect one considering the plethora of processes that c-di-GMP regulates. It is also possible that compound **4.1** acts on other receptors or processes, other than c-di-GMP signalling to affect swarming. Whether there are additional targets involved in the swarming regulation by compound **4.1**, the discovery of an inhibitor of RocR that affects swarming but not swimming is very interesting and provides an interesting probe that could be used to study swarming in *Pseudomonas aeruginosa*. Consistent with the lack of global modulation of c-di-GMP concentration by compound **4.1**, bacterial biofilm formation, a potential liability of c-di-GMP PDE inhibitors, was not enhanced (see Figure 4.17). Future studies, beyond the scope of this manuscript, will attempt to shed more light on this interesting finding.

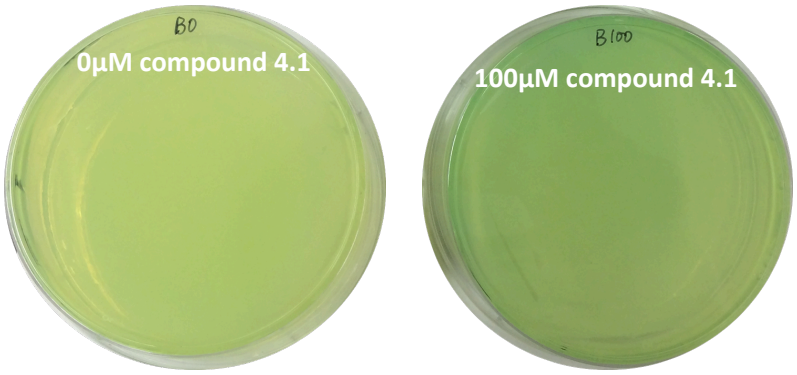

Figure 4.15. Pyoverdine test. 0 or 100 μM compound **4.1** was added to King agar B. Diluted PAO1 culture was spread evenly on the agar surface. After 24 h incubation, 100 μM compound **4.1** significantly increased pyoverdine production.

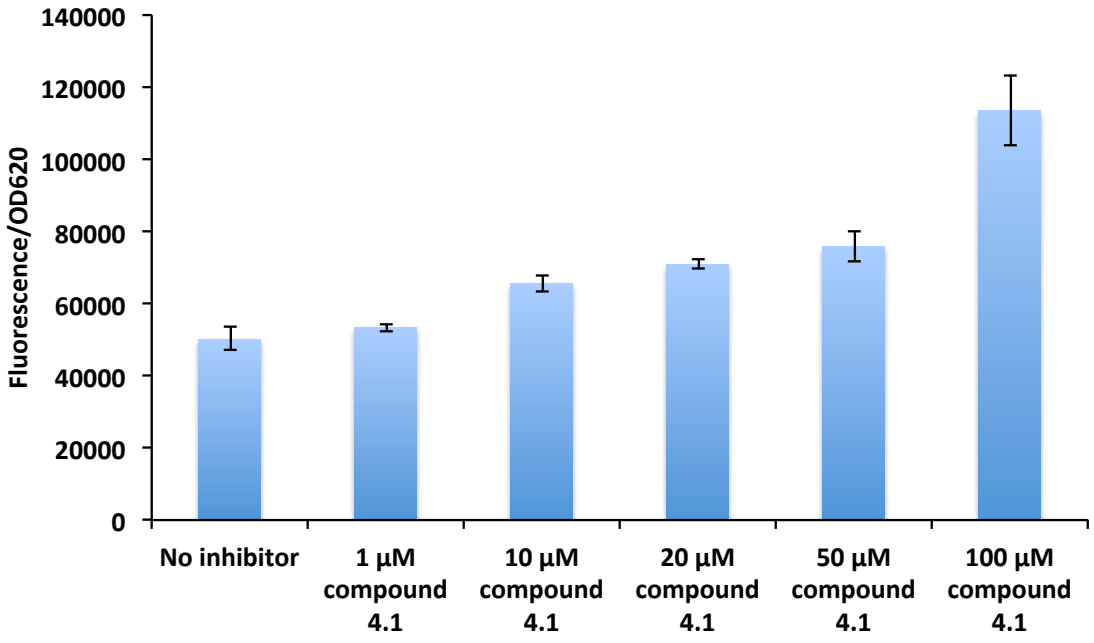

Figure 4.16. Compound 4.1 reduces rhamnolipid production. PAO1 was treated with DMSO or 100 μM compound **4.1**. Extraction and quantification of rhamnolipid followed the methods published by Blackwell.[248]

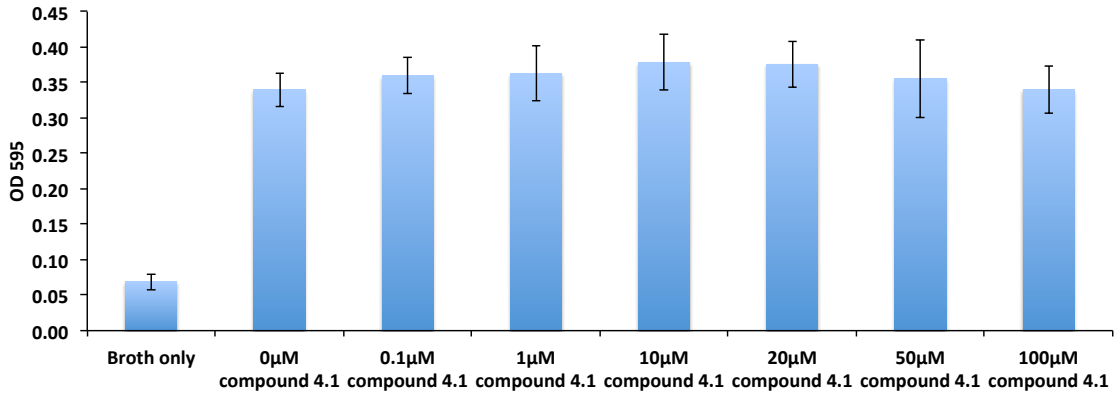

Figure 4.17. Biofilm tests of compound **4.1** on PAO1. PAO1 was treated with different concentrations of compound **4.1**, but biofilm formation was not inhibited by compound **4.1**.

4.3 Conclusions

C-di-GMP has emerged as an interesting second messenger in bacteria and there is a high interest in finding small molecules that perturb c-di-GMP signaling in bacteria. The majority of reports on small molecule inhibitors of c-di-GMP signaling have focused on the inhibition of c-di-GMP synthesis[76, 249, 250], probably due to the central role that c-di-GMP plays in most Gram-negative biofilm maturation[5] and resistance to stress.[251] However c-di-GMP and its degradation product, pGpG, probably have complex roles in bacterial virulence factor production and it is not clear yet whether the inhibition of c-di-GMP would have a therapeutic benefit. Chemical probes that inhibit cyclic dinucleotide related enzymes could play crucial roles in deciphering the complex c-di-GMP regulatory network. Compound **4.1** did not inhibit other cyclic dinucleotide metabolic enzymes such as WspR D70E (c-di-GMP synthase from *P. aeruginosa*), DisA (c-di-AMP synthase, from *B. subtilis*) and

GdpP (previously named YybT, c-di-AMP phosphodiesterase from *B. subtilis*), data not shown. Compound **4.1** also did not inhibit YahA (PDE from *E. coli*) or Snake venom phosphodiesterase (SVPD) or other c-di-GMP PDEs from *P. aeruginosa* (DipA, PvrR and PA4108) (See Figure 4.18).

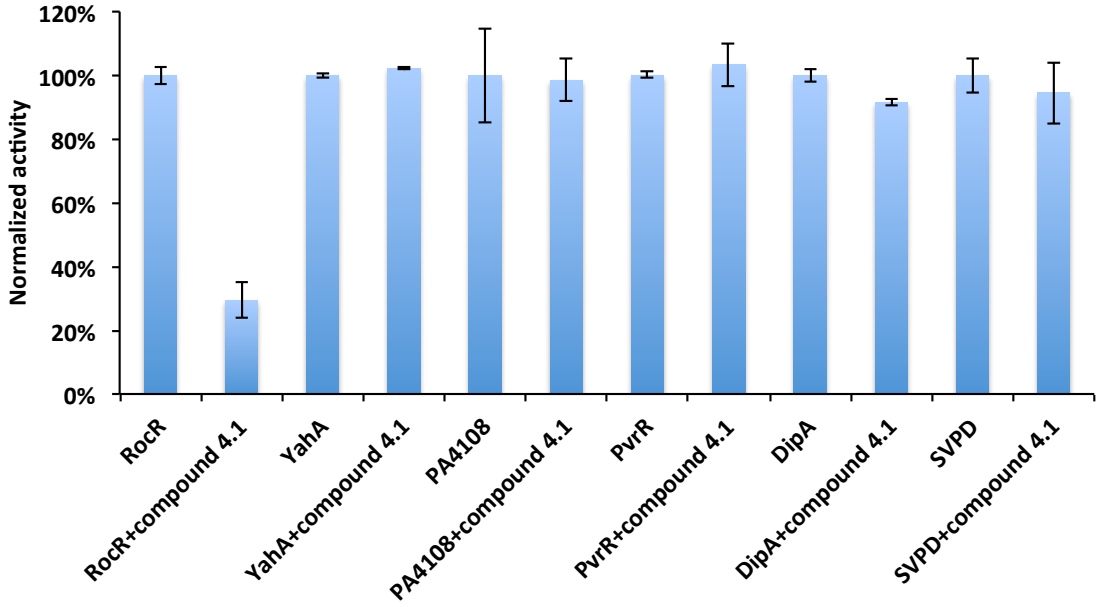

Figure 4.18. The enzymatic activities of different PDEs with or without compound **4.1** were analyzed by HPLC experiments or bis-pNPP cleavage assays. Compound **4.1** did not significantly inhibit YahA from *E. coli*, PA4108, PvrR or DipA from *P. aeruginosa* and Snake venom phosphodiesterase (SVPD) from *Crotalus atrox*.

We showed that this inhibitor could inhibit *P. aeruginosa* rhamnolipid production and swarming (a virulence factor for systemic invasion), but at the same time could also increase the production of other virulence factors (such as pyocyanin and pyoverdine) synthesis. It is known that quorum sensing regulates c-di-GMP signaling in a variety of bacteria, including *P. aeruginosa*, but the opposite regulation of

quorum sensing by c-di-GMP has not been extensively studied. The modulation of pyocyanin or pyoverdine or rhamnolipid (virulence factors that are mainly controlled by quorum sensing) by a c-di-GMP PDE inhibitor hints at a possible direct modulation of quorum sensing by c-di-GMP-related enzymes. Further work is needed to determine if the modulation of pyoverdine and pyocyanin or rhamnolipid by a c-di-GMP PDE inhibitor is via QS axis or via alternative pathways that also modulate pyoverdine and pyocyanin or rhamnolipid synthesis.[247] Recently, in a seminal disclosure by Blackwell and co-workers, it was revealed that modulation of RhIR, a quorum sensing receptor, with a small molecule inversely affected pyocyanin and rhamnolipid production (another example of unexpected modulation of virulence). It appears that a global approach needs to be taken towards developing an anti-virulence therapy.[248]

4.4. Experimental

4.4.1. Protein purification.

Snake venom phosphodiesterase (SVPD) from *Crotalus atrox* was purchased from Sigma-Aldrich. RocR, WspR, DisA, YahA and YybT purification were performed as described previously.[106] DipA, PA4108 and PvrR plasmids were transformed into BL21 (DE3) cells. When OD_{600} got 0.6, protein expression was induced by 1 mM IPTG. After expression at 16 °C overnight, cells were harvested by centrifugation (Sorvall LYNX 6000 Superspeed Centrifuge) at 5000 rpm for 30 min. Cells were resuspended in lysis buffer and lysed by sonication. Cell lysates were

centrifuged at 22,000 rpm for 25 min. Proteins were purified from supernatant by Nickel column (GE Healthcare HiTrap column). Lysis buffer for DipA contains 10 mM Tris-HCl, pH 8.0, 1 mM EDTA and 0.1% Tween 20. Lysis buffer for PA4108 contains 50 mM Tris-HCl, pH 8.0 and 50 mM NaCl. Lysis buffer for PvrR contains 10 mM Tris-HCl, pH 8.0 and 100 mM NaCl.

4.4.2. Radiolabeling experiments.

^{32}P-c-di-GMP was synthesized by incubating ^{32}P-GTP (333 nM), GTP (20 μM) and WspR D70E (5 μM) in a buffer containing 10 mM Tris-HCl, pH 8.0, 100 mM NaCl and 5 mM $MgCl_2$ at 37 °C overnight. For inhibition tests, c-di-GMP (50 μM) and ^{32}P-c-di-GMP (16 nM) were cleaved by RocR or YahA in the presence or absence of 100 μM potential inhibitors at 37 °C. The RocR reaction buffer, pH 8.0, contained 100 mM Tris-HCl, 20 mM KCl and 25 mM $MgCl_2$. YahA reaction buffer pH, 9.35, contained 50 mM Tris-HCl, 5 mM $MgCl_2$ and 50 mM NaCl. At different time points, 0.5 μL of reaction mixture was applied on a cellulose TLC plate (EMD Millipore). The TLC plates were developed in a buffer consisting of 1:1.5 (v/v) mixture of saturated $(NH_4)_2SO_4$: 1.5 M KH_2PO_4. To measure the kinetics of inhibition, radiolabeling experiments were conducted to monitor the reaction initial velocities with different concentrations of c-di-GMP and a fixed concentration of RocR (600 nM). 50 μM of compound **4.1** was used to determine K_i.

4.4.3. Bis-pNPP cleavage assays.

0.77 μM DipA or 4.7 μM PA4108 or 5 μM PvrR or 0.001 unit/mL SVPD reacted

with 1 mM bis-pNPP at 37 °C for 1 h in the presence or absence of 100 μM compound **4.1**. OD_{420} was monitored by BioTek Cytation 5 Cell Imaging Multi-Mode Reader.

4.4.4. Dissociation constant K_d measurement.

5 μM RocR and different concentrations of c-di-GMP were incubated at 4 °C for 1 h. Protein intrinsic fluorescence measurement (Excitation: 280 nm and Emission: 300 ~ 430 nm) was carried out on a Varian Cary Eclipse fluorescence spectrophotometer.

The dissociation constant was calculated by the following equations:

$$F = F_0 + \Delta F \frac{\left(K_d^{app} + P_t + L_t\right) - \sqrt{(K_d^{app} + P_t + L_t)^2 - 4P_tL_t}}{2P_t} \quad (4.1)^2$$

$$\log\left(\frac{F_0\text{-}F}{F}\right) = \log K_a + n \log[L_t] \quad (4.2)^{252}$$

Where F is the intrinsic fluorescence intensity at 340 nm. F_0 is the fluorescence intensity at 340 nm in the absence of compound **4.1**. ΔF is the fluorescence intensity change upon compound **4.1** binding. K_a is the association constant and K_d^{app} is the apparent dissociation constant of binding of compound **4.1** to RocR. P_t is the total protein concentration and L_t is the total compound **4.1** concentration.

4.4.5. Intracellular c-di-GMP and pGpG concentration quantification.

PAO1 overnight culture was diluted 1:100 into fresh TSB medium. 5 mL of the

diluted PAO1 cultures with or without 100 μM compound **4.1** were shaken at 37 °C for 24 h. Cells were harvested by centrifugation (Sorvall LYNX 6000 Superspeed Centrifuge) at 5000 rpm for 30 min. Cells were resuspended in 10 mM Tris-HCl, pH 8.0 and 100 mM NaCl and lysed by sonication. After centrifugation at 12,000 rpm for 10 min, the supernatant was evaporated to dryness in SpeedVac. The pellets were extracted by mixed solvent containing methanol: CH_3CN: water: 2:2:1 for 3 times. Protein concentration was determined using the pellet fraction. Combined all the extracted supernatants, filtered through 10K cut-off filter and evaporated to a final volume of 50 μL. Added 100 nM cXMP into supernatant as internal standard and c-di-GMP and pGpG concentration was quantified by Agilent 6460 Triple Quadrupole LC-MS/MS system using a Waters Atlantis T3 Column. Buffer A contains 0.1% formic acid in water and buffer B contains 0.1% in acetonitrile. The gradient is 0 → 16 min: 0% buffer B → 80% buffer B.

4.4.6. Viability test

P. aeruginosa PAO1 overnight culture was diluted to an OD_{600} of 0.02 in LB medium. 200 μL of bacterial culture was added to a 96 well microplate with 0, 0.1 μM, 1 μM, 10 μM, 20 μM, 50 μM or 100 μM compound **4.1**. After 24 h incubation at 37 °C, OD_{600} was measured by Molecular devices M5e microplate reader. Viability tests were done in triplicates.

4.4.7. Swimming and swarming assays

For swimming assay, 3 g agar in 800 mL deionized water was autoclaved and then mixed with sterile 200 mL of 5×M8 medium, 25 mL of 20% casamino acids, 10 mL of 20% glucose and 1 mL of 1 M $MgSO_4$.[253] 7.5 mL of mixed swimming agars with different concentrations of compound **4.1** were poured into 60 mm plates. The plates were dried for 30 min. PAO1 overnight culture was inoculated into the agar plates via an inoculating needle. Swimming plates were incubated at 37 °C for 24 h. For swarming assay, the components of the swarming agar were the same as swimming agar except that 5 g agar was added.[254] After drying for 30 min, 1 μL of PAO1 overnight culture was added onto the agar surface. Swarming plates were incubated at 37 °C for 24 h and then at room temperature for 24 h. Swimming and swarming experiments were done in duplicates.

4.4.8. Pyocyanin and pyoverdine test on agar plate

King agar A and King agar B were used for pyocyanin and pyoverdine tests. Different concentrations of compound **4.1** were added into agar. Overnight culture of PAO1 was diluted to an OD_{600} of 0.02 and diluted culture was spread evenly onto the plate surface. Plates were incubated at 37 °C for 24 h. Pyocyanin and pyoverdine tests were done in duplicates.

4.4.9. Pyocyanin and pyoverdine tests in liquid culture.

Overnight culture of PAO1 was diluted 1:100 in fresh TSB medium. 5 mL of diluted bacterial culture were mixed with different concentrations of compound **4.1**. After shaking at at 37 °C for 48 h, 1 mL of bacteria were used for OD_{600}

measurement. Spin down the cells in the other 4 mL of culture and collected the supernatant. 100 μL of supernatant was mixed with 100 mM Tris-HCl, pH 8.0 and went for pyoverdine fluorescence measurement (Ex: 400 nm and Em: 460 nm) on BioTek Cytation 5 Cell Imaging Multi-Mode Reader. 1 mL of supernatant was extracted by 1 mL of chloroform. The separated chloroform layer was mixed with 300 μL 1 mM HCl. Collected the pink HCl layer and measure OD_{520} on Jasco V-750 UV-Visible/NIR Spectrophotometer. Pyocyanin and pyoverdine tests were done in triplicates.

4.4.10. Rhamnolipid test

Rhamnolipid test was conducted according to the methods published by Blackwell in 2015.[248] *P. aeruginosa* PAO1 was grown in 15 mL LB medium overnight. Prepare 1 liter of Minimal Medium containing 49.3 mM Na_2HPO_4, 50 mM KH_2PO_4, 4.8 mM $MgSO_4$, 7.6 mM $(NH_4)_2SO_4$, 0.6 mM $CaCl_2$, 25 μM $FeSO_4$, 0.162 μM $(NH_4)_6Mo_7O_{24}$, 38 μM $ZnSO_4$, 14 μM $MnCl_2$, 1.6 μM $CuSO_4$, 0.86 μM $CoCl_2$, 1.9 μM boric acid, 5.5 μM $NiCl_2$, 6.72 μM EDTA, 0.6% glycerol in water. PAO1 overnight culture was diluted 1:100 into the fresh Minimal Medium. DMSO or 100 μM compound **4.1** was added to the culture. After 20 h shaking at 37 °C, cell culture supernatant was collected by centrifugation at 5000 rpm for 20 min using Sorvall LYNX 6000 Superspeed Centrifuge. Rhamonolipid was extracted by diethyl ether, evaporated to dryness and redissolved in 200 μL water. 50 μL of rhamnolipid solution was mixed with 450 μL of 0.19% (w/v) orcinol in 50% (v/v) concentrated H_2SO_4. After incubation at 80 °C for 30 min, the solutions were allowed to cool at RT for 15

min and the absorbance at 421 nm was measured by Jasco V-730 UV-Visible/NIR Spectrophotometer. Data were normalized to OD_{600} of PAO1 culture.

4.4.11. Biofilm test.

P. aeruginosa PAO1 overnight culture was diluted to an OD_{600} of 0.02 in 10 % TSB. 200 μL of bacterial culture was added to a MBEC plate (Innovotech) with 0, 0.1 μM, 1 μM, 10 μM, 20 μM, 50 μM or 100 μM compound **4.1**. After 4 hour incubation at 37 °C, pegs were stained with 0.1% crystal violet and washed three times with distilled water. Then air-dried pegs were dipped into ethanol until crystal violet was completely dissolved. OD_{595} was measured by Molecular devices M5e microplate reader. Biofilms tests were repeated eight times.

Chapter 5 : Conclusion and Future Perspectives

5.1. Conclusion and future perspectives

It is widely accepted that c-di-GMP and c-di-AMP are dominant second messengers in bacteria.[5] Their signaling networks are complicated and intricate. In Gram-negative and a few Gem-positive bacteria, increased intracellular concentrations of c-di-GMP lead to exopolysaccharide production and biofilm formation, which is very difficult to eliminate.[6] On the other hand, decreased concentrations of c-di-GMP promote swimming and swarming activities and trigger acute virulence factor production.[14] C-di-AMP is essential for the viability and growth of Gram-positive and mycobacterium.[7] It is considered as a promising drug target because of its key roles in cell wall homeostasis and DNA damage sensing regulations.[7] But in some cases, for example, for the intracellular bacterium, the ability of c-di-AMP to bind to STING and induce Type I interferon response is a threat to its survival.[126] The intracellular concentrations of cyclic dinucleotides are fine-tuned by their metabolism enzymes. Usually there are multi-types of synthases and hydrolases existing in one bacterium and these cooperate to regulate cyclic dinucleotide concentrations.[194] Small molecules that disrupt the function of cyclic dinucleotide metabolism enzymes would provide an effective way to elucidate the details of signaling transduction, could inhibit biofilm formation, control virulence factor production and/or decrease bacterial viability. A lot of efforts have been put into the identification of inhibitors of c-di-GMP synthase DGC.[52] Only a few c-di-

GMP analogs, containing negative charged phosphodiester bonds, have been designed to inhibit c-di-GMP phosphodiesterase.[8] These analogs are however unlikely to cross bacterial cell membrane.[79] For the newly discovered second messenger c-di-AMP, there was no reported inhibitor for the synthases or phosphodiesterases of this dinucleotide before my Ph.D. study. So during my Ph.D., I focused on the identification of small molecules that intercept cyclic dinucleotide signaling.

In Chapter 2, I reported the identification of the first small molecule inhibitor of c-di-AMP synthase DisA from a 1000 compound library by using the coralyne assay. I demonstrated that the coralyne assay is an easy, cheap and powerful method for real-time c-di-AMP detection and it could be utilized for high though-put screening. Although some false positives showed up in the screening, it successfully ruled out 99% of non-inhibitors. The DisA inhibitor bromophenol-TH contains halogenated phenol and thiohydantoin groups. Compounds with similar structures did not have DisA inhibition effects, indicating the specificity of bromophenol-TH inhibition. Bromophenol-TH binds to DisA with a K_d of 21 μM and high concentrations of ATP did not abolish bromophenol-TH binding, indicating that bromophenol-TH is a non-competitive inhibitor. Although bromophenol-TH has a Michael acceptor, it doesn't react with cysteine and it is not a covalent inhibitor. The IC_{50} of 56 μM (5 μM DisA and 50 μM ATP) for bromophenol-TH is not ideal. We also worked on Structure Activity Relationship studies to optimize the inhibition effects of this inhibitor. So we designed and synthesized four types of BTH analogs. Type A analogs contain mixed halogens whereas type B analogs consist of only one type of halogens. Type C analog

has modifications on the phenolic group and type D has other kinds of heterocyclic rings. None of the analogs have stronger inhibition effects than bromophenol-TH, indicating that halogen substitution causes dramatic changes in enzyme affinity for a ligand. Future work will involve the screening for new scaffolds of c-di-AMP synthase inhibitors using the coralyne assay. A graduate student in the Sintim group, Clement Opoku-Temeng, is currently working on the identification of more potent DisA inhibitors. He screened a library of 2000 known drugs and successfully identified the antiparasitic drug Suramin as a more efficient DisA inhibitor than bromophenol-TH.

In Chapter 3, I characterized a cyclic dinucleotide phosphodiesterase CdnP from *M. tuberculosis*. The DHH-DHH1 domain protein CdnP efficiently cleaves c-di-AMP to AMP and it also cleaves c-di-GMP to GMP. The cleavage is enhanced at higher pH and in the presence of Mn^{2+}. Ca^{2+} slows down the cleavage process. Interesting, the host-derived second messenger 2'3'-cGAMP is also a substrate of CdnP, but not other cyclic dinucleotide PDE, indicating the possibility of CdnP disrupting host signaling transduction. The cleavage product of 2'3'-cGAMP, pGp(2'-5')A was ascertained by HPLC co-injection with synthesized compounds. Our collaborator in the Tuberculosis center at Johns Hopkins University demonstrated CdnP decreases the intracellular concentration of 2'3'-cGAMP in macrophages and CdnP reduces macrophage Type I IFN responses during infection in a STING-IRF3-dependent manner. In a mouse infection model, the virulence of *M. tuberculosis* with *cdnP* mutant significantly decreased. Since CdnP is important in *M. tuberculosis*, we designed and synthesized some CdnP inhibitors, which has similar structure to ApA.

Out of the four inhibitors, Ap(S)A showed the best inhibition effects (K_i = 65 ± 23 μM) and it is resistant to CdnP cleavage. Our collaborators evaluated the activity of Ap(S)A *in vivo* and found that Ap(S)A significantly reduced CDN mediated IRF induction. Future work will involve the screening for CdnP small molecule inhibitors using the fluorescent probes developed by Dr. Benjamin Roembke and Dr. Jie Zhou in Sintim group. A graduate student Clement Opoku-Temeng will conduct the screening experiments in the screening center at Purdue University.

In Chapter 4, I reported a novel small molecule inhibitor for c-di-GMP phosphodiesterase RocR from *P. aeruginosa*. Although this compound is identified as a promising inhibitor of YahA (a c-di-GMP PDE in *E. coli*) in a computer-based screening, it did not inhibit YahA activity. Interestingly, it inhibits RocR (K_i = 83 ± 7 μM), which is responsible for the virulence of human pathogen *P. aeruginosa*.[194] We showed that this RocR inhibitor could inhibit *P. aeruginosa* swarming motility, which is essential for infection, by increasing the production of surfactant rhamnolipid. However, at the same time RocR inhibitor could also increase the production of other virulence factor synthesis, such as pyocyanin and pyoverdine, which are mainly controlled by quorum sensing system. Two analogs of RocR inhibitor were synthesized with minor modification on the benzoisothiazolone core, these analogs lost most or all RocR inhibition activities. Future work involves the structure-activity relationship study of RocR inhibitor. More generations of analogs will be synthesized by Dr. Genichiro Tsuji. RocR activity inhibition and bacterial tests will be conducted by a graduate student Clement Opoku-Temeng.

Appendices

1. Compound ID of 1000 compound library for DisA inhibitor screening

Plate	Well	IDNUMBER	Plate	Well	IDNUMBER	Plate	Well	IDNUMBER	Plate	Well	IDNUMBER	Plate	Well	IDNUMBER	Plate	Well	IDNUMBER
1	A3	ST000136	2	A3	ST006415	3	A3	ST011913	4	A3	ST018800	5	A3	ST021056	6	A3	ST025589
1	B3	ST000137	2	B3	ST006418	3	B3	ST011924	4	B3	ST018811	5	B3	ST021121	6	B3	ST025590
1	C3	ST000235	2	C3	ST006422	3	C3	ST011928	4	C3	ST018868	5	C3	ST021131	6	C3	ST025594
1	D3	ST000348	2	D3	ST006428	3	D3	ST011981	4	D3	ST018876	5	D3	ST021145	6	D3	ST025613
1	E3	ST000412	2	E3	ST006431	3	E3	ST012001	4	E3	ST018936	5	E3	ST021200	6	E3	ST025619
1	F3	ST000460	2	F3	ST006433	3	F3	ST012157	4	F3	ST018946	5	F3	ST022328	6	F3	ST025656
1	G3	ST000472	2	G3	ST006434	3	G3	ST012202	4	G3	ST018950	5	G3	ST022370	6	G3	ST025744
1	H3	ST000480	2	H3	ST006435	3	H3	ST012256	4	H3	ST018953	5	H3	ST022488	6	H3	ST025746
1	A4	ST000481	2	A4	ST006437	3	A4	ST012278	4	A4	ST018961	5	A4	ST022491	6	A4	ST025752
1	B4	ST000482	2	B4	ST006440	3	B4	ST012279	4	B4	ST019349	5	B4	ST023274	6	B4	ST025753
1	C4	ST000485	2	C4	ST006442	3	C4	ST012280	4	C4	ST019590	5	C4	ST023483	6	C4	ST025757
1	D4	ST000489	2	D4	ST006448	3	D4	ST012283	4	D4	ST019599	5	D4	ST023501	6	D4	ST025995
1	E4	ST000610	2	E4	ST006451	3	E4	ST012294	4	E4	ST019647	5	E4	ST023505	6	E4	ST025996
1	F4	ST000616	2	F4	ST006452	3	F4	ST012337	4	F4	ST019706	5	F4	ST023510	6	F4	ST026264
1	G4	ST000691	2	G4	ST006455	3	G4	ST012339	4	G4	ST019707	5	G4	ST024145	6	G4	ST026286
1	H4	ST000753	2	H4	ST006456	3	H4	ST012343	4	H4	ST019720	5	H4	ST024156	6	H4	ST026289
1	A5	ST000868	2	A5	ST006458	3	A5	ST012365	4	A5	ST019727	5	A5	ST024175	6	A5	ST026291
1	B5	ST000900	2	B5	ST006459	3	B5	ST012372	4	B5	ST019728	5	B5	ST024204	6	B5	ST026292
1	C5	ST001021	2	C5	ST006460	3	C5	ST012376	4	C5	ST019729	5	C5	ST024205	6	C5	ST026293
1	D5	ST001025	2	D5	ST006468	3	D5	ST012435	4	D5	ST019736	5	D5	ST024226	6	D5	ST026296
1	E5	ST001109	2	E5	ST006472	3	E5	ST012443	4	E5	ST019739	5	E5	ST024228	6	E5	ST026300
1	F5	ST001112	2	F5	ST006482	3	F5	ST012465	4	F5	ST019747	5	F5	ST024231	6	F5	ST026442
1	G5	ST001113	2	G5	ST006486	3	G5	ST012482	4	G5	ST019756	5	G5	ST024293	6	G5	ST026451
1	H5	ST001153	2	H5	ST006494	3	H5	ST012499	4	H5	ST019797	5	H5	ST024297	6	H5	ST026460
1	A6	ST001191	2	A6	ST006503	3	A6	ST012544	4	A6	ST019829	5	A6	ST024298	6	A6	ST026461
1	B6	ST001615	2	B6	ST006512	3	B6	ST012574	4	B6	ST019830	5	B6	ST024299	6	B6	ST026557
1	C6	ST001670	2	C6	ST006518	3	C6	ST012641	4	C6	ST019848	5	C6	ST024300	6	C6	ST026564
1	D6	ST001766	2	D6	ST006520	3	D6	ST012802	4	D6	ST019878	5	D6	ST024303	6	D6	ST026577
1	E6	ST002482	2	E6	ST006540	3	E6	ST012807	4	E6	ST019884	5	E6	ST024311	6	E6	ST026599
1	F6	ST002485	2	F6	ST006545	3	F6	ST012814	4	F6	ST019919	5	F6	ST024313	6	F6	ST026666
1	G6	ST002605	2	G6	ST006590	3	G6	ST012816	4	G6	ST019920	5	G6	ST024314	6	G6	ST026784
1	H6	ST002824	2	H6	ST006635	3	H6	ST012820	4	H6	ST019923	5	H6	ST024318	6	H6	ST026818
1	A7	ST003014	2	A7	ST006780	3	A7	ST012825	4	A7	ST019924	5	A7	ST024323	6	A7	ST026959
1	B7	ST003110	2	B7	ST006805	3	B7	ST013077	4	B7	ST019940	5	B7	ST024333	6	B7	ST026975
1	C7	ST003148	2	C7	ST006923	3	C7	ST013227	4	C7	ST019945	5	C7	ST024334	6	C7	ST027014
1	D7	ST003203	2	D7	ST007036	3	D7	ST013366	4	D7	ST019964	5	D7	ST024335	6	D7	ST027104
1	E7	ST003207	2	E7	ST007130	3	E7	ST013369	4	E7	ST019965	5	E7	ST024337	6	E7	ST027105
1	F7	ST003391	2	F7	ST007228	3	F7	ST013389	4	F7	ST019976	5	F7	ST024339	6	F7	ST027110
1	G7	ST003425	2	G7	ST007374	3	G7	ST013432	4	G7	ST020004	5	G7	ST024341	6	G7	ST027123
1	H7	ST003440	2	H7	ST007375	3	H7	ST013554	4	H7	ST020006	5	H7	ST024342	6	H7	ST027174
1	A8	ST003442	2	A8	ST007517	3	A8	ST013652	4	A8	ST020016	5	A8	ST024343	6	A8	ST027181
1	B8	ST003469	2	B8	ST007520	3	B8	ST013779	4	B8	ST020019	5	B8	ST024345	6	B8	ST027184
1	C8	ST003473	2	C8	ST007521	3	C8	ST013849	4	C8	ST020042	5	C8	ST024371	6	C8	ST027202
1	D8	ST003475	2	D8	ST007525	3	D8	ST013855	4	D8	ST020043	5	D8	ST024372	6	D8	ST027205
1	E8	ST003489	2	E8	ST007535	3	E8	ST013880	4	E8	ST020048	5	E8	ST024373	6	E8	ST027277
1	F8	ST003517	2	F8	ST007546	3	F8	ST013881	4	F8	ST020055	5	F8	ST024374	6	F8	ST027411
1	G8	ST003540	2	G8	ST008121	3	G8	ST014006	4	G8	ST020504	5	G8	ST024376	6	G8	ST027416
1	H8	ST003595	2	H8	ST008330	3	H8	ST014014	4	H8	ST020598	5	H8	ST024386	6	H8	ST027425
1	A9	ST003651	2	A9	ST008331	3	A9	ST014296	4	A9	ST020608	5	A9	ST024387	6	A9	ST027427
1	B9	ST003720	2	B9	ST008384	3	B9	ST014620	4	B9	ST020612	5	B9	ST024435	6	B9	ST027452
1	C9	ST004068	2	C9	ST008445	3	C9	ST014640	4	C9	ST020618	5	C9	ST024450	6	C9	ST027455
1	D9	ST004080	2	D9	ST009099	3	D9	ST014683	4	D9	ST020635	5	D9	ST024471	6	D9	ST027464
1	E9	ST004089	2	E9	ST009153	3	E9	ST014858	4	E9	ST020639	5	E9	ST024494	6	E9	ST027472
1	F9	ST004304	2	F9	ST009299	3	F9	ST014902	4	F9	ST020711	5	F9	ST024504	6	F9	ST027492
1	G9	ST004439	2	G9	ST009305	3	G9	ST014979	4	G9	ST020725	5	G9	ST024511	6	G9	ST027506
1	H9	ST004727	2	H9	ST009309	3	H9	ST014992	4	H9	ST020770	5	H9	ST024524	6	H9	ST027512
1	A10	ST004883	2	A10	ST009310	3	A10	ST015439	4	A10	ST020771	5	A10	ST024560	6	A10	ST027516
1	B10	ST004916	2	B10	ST009315	3	B10	ST016438	4	B10	ST020777	5	B10	ST024562	6	B10	ST027552
1	C10	ST005123	2	C10	ST009320	3	C10	ST016477	4	C10	ST020788	5	C10	ST024740	6	C10	ST027573
1	D10	ST005226	2	D10	ST009322	3	D10	ST016560	4	D10	ST020792	5	D10	ST024806	6	D10	ST027574
1	E10	ST005387	2	E10	ST009479	3	E10	ST016562	4	E10	ST020798	5	E10	ST024819	6	E10	ST027625
1	F10	ST005392	2	F10	ST009498	3	F10	ST016603	4	F10	ST020805	5	F10	ST024909	6	F10	ST027677
1	G10	ST005395	2	G10	ST009499	3	G10	ST016608	4	G10	ST020806	5	G10	ST024910	6	G10	ST027720
1	H10	ST005398	2	H10	ST009506	3	H10	ST016610	4	H10	ST020807	5	H10	ST024912	6	H10	ST027724
1	A11	ST005523	2	A11	ST009511	3	A11	ST018293	4	A11	ST020808	5	A11	ST024965	6	A11	ST027829
1	B11	ST005543	2	B11	ST009787	3	B11	ST018295	4	B11	ST020809	5	B11	ST025224	6	B11	ST027857
1	C11	ST005570	2	C11	ST010080	3	C11	ST018296	4	C11	ST020810	5	C11	ST025226	6	C11	ST027858
1	D11	ST005585	2	D11	ST010082	3	D11	ST018314	4	D11	ST020829	5	D11	ST025248	6	D11	ST027868
1	E11	ST005621	2	E11	ST010095	3	E11	ST018481	4	E11	ST020831	5	E11	ST025272	6	E11	ST027874
1	F11	ST005646	2	F11	ST010119	3	F11	ST018532	4	F11	ST020925	5	F11	ST025419	6	F11	ST027881
1	G11	ST006213	2	G11	ST010137	3	G11	ST018549	4	G11	ST020926	5	G11	ST025457	6	G11	ST027883
1	H11	ST006269	2	H11	ST010152	3	H11	ST018559	4	H11	ST020927	5	H11	ST025489	6	H11	ST027923
1	A12	ST006361	2	A12	ST010156	3	A12	ST018584	4	A12	ST020929	5	A12	ST025507	6	A12	ST028181
1	B12	ST006394	2	B12	ST010160	3	B12	ST018596	4	B12	ST020930	5	B12	ST025524	6	B12	ST028198
1	C12	ST006400	2	C12	ST010215	3	C12	ST018601	4	C12	ST020932	5	C12	ST025547	6	C12	ST028199
1	D12	ST006401	2	D12	ST010300	3	D12	ST018704	4	D12	ST020937	5	D12	ST025548	6	D12	ST028202
1	E12	ST006402	2	E12	ST010460	3	E12	ST018720	4	E12	ST020941	5	E12	ST025556	6	E12	ST028219
1	F12	ST006404	2	F12	ST010467	3	F12	ST018722	4	F12	ST020946	5	F12	ST025577	6	F12	ST028220
1	G12	ST006406	2	G12	ST011904	3	G12	ST018724	4	G12	ST020948	5	G12	ST025584	6	G12	ST028230
1	H12	ST006413	2	H12	ST011910	3	H12	ST018786	4	H12	ST020981	5	H12	ST025585	6	H12	ST028231

Plate	Well	IDNUMBER	Plate	Well	IDNUMBER	Plate	Well	IDNUMBER	Plate	Well	IDNUMBER	Plate	Well	IDNUMBER	Plate	Well	IDNUMBER
7	A3	ST028232	8	A3	ST033372	9	A3	ST035796	10	A3	ST041259	11	A3	ST050109	12	A3	ST055362
7	B3	ST028233	8	B3	ST033378	9	B3	ST035937	10	B3	ST041264	11	B3	ST050125	12	B3	ST055369
7	C3	ST028246	8	C3	ST033380	9	C3	ST036220	10	C3	ST041573	11	C3	ST050126	12	C3	ST055374
7	D3	ST028249	8	D3	ST033384	9	D3	ST036268	10	D3	ST041608	11	D3	ST050174	12	D3	ST055375
7	E3	ST028254	8	E3	ST033385	9	E3	ST036284	10	E3	ST041618	11	E3	ST050184	12	E3	ST055384
7	F3	ST028255	8	F3	ST033386	9	F3	ST036285	10	F3	ST041720	11	F3	ST050193	12	F3	ST055403
7	G3	ST028264	8	G3	ST033390	9	G3	ST036288	10	G3	ST041808	11	G3	ST050208	12	G3	ST055412
7	H3	ST028280	8	H3	ST033419	9	H3	ST036315	10	H3	ST041838	11	H3	ST050241	12	H3	ST055636
7	A4	ST028313	8	A4	ST033465	9	A4	ST036363	10	A4	ST041861	11	A4	ST050256	12	A4	ST055797
7	B4	ST028314	8	B4	ST033526	9	B4	ST036422	10	B4	ST041904	11	B4	ST050260	12	B4	ST055950
7	C4	ST028317	8	C4	ST033560	9	C4	ST036427	10	C4	ST041906	11	C4	ST050261	12	C4	ST055965
7	D4	ST028320	8	D4	ST033562	9	D4	ST036451	10	D4	ST041925	11	D4	ST050276	12	D4	ST055982
7	E4	ST028334	8	E4	ST033578	9	E4	ST036457	10	E4	ST041949	11	E4	ST050285	12	E4	ST055983
7	F4	ST028379	8	F4	ST033626	9	F4	ST036476	10	F4	ST041951	11	F4	ST050288	12	F4	ST055987
7	G4	ST028452	8	G4	ST033645	9	G4	ST036478	10	G4	ST041954	11	G4	ST051981	12	G4	ST055997
7	H4	ST028454	8	H4	ST033647	9	H4	ST036501	10	H4	ST041960	11	H4	ST051982	12	H4	ST055998
7	A5	ST028457	8	A5	ST033680	9	A5	ST036521	10	A5	ST042048	11	A5	ST052055	12	A5	ST056004
7	B5	ST028652	8	B5	ST034265	9	B5	ST036523	10	B5	ST042049	11	B5	ST052591	12	B5	ST056010
7	C5	ST028653	8	C5	ST034608	9	C5	ST036528	10	C5	ST042100	11	C5	ST052617	12	C5	ST056083
7	D5	ST028687	8	D5	ST034820	9	D5	ST036532	10	D5	ST042539	11	D5	ST052625	12	D5	ST056106
7	E5	ST028697	8	E5	ST034834	9	E5	ST036533	10	E5	ST043505	11	E5	ST052829	12	E5	ST056229
7	F5	ST028710	8	F5	ST034848	9	F5	ST036555	10	F5	ST043619	11	F5	ST053033	12	F5	ST056246
7	G5	ST028951	8	G5	ST034858	9	G5	ST036572	10	G5	ST043621	11	G5	ST053109	12	G5	ST056247
7	H5	ST028954	8	H5	ST034864	9	H5	ST036632	10	H5	ST044001	11	H5	ST053113	12	H5	ST056249
7	A6	ST028966	8	A6	ST034871	9	A6	ST036637	10	A6	ST044185	11	A6	ST053114	12	A6	ST056250
7	B6	ST028967	8	B6	ST034883	9	B6	ST036643	10	B6	ST044277	11	B6	ST053115	12	B6	ST056251
7	C6	ST028968	8	C6	ST034885	9	C6	ST036649	10	C6	ST044315	11	C6	ST053116	12	C6	ST056252
7	D6	ST028969	8	D6	ST034889	9	D6	ST036826	10	D6	ST044457	11	D6	ST053132	12	D6	ST056258
7	E6	ST028975	8	E6	ST034895	9	E6	ST037188	10	E6	ST044513	11	E6	ST053133	12	E6	ST056314
7	F6	ST028978	8	F6	ST034902	9	F6	ST037535	10	F6	ST044541	11	F6	ST053231	12	F6	ST056322
7	G6	ST029024	8	G6	ST034922	9	G6	ST037673	10	G6	ST044625	11	G6	ST053241	12	G6	ST056520
7	H6	ST029026	8	H6	ST034931	9	H6	ST037712	10	H6	ST044744	11	H6	ST053256	12	H6	ST056653
7	A7	ST029099	8	A7	ST034941	9	A7	ST037833	10	A7	ST044758	11	A7	ST053293	12	A7	ST056706
7	B7	ST029220	8	B7	ST034951	9	B7	ST037989	10	B7	ST044912	11	B7	ST053294	12	B7	ST056760
7	C7	ST029244	8	C7	ST034952	9	C7	ST038015	10	C7	ST045230	11	C7	ST053298	12	C7	ST056761
7	D7	ST029246	8	D7	ST034958	9	D7	ST038161	10	D7	ST045510	11	D7	ST053300	12	D7	ST056763
7	E7	ST029251	8	E7	ST034960	9	E7	ST038232	10	E7	ST045589	11	E7	ST053305	12	E7	ST056765
7	F7	ST029253	8	F7	ST034961	9	F7	ST039178	10	F7	ST045665	11	F7	ST053308	12	F7	ST056767
7	G7	ST029255	8	G7	ST034962	9	G7	ST039320	10	G7	ST045666	11	G7	ST053334	12	G7	ST056770
7	H7	ST029257	8	H7	ST034963	9	H7	ST039538	10	H7	ST045882	11	H7	ST053363	12	H7	ST056777
7	A8	ST029259	8	A8	ST034968	9	A8	ST039546	10	A8	ST045966	11	A8	ST053367	12	A8	ST056806
7	B8	ST029264	8	B8	ST034978	9	B8	ST039551	10	B8	ST047310	11	B8	ST053373	12	B8	ST056969
7	C8	ST029265	8	C8	ST034992	9	C8	ST039565	10	C8	ST047697	11	C8	ST053374	12	C8	ST057069
7	D8	ST029270	8	D8	ST034996	9	D8	ST039668	10	D8	ST047995	11	D8	ST053378	12	D8	ST057110
7	E8	ST029276	8	E8	ST035014	9	E8	ST040000	10	E8	ST048007	11	E8	ST053380	12	E8	ST057209
7	F8	ST029277	8	F8	ST035018	9	F8	ST040111	10	F8	ST048136	11	F8	ST053406	12	F8	ST057268
7	G8	ST029288	8	G8	ST035029	9	G8	ST040314	10	G8	ST048909	11	G8	ST053408	12	G8	ST057269
7	H8	ST029303	8	H8	ST035037	9	H8	ST040325	10	H8	ST048953	11	H8	ST053412	12	H8	ST057372
7	A9	ST029309	8	A9	ST035039	9	A9	ST040329	10	A9	ST048963	11	A9	ST053413	12	A9	ST057425
7	B9	ST029392	8	B9	ST035041	9	B9	ST040345	10	B9	ST048964	11	B9	ST053417	12	B9	ST057449
7	C9	ST029393	8	C9	ST035045	9	C9	ST040383	10	C9	ST048965	11	C9	ST053418	12	C9	ST057477
7	D9	ST029538	8	D9	ST035046	9	D9	ST040389	10	D9	ST048966	11	D9	ST053419	12	D9	ST057626
7	E9	ST029543	8	E9	ST035054	9	E9	ST040392	10	E9	ST048968	11	E9	ST053432	12	E9	ST057635
7	F9	ST029570	8	F9	ST035057	9	F9	ST040393	10	F9	ST048978	11	F9	ST053436	12	F9	ST057636
7	G9	ST029587	8	G9	ST035060	9	G9	ST040400	10	G9	ST049052	11	G9	ST053441	12	G9	ST057637
7	H9	ST029626	8	H9	ST035072	9	H9	ST040406	10	H9	ST049053	11	H9	ST053455	12	H9	ST057638
7	A10	ST029668	8	A10	ST035090	9	A10	ST040410	10	A10	ST049062	11	A10	ST053456	12	A10	ST057683
7	B10	ST029803	8	B10	ST035094	9	B10	ST040412	10	B10	ST049067	11	B10	ST053680	12	B10	ST057709
7	C10	ST029981	8	C10	ST035129	9	C10	ST040414	10	C10	ST049070	11	C10	ST053694	12	C10	ST057710
7	D10	ST030428	8	D10	ST035130	9	D10	ST040419	10	D10	ST049071	11	D10	ST054069	12	D10	ST057711
7	E10	ST030562	8	E10	ST035131	9	E10	ST040425	10	E10	ST049073	11	E10	ST054354	12	E10	ST058249
7	F10	ST030733	8	F10	ST035169	9	F10	ST040426	10	F10	ST049074	11	F10	ST054407	12	F10	ST058274
7	G10	ST031049	8	G10	ST035173	9	G10	ST040427	10	G10	ST049079	11	G10	ST054625	12	G10	ST058282
7	H10	ST031162	8	H10	ST035174	9	H10	ST040429	10	H10	ST049143	11	H10	ST054687	12	H10	ST058283
7	A11	ST031166	8	A11	ST035177	9	A11	ST040432	10	A11	ST049356	11	A11	ST054708	12	A11	ST058284
7	B11	ST031272	8	B11	ST035186	9	B11	ST040445	10	B11	ST049416	11	B11	ST054780	12	B11	ST058285
7	C11	ST031415	8	C11	ST035224	9	C11	ST040459	10	C11	ST049455	11	C11	ST054939	12	C11	ST058293
7	D11	ST031702	8	D11	ST035648	9	D11	ST040466	10	D11	ST049477	11	D11	ST054947	12	D11	ST058459
7	E11	ST031721	8	E11	ST035656	9	E11	ST040468	10	E11	ST049494	11	E11	ST055031	12	E11	ST058522
7	F11	ST031725	8	F11	ST035670	9	F11	ST040516	10	F11	ST049754	11	F11	ST055044	12	F11	ST058739
7	G11	ST031791	8	G11	ST035688	9	G11	ST040549	10	G11	ST049803	11	G11	ST055060	12	G11	ST058927
7	H11	ST031947	8	H11	ST035692	9	H11	ST040554	10	H11	ST049855	11	H11	ST055062	12	H11	ST058928
7	A12	ST032360	8	A12	ST035719	9	A12	ST040555	10	A12	ST049871	11	A12	ST055063	12	A12	ST058933
7	B12	ST032369	8	B12	ST035745	9	B12	ST040634	10	B12	ST049900	11	B12	ST055076	12	B12	ST058938
7	C12	ST032605	8	C12	ST035746	9	C12	ST040665	10	C12	ST049949	11	C12	ST055077	12	C12	ST059001
7	D12	ST032974	8	D12	ST035759	9	D12	ST040666	10	D12	ST049974	11	D12	ST055086	12	D12	ST059053
7	E12	ST033197	8	E12	ST035784	9	E12	ST040691	10	E12	ST049975	11	E12	ST055132	12	E12	ST059207
7	F12	ST033361	8	F12	ST035787	9	F12	ST040872	10	F12	ST049988	11	F12	ST055144	12	F12	ST059224
7	G12	ST033370	8	G12	ST035789	9	G12	ST040908	10	G12	ST049995	11	G12	ST055176	12	G12	ST059348
7	H12	ST033371	8	H12	ST035794	9	H12	ST041026	10	H12	ST050006	11	H12	ST055328	12	H12	ST059407

Plate	Well	MDL number	Plate	Well	MDL number	Plate	Well	MDL number	Plate	Well	MDL number
Sigma	A1	MFCD00133539	Sigma	B1	MFCD04974495	Sigma	C1	MFCD00157720	Sigma	D1	MFCD00005607
Sigma	A2	MFCD08705319	Sigma	B2	MFCD00055790	Sigma	C2	MFCD00136466	Sigma	D2	MFCD00002497
Sigma	A3	MFCD00079619	Sigma	B3	MFCD00187724	Sigma	C3	MFCD00093078	Sigma	D3	MFCD00005183
Sigma	A4	MFCD11045307	Sigma	B4	MFCD00085853	Sigma	C4	MFCD00032240	Sigma	D4	MFCD00012780
Sigma	A5	MFCD08276917	Sigma	B5	MFCD00020684	Sigma	C5	MFCD09865273	Sigma	D5	MFCD00002339
Sigma	A6	MFCD00010555	Sigma	B6	MFCD00017824	Sigma	C6	MFCD08272809	Sigma	D6	MFCD00019481
Sigma	A7	MFCD08277040	Sigma	B7	MFCD00088782	Sigma	C7	MFCD06411391	Sigma	D7	MFCD00151027
Sigma	A8	MFCD16875436	Sigma	B8	MFCD00030041	Sigma	C8	MFCD21608518			
Sigma	A9	MFCD00864692	Sigma	B9	MFCD00030033	Sigma	C9	MFCD12828770			
Sigma	A10	MFCD00083192	Sigma	B10	MFCD00028696	Sigma	C10	MFCD00099612			
Sigma	A11	MFCD01657514	Sigma	B11	MFCD00030043	Sigma	C11	MFCD01076570			

2. Coralyne assay screening result

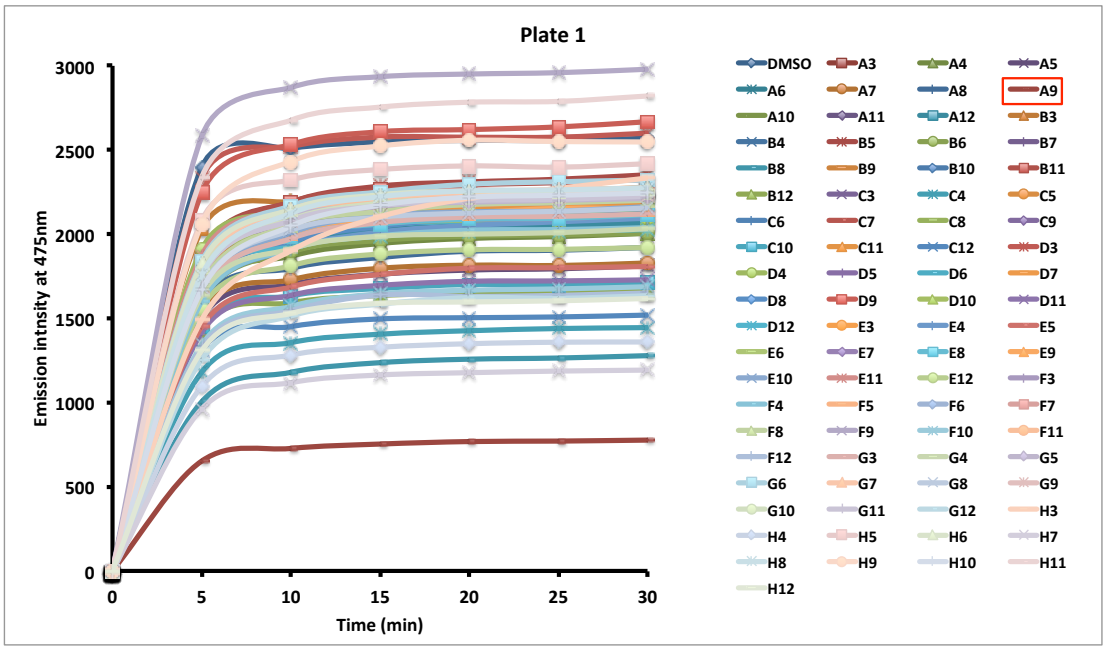

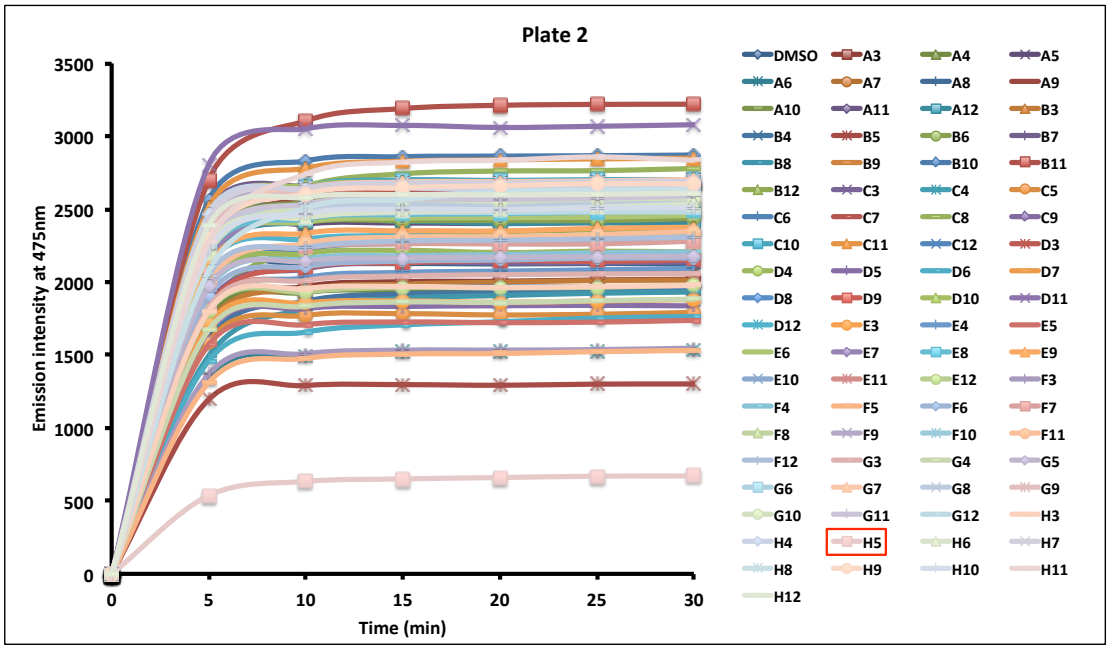

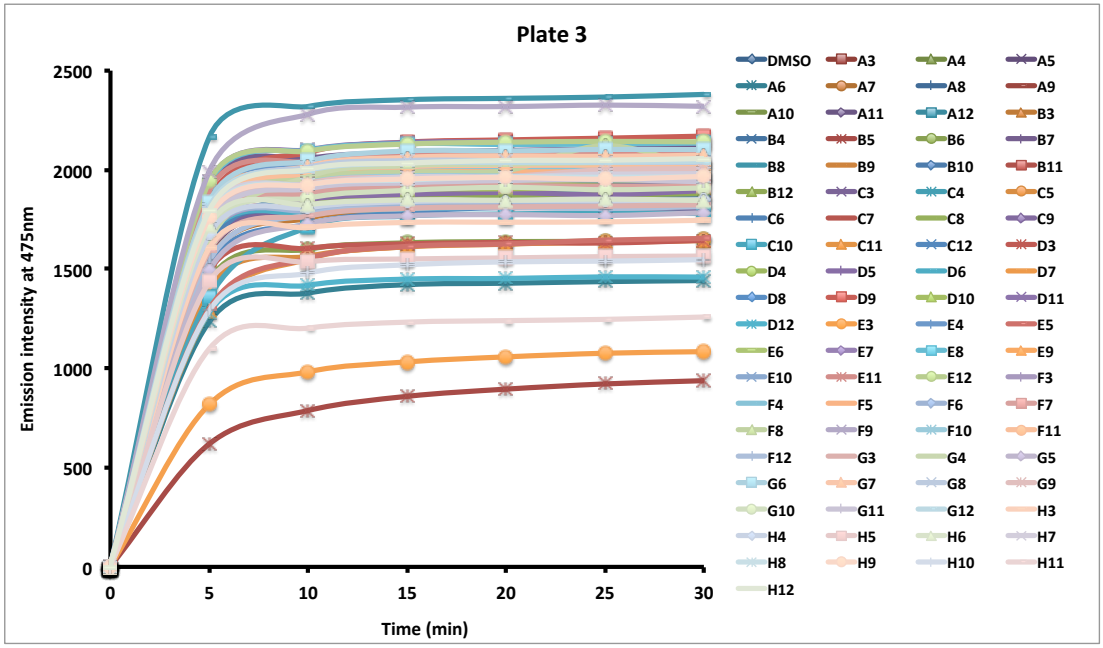
Plate 3
Emission intensity at 475nm
Time (min)
0
500
1000
1500
2000
2500
0
5
10
15
20
25
30
DMSO A3 A4 A5
A6 A7 A8 A9
A10 A11 A12 B3
B4 B5 B6 B7
B8 B9 B10 B11
B12 C3 C4 C5
C6 C7 C8 C9
C10 C11 C12 D3
D4 D5 D6 D7
D8 D9 D10 D11
D12 E3 E4 E5
E6 E7 E8 E9
E10 E11 E12 F3
F4 F5 F6 F7
F8 F9 F10 F11
F12 G3 G4 G5
G6 G7 G8 G9
G10 G11 G12 H3
H4 H5 H6 H7
H8 H9 H10 H11
H12

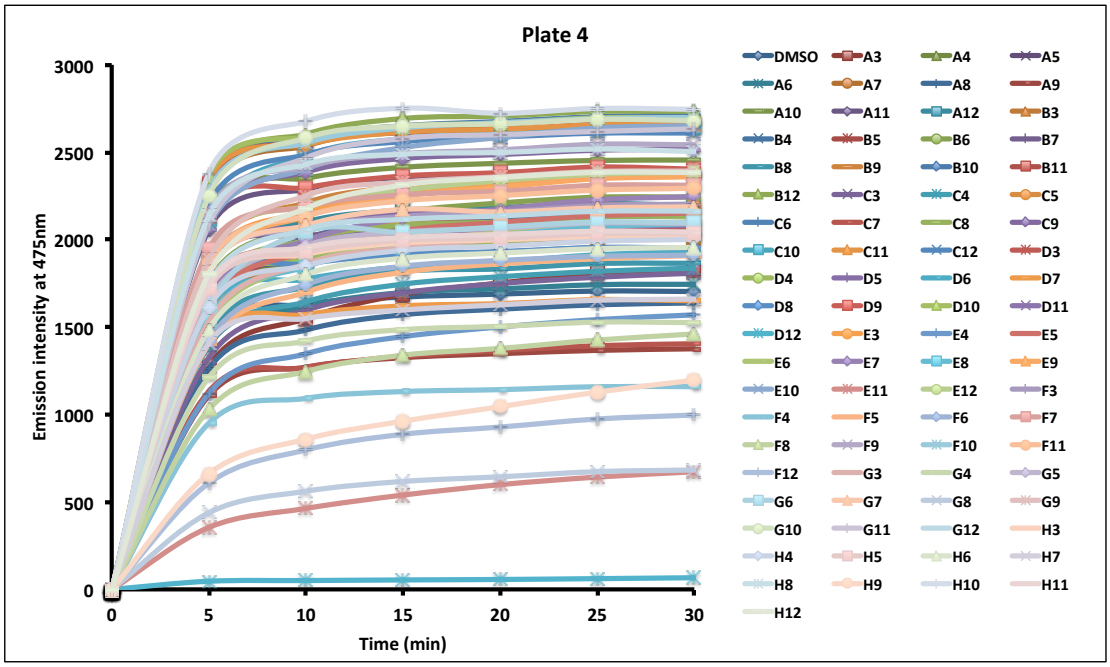
Plate 4
Emission intensity at 475nm
Time (min)
0
500
1000
1500
2000
2500
3000
0
5
10
15
20
25
30
DMSO A3 A4 A5
A6 A7 A8 A9
A10 A11 A12 B3
B4 B5 B6 B7
B8 B9 B10 B11
B12 C3 C4 C5
C6 C7 C8 C9
C10 C11 C12 D3
D4 D5 D6 D7
D8 D9 D10 D11
D12 E3 E4 E5
E6 E7 E8 E9
E10 E11 E12 F3
F4 F5 F6 F7
F8 F9 F10 F11
F12 G3 G4 G5
G6 G7 G8 G9
G10 G11 G12 H3
H4 H5 H6 H7
H8 H9 H10 H11
H12

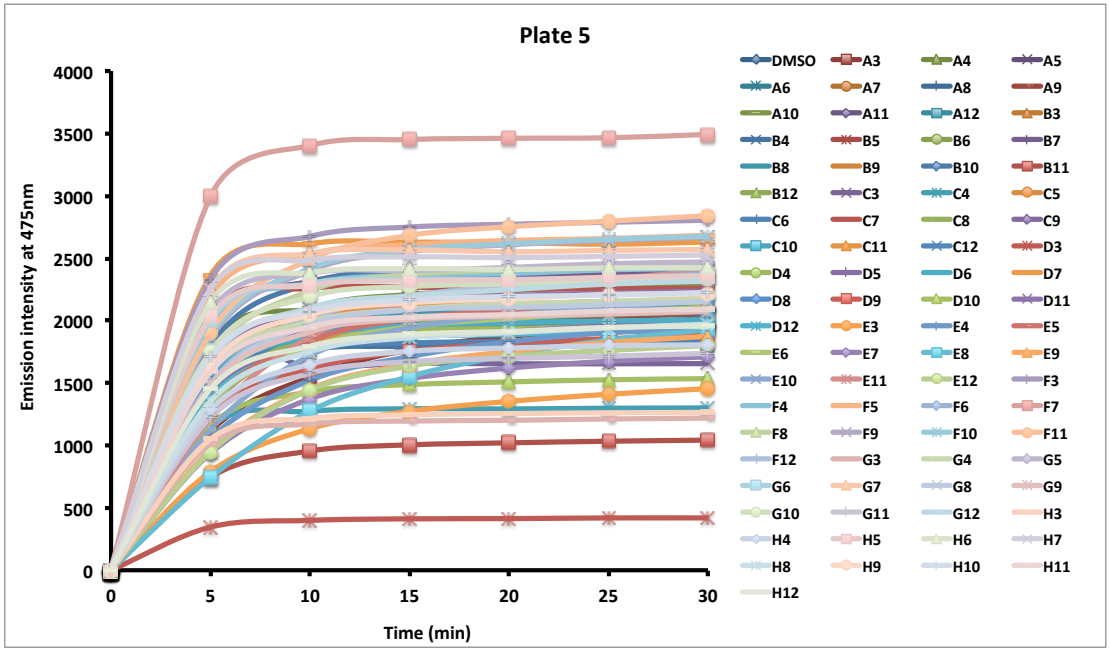
Plate 5
Emission intensity at 475nm
Time (min)
0
500
1000
1500
2000
2500
3000
3500
4000
0
5
10
15
20
25
30
DMSO A3 A4 A5
A6 A7 A8 A9
A10 A11 A12 B3
B4 B5 B6 B7
B8 B9 B10 B11
B12 C3 C4 C5
C6 C7 C8 C9
C10 C11 C12 D3
D4 D5 D6 D7
D8 D9 D10 D11
D12 E3 E4 E5
E6 E7 E8 E9
E10 E11 E12 F3
F4 F5 F6 F7
F8 F9 F10 F11
F12 G3 G4 G5
G6 G7 G8 G9
G10 G11 G12 H3
H4 H5 H6 H7
H8 H9 H10 H11
H12

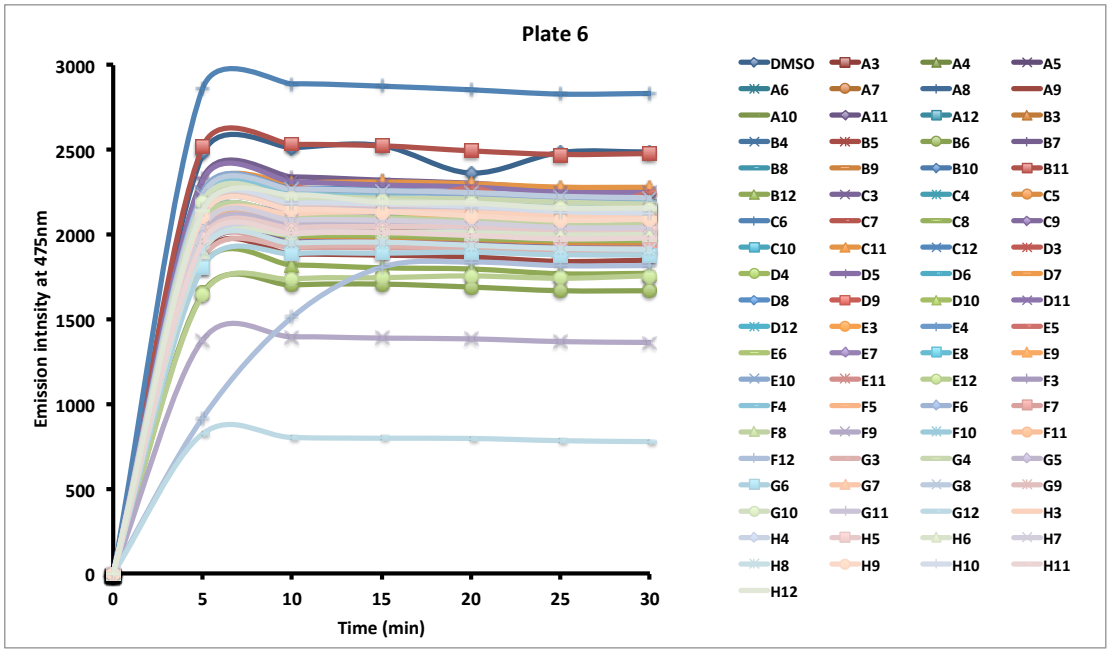
Plate 6
Emission intnsity at 475nm
Time (min)
0
500
1000
1500
2000
2500
3000
0
5
10
15
20
25
30
DMSO A3 A4 A5
A6 A7 A8 A9
A10 A11 A12 B3
B4 B5 B6 B7
B8 B9 B10 B11
B12 C3 C4 C5
C6 C7 C8 C9
C10 C11 C12 D3
D4 D5 D6 D7
D8 D9 D10 D11
D12 E3 E4 E5
E6 E7 E8 E9
E10 E11 E12 F3
F4 F5 F6 F7
F8 F9 F10 F11
F12 G3 G4 G5
G6 G7 G8 G9
G10 G11 G12 H3
H4 H5 H6 H7
H8 H9 H10 H11
H12

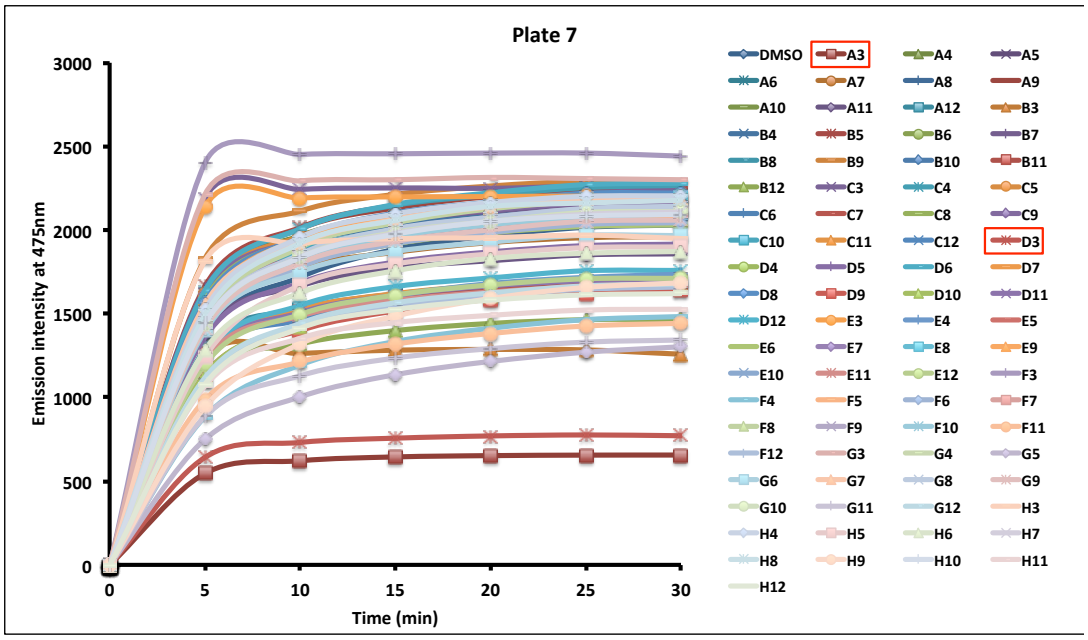
Plate 7
Emission intensity at 475nm
Time (min)
0
500
1000
1500
2000
2500
3000
0
5
10
15
20
25
30
DMSO A3 A4 A5
A6 A7 A8 A9
A10 A11 A12 B3
B4 B5 B6 B7
B8 B9 B10 B11
B12 C3 C4 C5
C6 C7 C8 C9
C10 C11 C12 D3
D4 D5 D6 D7
D8 D9 D10 D11
D12 E3 E4 E5
E6 E7 E8 E9
E10 E11 E12 F3
F4 F5 F6 F7
F8 F9 F10 F11
F12 G3 G4 G5
G6 G7 G8 G9
G10 G11 G12 H3
H4 H5 H6 H7
H8 H9 H10 H11
H12

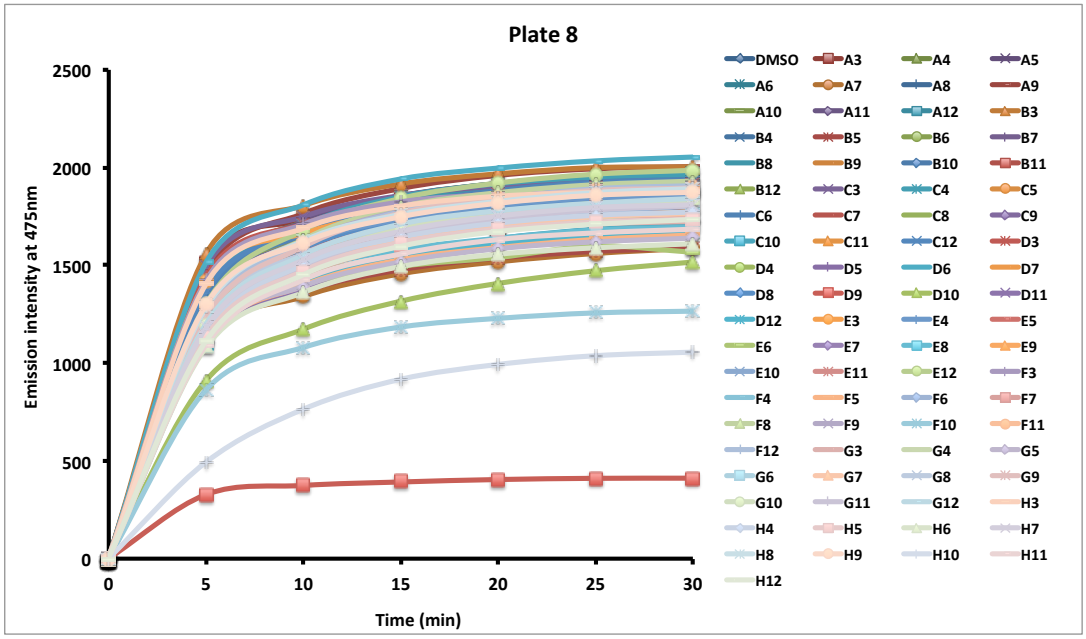
Plate 8
Emission intensity at 475nm
Time (min)
0
500
1000
1500
2000
2500
0
5
10
15
20
25
30
DMSO A3 A4 A5
A6 A7 A8 A9
A10 A11 A12 B3
B4 B5 B6 B7
B8 B9 B10 B11
B12 C3 C4 C5
C6 C7 C8 C9
C10 C11 C12 D3
D4 D5 D6 D7
D8 D9 D10 D11
D12 E3 E4 E5
E6 E7 E8 E9
E10 E11 E12 F3
F4 F5 F6 F7
F8 F9 F10 F11
F12 G3 G4 G5
G6 G7 G8 G9
G10 G11 G12 H3
H4 H5 H6 H7
H8 H9 H10 H11
H12

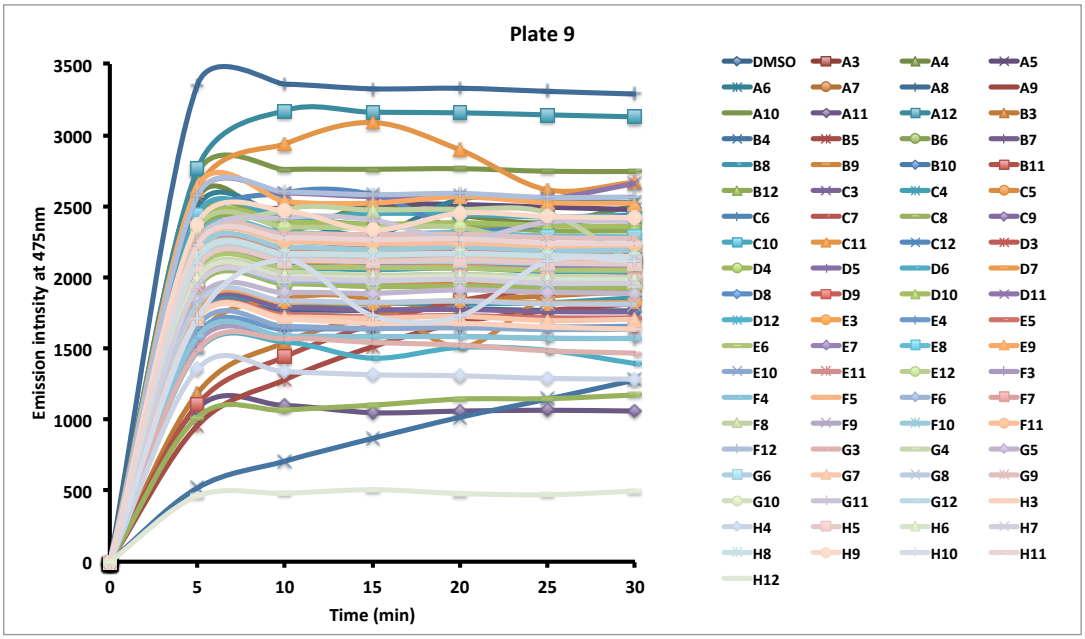
Plate 9
Emission intnsity at 475nm
Time (min)
0
500
1000
1500
2000
2500
3000
3500
0
5
10
15
20
25
30
DMSO A3 A4 A5
A6 A7 A8 A9
A10 A11 A12 B3
B4 B5 B6 B7
B8 B9 B10 B11
B12 C3 C4 C5
C6 C7 C8 C9
C10 C11 C12 D3
D4 D5 D6 D7
D8 D9 D10 D11
D12 E3 E4 E5
E6 E7 E8 E9
E10 E11 E12 F3
F4 F5 F6 F7
F8 F9 F10 F11
F12 G3 G4 G5
G6 G7 G8 G9
G10 G11 G12 H3
H4 H5 H6 H7
H8 H9 H10 H11
H12

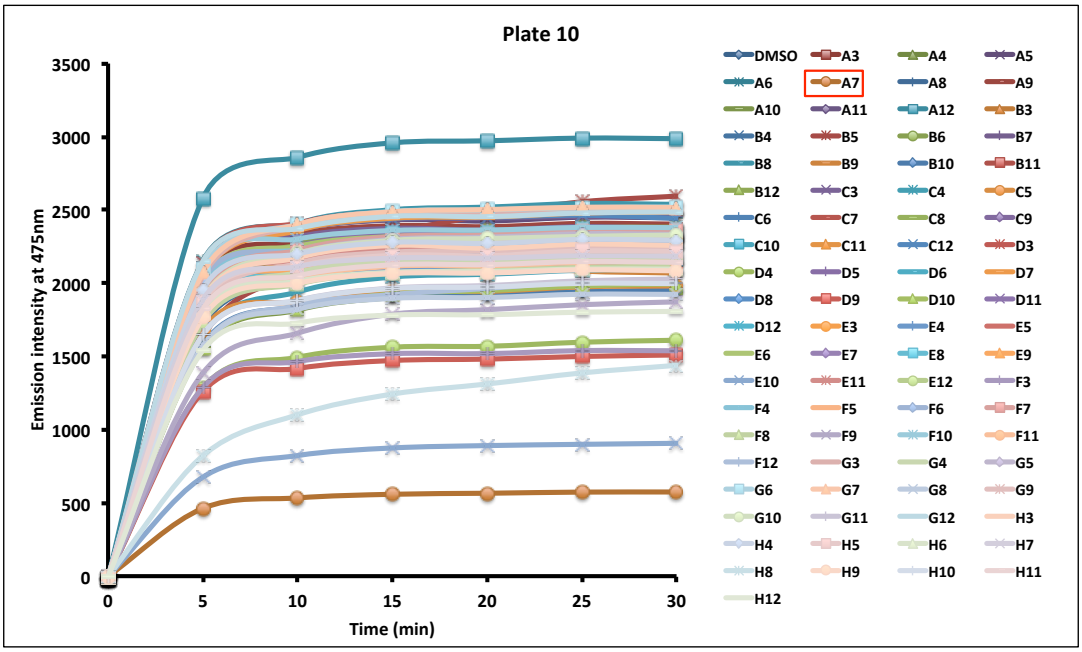
Plate 10
Emission intensity at 475nm
Time (min)
0
500
1000
1500
2000
2500
3000
3500
0
5
10
15
20
25
30
DMSO A3 A4 A5
A6 A7 A8 A9
A10 A11 A12 B3
B4 B5 B6 B7
B8 B9 B10 B11
B12 C3 C4 C5
C6 C7 C8 C9
C10 C11 C12 D3
D4 D5 D6 D7
D8 D9 D10 D11
D12 E3 E4 E5
E6 E7 E8 E9
E10 E11 E12 F3
F4 F5 F6 F7
F8 F9 F10 F11
F12 G3 G4 G5
G6 G7 G8 G9
G10 G11 G12 H3
H4 H5 H6 H7
H8 H9 H10 H11
H12

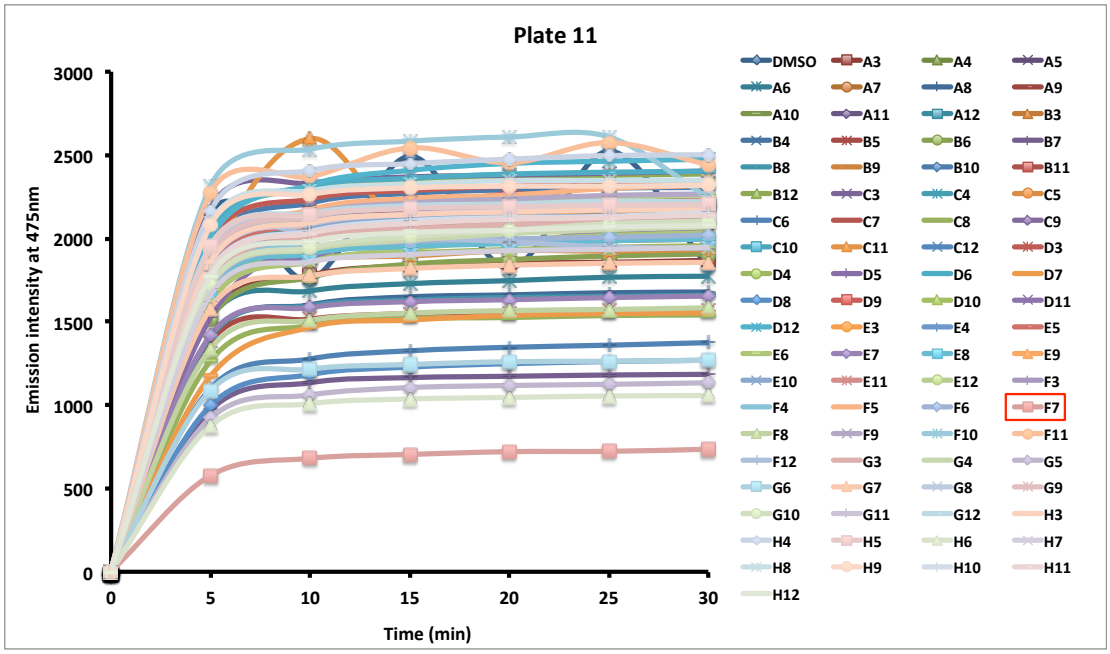
Plate 11
Emission intensity at 475nm
Time (min)
0
500
1000
1500
2000
2500
3000
0
5
10
15
20
25
30
DMSO A3 A4 A5
A6 A7 A8 A9
A10 A11 A12 B3
B4 B5 B6 B7
B8 B9 B10 B11
B12 C3 C4 C5
C6 C7 C8 C9
C10 C11 C12 D3
D4 D5 D6 D7
D8 D9 D10 D11
D12 E3 E4 E5
E6 E7 E8 E9
E10 E11 E12 F3
F4 F5 F6 F7
F8 F9 F10 F11
F12 G3 G4 G5
G6 G7 G8 G9
G10 G11 G12 H3
H4 H5 H6 H7
H8 H9 H10 H11
H12

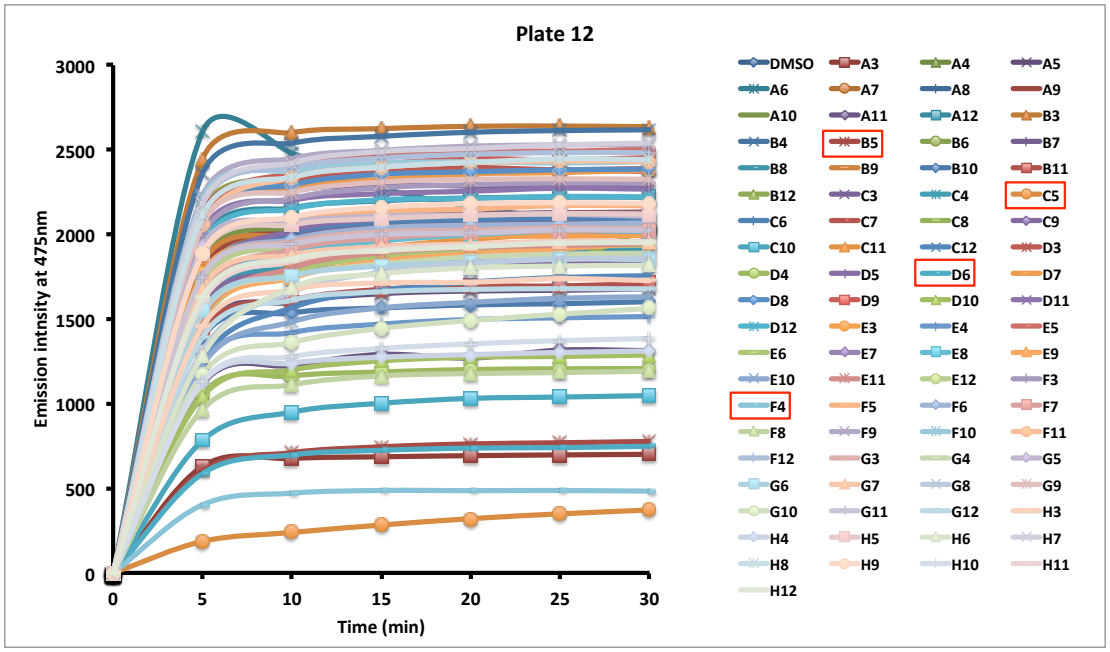
Plate 12
Emission intnsity at 475nm
Time (min)
0
500
1000
1500
2000
2500
3000
0
5
10
15
20
25
30
DMSO A3 A4 A5
A6 A7 A8 A9
A10 A11 A12 B3
B4 B5 B6 B7
B8 B9 B10 B11
B12 C3 C4 C5
C6 C7 C8 C9
C10 C11 C12 D3
D4 D5 D6 D7
D8 D9 D10 D11
D12 E3 E4 E5
E6 E7 E8 E9
E10 E11 E12 F3
F4 F5 F6 F7
F8 F9 F10 F11
F12 G3 G4 G5
G6 G7 G8 G9
G10 G11 G12 H3
H4 H5 H6 H7
H8 H9 H10 H11
H12

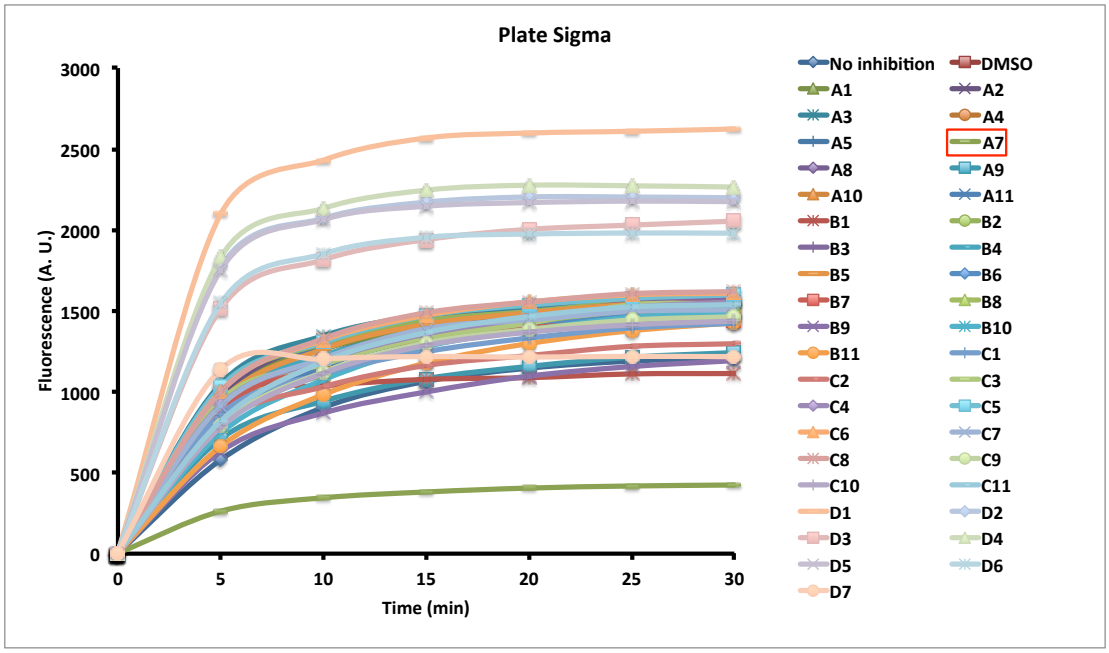
Plate Sigma
Fluorescence (A. U.)
3000
2500
2000
1500
1000
500
0
0
5
10
15
20
25
30
Time (min)
No inhibition
DMSO
A1
A2
A3
A4
A5
A7
A8
A9
A10
A11
B1
B2
B3
B4
B5
B6
B7
B8
B9
B10
B11
C1
C2
C3
C4
C5
C6
C7
C8
C9
C10
C11
D1
D2
D3
D4
D5
D6
D7

Bibliography

1. Y. Zheng, J. Zhou, S. M. Cooper Jr, C. Opoku-Temeng, A. M. De Brito and H. O. Sintim, *Tetrahedron*. DOI: 10.1016/j.tet.2015.10.073.
2. C. Bodenreider, D. Beer, T. H. Keller, S. Sonntag, D. Wen, L. Yap, Y. H. Yau, S. G. Shochat, D. Huang, T. Zhou, A. Caflisch, X. C. Su, K. Ozawa, G. Otting, S. G. Vasudevan, J. Lescar and S. P. Lim, *Anal. Biochem.*, 2009, **395**, 195-204.
3. K. Lewis, *Nat. Rev. Drug Discov.*, 2013, **12**, 371-387.
4. V. Nizet, *Sci. Transl. Med.*, 2015, **7**, 295ed298.
5. D. Kalia, G. Merey, S. Nakayama, Y. Zheng, J. Zhou, Y. Luo, M. Guo, B. T. Roembke and H. O. Sintim, *Chem. Soc. Rev.*, 2013, **42**, 305-341.
6. U. Romling, M. Gomelsky and M. Y. Galperin, *Mol. Microbiol.*, 2005, **57**, 629-639.
7. R. M. Corrigan and A. Gründling, *Nat. Rev. Microbiol.*, 2013, **11**, 513-524.
8. B. W. Davies, R. W. Bogard, T. S. Young and J. J. Mekalanos, *Cell*, 2012, **149**, 358-370.
9. E. J. Diner, D. L. Burdette, S. C. Wilson, K. M. Monroe, C. A. Kellenberger, M. Hyodo, Y. Hayakawa, M. C. Hammond and R. E. Vance, *Cell Rep.*, 2013, **3**, 1355-1361.
10. P. Ross, H. Weinhouse, Y. Aloni, D. Michaeli, P. Weinbergerohana, R. Mayer, S. Braun, E. Devroom, G. A. Vandermarel, J. H. Vanboom and M. Benziman, *Nature*, 1987, **325**, 279-281.
11. U. Romling, M. Y. Galperin and M. Gomelsky, *Microbiol. Mol. Biol. Rev.*, 2013, **77**, 1-52.
12. C. D. Boyd and G. A. O'Toole, *Annu. Rev. Cell Dev. Biol.*, 2012, **28**, 439-462.
13. A. J. Wolfe and K. L. Visick, *J. Bacteriol.*, 2008, **190**, 463-475.
14. R. Hengge, *Nat. Rev. Microbiol.*, 2009, **7**, 263-273.
15. N. Sudarsan, E. R. Lee, Z. Weinberg, R. H. Moy, J. N. Kim, K. H. Link and R. R. Breaker, *Science*, 2008, **321**, 411-413.
16. G. B. Hecht and A. Newton, *J. Bacteriol.*, 1995, **177**, 6223-6229.
17. R. Paul, S. Weiser, N. C. Amiot, C. Chan, T. Schirmer, B. Giese and U. Jenal, *Genes Dev.*, 2004, **18**, 715-727.
18. C. Chan, R. Paul, D. Samoray, N. C. Amiot, B. Giese, U. Jenal and T. Schirmer, *Proc. Natl. Acad. Sci. U. S. A.*, 2004, **101**, 17084-17089.
19. R. Tal, H. C. Wong, R. Calhoon, D. Gelfand, A. L. Fear, G. Volman, R. Mayer, P. Ross, D. Amikam, H. Weinhouse, A. Cohen, S. Sapir, P. Ohana and M. Benziman, *J. Bacteriol.*, 1998, **180**, 4416-4425.
20. N. De, M. V. A. S. Navarro, R. V. Raghavan and H. Sondermann, *J. Mol. Biol.*, 2009, **393**, 619-633.
21. R. Simm, M. Morr, A. Kader, M. Nimtz and U. Romling, *Mol. Microbiol.*, 2004, **53**, 1123-1134.

22. M. Tarnawski, T. R. Barends and I. Schlichting, *Acta Crystallogr. D. Biol. Crystallogr.*, 2015, **71**, 2158-2177.
23. J. L. Hunter, G. B. Severin, B. J. Koestler and C. M. Waters, *BMC Microbiol.*, 2014, **14**, 22.
24. D. Pérez-Mendoza, S. J. Coulthurst, S. Humphris, E. Campbell, M. Welch, I. K. Toth and G. P. Salmond, *Mol. Microbiol.*, 2011, **82**, 719-733.
25. N. De, M. Pirruccello, P. V. Krasteva, N. Bae, R. V. Raghavan and H. Sondermann, *PLoS Biol.*, 2008, **6**, e67.
26. M. W. Chen, M. Kotaka, C. Vonrhein, G. Bricogne, F. Rao, M. L. C. Chuah, D. Svergun, G. Schneider, Z.-X. Liang and J. Lescar, *J. Bacteriol.*, 2012, **194**, 4837-4846.
27. F. Rao, Y. Yang, Y. Qi and Z. X. Liang, *J. Bacteriol.*, 2008, **190**, 3622-3631.
28. A. Sundriyal, C. Massa, D. Samoray, F. Zehender, T. Sharpe, U. Jenal and T. Schirmer, *J. Biol. Chem.*, 2014, **289**, 6978-6990.
29. M. Y. Galperin, A. N. Nikolskaya and E. V. Koonin, *FEMS Microbiol. Lett.*, 2001, **204**, 213-214.
30. R. P. Ryan, Y. Fouhy, J. F. Lucey, L. C. Crossman, S. Spiro, Y. W. He, L. H. Zhang, S. Heeb, M. Camara, P. Williams and J. M. Dow, *Proc. Natl. Acad. Sci. U. S. A.*, 2006, **103**, 6712-6717.
31. A. L. Lovering, M. J. Capeness, C. Lambert, L. Hobley and R. E. Sockett, *MBio*, 2011, **2**, e00163-11.
32. D. Bellini, D. L. Caly, Y. McCarthy, M. Bumann, S. Q. An, J. M. Dow, R. P. Ryan and M. A. Walsh, *Mol. Microbiol.*, 2014, **91**, 26-38.
33. S. Rinaldo, A. Paiardini, V. Stelitano, P. Brunotti, L. Cervoni, S. Fernicola, C. Protano, M. Vitali, F. Cutruzzolà and G. Giardina, *J. Bacteriol.*, 2015, **197**, 1525-1535.
34. D. Amikam and M. Y. Galperin, *Bioinformatics*, 2006, **22**, 3-6.
35. D. A. Ryjenkov, R. Simm, U. Romling and M. Gomelsky, *J. Biol. Chem.*, 2006, **281**, 30310-30314.
36. J. C. Whitney, G. B. Whitfield, L. S. Marmont, P. Yip, A. M. Neculai, Y. D. Lobsanov, H. Robinson, D. E. Ohman and P. L. Howell, *J. Biol. Chem.*, 2015, **290**, 12451-12462.
37. M. Christen, B. Christen, M. G. Allan, M. Folcher, P. Jenö, S. Grzesiek and U. Jenal, *Proc. Natl. Acad. Sci. U. S. A.*, 2007, **104**, 4112-4117.
38. J. T. Pratt, R. Tamayo, A. D. Tischler and A. Camilli, *J. Biol. Chem.*, 2007, **282**, 12860-12870.
39. M. V. A. S. Navarro, N. De, N. Bae, Q. Wang and H. Sondermann, *Structure*, 2009, **17**, 1104-1116.
40. S. Ozaki, A. Schalch-Moser, L. Zumthor, P. Manfredi, A. Ebbensgaard, T. Schirmer and U. Jenal, *Mol. Microbiol.*, 2014, **94**, 580-594.
41. T. Su, S. Liu, K. Wang, K. Chi, D. Zhu, T. Wei, Y. Huang, L. Guo, W. Hu, S. Xu, Z. Lin and L. Gu, *J. Struct. Biol.*, 2015, **192**, 1-13.
42. B. Y. Matsuyama, P. V. Krasteva, C. Baraquet, C. S. Harwood, H. Sondermann and M. V. Navarro, *Proc. Natl. Acad. Sci. U. S. A.*, 2016, **113**, e209-218.

43. P. V. Krasteva, J. C. Fong, N. J. Shikuma, S. Beyhan, M. V. Navarro, F. H. Yildiz and H. Sondermann, *Science*, 2010, **327**, 866-868.
44. E. R. Lee, J. L. Baker, Z. Weinberg, N. Sudarsan and R. R. Breaker, *Science*, 2010, **329**, 845-848.
45. S. Nakayama, Y. Luo, J. Zhou, T. K. Dayie and H. O. Sintim, *Chem. Commun.*, 2012, **48**, 9059-9061.
46. C. C. de Carvalho, *Recent Pat. Biotechnol.*, 2012, **6**, 13-22.
47. H. C. Flemming and J. Wingender, *Nat. Rev. Microbiol.*, 2010, **8**, 623-633.
48. M. R. Hall, E. McGillicuddy and L. J. Kaplan, *Surg. Infect. (Larchmt)*, 2014, **15**, 1-7.
49. J. B. Lucks, S. A. Mortimer, C. Trapnell, S. J. Luo, S. Aviran, G. P. Schroth, L. Pachter, J. A. Doudna and A. P. Arkin, *Proc. Natl. Acad. Sci. U. S. A.*, 2011, **108**, 11063-11068.
50. A. Bridier, P. Sanchez-Vizuete, M. Guilbaud, J. C. Piard, M. Naïtali and R. Briandet, *Food Microbiol.*, 2015, **45**, 167-178.
51. K. Sambanthamoorthy, C. Luo, N. Pattabiraman, X. Feng, B. Koestler, C. M. Waters and T. J. Palys, *Biofouling*, 2014, **30**, 17-28.
52. K. Sambanthamoorthy, R. E. Sloup, V. Parashar, J. M. Smith, E. E. Kim, M. F. Semmelhack, M. B. Neiditch and C. M. Waters, *Antimicrob. Agents Chemother.*, 2012, **56**, 5202-5211.
53. D. G. Ha and G. A. O'Toole, *Microbiol. Spectr.*, 2015, **3**, MB-0003-2014.
54. D. O. Serra, A. M. Richter and R. Hengge, *J. Bacteriol.*, 2013, **195**, 5540-5554.
55. T. Fujiwara, K. Komoda, N. Sakurai, K. Tajima, I. Tanaka and M. Yao, *Biochem. Biophys. Res. Commun.*, 2013, **431**, 802-807.
56. A. Boyd and A. M. Chakrabarty, *J. Ind. Microbiol.*, 1995, **15**, 162-168.
57. K. M. Colvin, Y. Irie, C. S. Tart, R. Urbano, J. C. Whitney, C. Ryder, P. L. Howell, D. J. Wozniak and M. R. Parsek, *Environ. Microbiol.*, 2012, **14**, 1913-1928.
58. K. M. Colvin, V. D. Gordon, K. Murakami, B. R. Borlee, D. J. Wozniak, G. C. Wong and M. R. Parsek, *PLoS Pathog.*, 2011, **7**, e1001264.
59. V. T. Lee, J. M. Matewish, J. L. Kessler, M. Hyodo, Y. Hayakawa and S. Lory, *Mol. Microbiol.*, 2007, **65**, 1474-1484.
60. J. W. Hickman and C. S. Harwood, *Mol. Microbiol.*, 2008, **69**, 376-389.
61. A. Siitonen and M. Nurminen, *Infect. Immun.*, 1992, **60**, 3918-3920.
62. M. N. Guentzel and L. J. Berry, *Infect. Immun.*, 1975, **11**, 890-897.
63. C. Allison, N. Coleman, P. L. Jones and C. Hughes, *Infect. Immun.*, 1992, **60**, 4740-4746.
64. Y. Hou, d. F. Li and d. C. Wang, *Acta. Crystallogr. Sect. F. Struct. Biol. Cryst. Commun.*, 2013, **69**, 663-665.
65. J. Zhou, S. A. Lloyd and D. F. Blair, *Proc. Natl. Acad. Sci. U. S. A.*, 1998, **95**, 6436-6441.
66. J. P. Armitage and R. M. Berry, *Cell*, 2010, **141**, 24-26.
67. C. Baraquet and C. S. Harwood, *Proc. Natl. Acad. Sci. U. S. A.*, 2013, **110**, 18478-18483.

68. C. M. Toutain, M. E. Zegans and G. A. O'Toole, *J. Bacteriol.*, 2005, **187**, 771-777.
69. L. L. McCarter and M. Gomelsky, *J. Bacteriol.*, 2015, **197**, 406-409.
70. S. L. Kuchma, N. J. Delalez, L. M. Filkins, E. A. Snavely, J. P. Armitage and G. A. O'Toole, *J. Bacteriol.*, 2015, **197**, 420-430.
71. A. D. Tischler and A. Camilli, *Infect. Immun.*, 2005, **73**, 5873-5882.
72. X. Zogaj, G. C. Wyatt and K. E. Klose, *Infect. Immun.*, 2012, **80**, 4239-4247.
73. J. Engel and P. Balachandran, *Curr. Opin. Microbiol.*, 2009, **12**, 61-66.
74. S. L. Gellatly and R. E. Hancock, *Pathog. Dis.*, 2013, **67**, 159-173.
75. J. A. Moscoso, H. Mikkelsen, S. Heeb, P. Williams and A. Filloux, *Environ. Microbiol.*, 2011, **13**, 3128-3138.
76. P. Ohana, D. P. Delmer, R. W. Carlson, J. Glushka, P. Azadi, T. Bacic and M. Benziman, *Plant Cell Physiol.*, 1998, **39**.
77. P. Ohana, D. P. Delmer, G. Volman and M. Benziman, *Plant Cell Physiol.*, 1998, **39**, 153-159.
78. P. Ross, R. Mayer, H. Weinhouse, D. Amikam, Y. Huggirat, M. Benziman, E. de Vroom, A. Fidder, P. de Paus and L. A. Sliedregt, *J. Biol. Chem.*, 1990, **265**, 18933-18943.
79. J. Wang, J. Zhou, G. P. Donaldson, S. Nakayama, L. Yan, Y. F. Lam, V. T. Lee and H. O. Sintim, *J. Am. Chem. Soc.*, 2011, **133**, 9320-9330.
80. G. Witte, S. Hartung, K. Buettner and K.-P. Hopfner, *Mol. Cell*, 2008, **30**, 167-178.
81. M. Bejerano-Sagie, Y. Oppenheimer-Shaanan, I. Berlatzky, A. Rouvinski, M. Meyerovich and S. Ben-Yehuda, *Cell*, 2006, **125**, 679-690.
82. Y. Oppenheimer-Shaanan, E. Wexselblatt, J. Katzhendler, E. Yavin and S. Ben-Yehuda, *EMBO Rep.*, 2011, **12**, 594-601.
83. L. Zhang, W. Li and Z. G. He, *J. Biol. Chem.*, 2013, **288**, 3085-3096.
84. Y. Bai, J. Yang, T. M. Zarrella, Y. Zhang, D. W. Metzger and G. Bai, *J. Bacteriol.*, 2014, **196**, 614-623.
85. C. E. Witte, A. T. Whiteley, T. P. Burke, J.-D. Sauer, D. A. Portnoy and J. J. Woodward, *Mbio*, 2013, **4**, e00282-13.
86. J. J. Woodward, A. T. Iavarone and D. A. Portnoy, *Science*, 2010, **328**, 1703-1705.
87. F. M. Mehne, K. Schröder-Tittmann, R. T. Eijlander, C. Herzberg, L. Hewitt, V. Kaever, R. J. Lewis, O. P. Kuipers, K. Tittmann and J. Stülke, *J. Biol. Chem.*, 2014, **289**, 21098-21107.
88. T. Kamegaya, K. Kuroda and Y. Hayakawa, *Nagoya. J. Med. Sci.*, 2011, **73**, 49-57.
89. Y. Bai, J. Yang, L. E. Eisele, A. J. Underwood, B. J. Koestler, C. M. Waters, D. W. Metzger and G. Bai, *J. Bacteriol.*, 2013, **195**, 5123-5132.
90. Y. Bai, J. Yang, X. Zhou, X. Ding, L. E. Eisele and G. Bai, *PLoS One*, 2012, **7**.
91. F. Rao, R. Y. See, D. Zhang, D. C. Toh, Q. Ji and Z.-X. Liang, *J. Biol. Chem.*, 2010, **285**, 473-482.
92. R. M. Corrigan, J. C. Abbott, H. Burhenne, V. Kaever and A. Grüendling, *PLoS Pathog.*, 2011, **7**, e1002217.

93. K. Manikandan, V. Sabareesh, N. Singh, K. Saigal, U. Mechold and K. M. Sinha, *PLoS One*, 2014, **9**, e86096.
94. M. Ye, J. J. Zhang, X. Fang, G. B. Lawlis, B. Troxell, Y. Zhou, M. Gomelsky, Y. Lou and X. F. Yang, *Infect. Immun.*, 2014, **82**, 1840-1849.
95. T. N. Huynh, S. Luo, D. Pensinger, J. D. Sauer, L. Tong and J. J. Woodward, *Proc. Natl. Acad. Sci. U. S. A.*, 2015, **112**, e747-756.
96. R. M. Corrigan, I. Campeotto, T. Jeganathan, K. G. Roelofs, V. T. Lee and A. Gründling, *Proc. Natl. Acad. Sci. U. S. A.*, 2013, **110**, 9084-9089.
97. I. Campeotto, Y. Zhang, M. G. Mladenov, P. S. Freemont and A. Gründling, *J. Biol. Chem.*, 2014, **290**, 2888-2901.
98. J. Gundlach, A. Dickmanns, K. Schröder-Tittmann, P. Neumann, J. Kaesler, J. Kampf, C. Herzberg, E. Hammer, F. Schwede, V. Kaever, K. Tittmann, J. Stülke and R. Ficner, *J. Biol. Chem.*, 2014, **290**, 3069-3080.
99. J. W. Nelson, N. Sudarsan, K. Furukawa, Z. Weinberg, J. X. Wang and R. R. Breaker, *Nat. Chem. Biol.*, 2013, **9**, 834-839.
100. A. Ren and D. J. Patel, *Nat. Chem. Biol.*, 2014, **10**, 780-786.
101. A. Gao and A. Serganov, *Nat. Chem. Biol.*, 2014, **10**, 787-792.
102. C. A. Kellenberger, C. Chen, A. T. Whiteley, D. A. Portnoy and M. C. Hammond, *J. Am. Chem. Soc.*, 2015, **137**, 6432-6435.
103. F. M. Mehne, K. Gunka, H. Eilers, C. Herzberg, V. Kaever and J. Stülke, *J. Biol. Chem.*, 2013, **288**, 2004-2017.
104. J. Yang, Y. Bai, Y. Zhang, V. D. Gabrielle, L. Jin and G. Bai, *Mol. Microbiol.*, 2014, **93**, 65-79.
105. J. Zhou, D. A. Sayre, Y. Zheng, H. Szmacinski and H. O. Sintim, *Anal. Chem.*, 2014, **86**, 2412-2420.
106. Y. Zheng, J. Zhou, D. A. Sayre and H. O. Sintim, *Chem. Commun. (Camb)*, 2014, **50**, 11234-11237.
107. M. Müller, T. Deimling, K. P. Hopfner and G. Witte, *Biochem. J.*, 2015, **469**, 367-374.
108. C. Opoku-Temeng and H. O. Sintim, *Chem. Commun. (Camb)*, 2016.
109. R. M. Corrigan, L. Bowman, A. R. Willis, V. Kaever and A. Gründling, *J. Biol. Chem.*, 2015, **290**, 5826-5839.
110. J. Gao, J. Tao, W. Liang, M. Zhao, X. Du, S. Cui, H. Duan, B. Kan, X. Su and Z. Jiang, *Cell Res.*, 2015, **25**, 539-550.
111. C. A. Shanahan, B. L. Gaffney, R. A. Jones and S. A. Strobel, *J. Am. Chem. Soc.*, 2011, **133**, 15578-15592.
112. C. A. Kellenberger, S. C. Wilson, S. F. Hickey, T. L. Gonzalez, Y. Su, Z. F. Hallberg, T. F. Brewer, A. T. Iavarone, H. K. Carlson, Y. F. Hsieh and M. C. Hammond, *Proc. Natl. Acad. Sci. U. S. A.*, 2015, **112**, 5383-5388.
113. J. W. Nelson, N. Sudarsan, G. E. Phillips, S. Stav, C. E. Lünse, P. J. McCown and R. R. Breaker, *Proc. Natl. Acad. Sci. U. S. A.*, 2015, **112**, 5389-5394.
114. A. Ablasser, M. Goldeck, T. Cavlar, T. Deimling, G. Witte, I. Roehl, K.-P. Hopfner, J. Ludwig and V. Hornung, *Nature*, 2013, **498**, 380-+.
115. X. Zhang, H. Shi, J. Wu, X. Zhang, L. Sun, C. Chen and Z. J. Chen, *Mol. Cell*, 2013, **51**, 226-235.

116. P. Gao, M. Ascano, Y. Wu, W. Barchet, B. L. Gaffney, T. Zillinger, A. A. Serganov, Y. Liu, R. A. Jones, G. Hartmann, T. Tuschl and D. J. Patel, *Cell*, 2013, **153**, 1094-1107.
117. J. Wu, L. Sun, X. Chen, F. Du, H. Shi, C. Chen and Z. J. Chen, *Science*, 2013, **339**, 826-830.
118. L. Sun, J. Wu, F. Du, X. Chen and Z. J. Chen, *Science*, 2013, **339**, 786-791.
119. L. Li, Q. Yin, P. Kuss, Z. Maliga, J. L. Millán, H. Wu and T. J. Mitchison, *Nat. Chem. Biol.*, 2014, **10**, 1043-1048.
120. K. Kato, H. Nishimasu, S. Okudaira, E. Mihara, R. Ishitani, J. Takagi, J. Aoki and O. Nureki, *Proc. Natl. Acad. Sci. U. S. A.*, 2012, **109**, 16876-16881.
121. X. Zhang, J. Wu, F. Du, H. Xu, L. Sun, Z. Chen, C. A. Brautigam and Z. J. Chen, *Cell Rep.*, 2014, **6**, 421-430.
122. V. Hornung and E. Latz, *Nat. Rev. Immunol.*, 2010, **10**, 123-130.
123. Y. Tanaka and Z. J. Chen, *Sci. Signal.*, 2012, **5**, ra20.
124. T. Abe, A. Harashima, T. Xia, H. Konno, K. Konno, A. Morales, J. Ahn, D. Gutman and G. N. Barber, *Mol. Cell*, 2013, **50**, 5-15.
125. D. L. Burdette, K. M. Monroe, K. Sotelo-Troha, J. S. Iwig, B. Eckert, M. Hyodo, Y. Hayakawa and R. E. Vance, *Nature*, 2011, **478**, 515-518.
126. J. R. Barker, B. J. Koestler, V. K. Carpenter, D. L. Burdette, C. M. Waters, R. E. Vance and R. H. Valdivia, *MBio*, 2013, **4**, e00018-00013.
127. C. Pozzi, E. M. Waters, J. K. Rudkin, C. R. Schaeffer, A. J. Lohan, P. Tong, B. J. Loftus, G. B. Pier, P. D. Fey, R. C. Massey and J. P. O'Gara, *PLoS Pathog.*, 2012, **8**, e1002626.
128. V. Dengler, N. McCallum, P. Kiefer, P. Christen, A. Patrignani, J. A. Vorholt, B. Berger-Baechi and M. M. Senn, *PLoS One*, 2013, **8**, e73512.
129. K. H. Cho and S. O. Kang, *PLoS One*, 2013, **8**, e69425.
130. K. Tadmor, Y. Pozniak, T. Burg Golani, L. Lobel, M. Brenner, N. Sigal and A. A. Herskovits, *Front. Cell Infect. Microbiol.*, 2014, **4**, 16.
131. T. Yamamoto, H. Hara, K. Tsuchiya, S. Sakai, R. Fang, M. Matsuura, T. Nomura, F. Sato, M. Mitsuyama and I. Kawamura, *Infect. Immun.*, 2012, **80**, 2323-2332.
132. M. Kaplan Zeevi, N. S. Shafir, S. Shaham, S. Friedman, N. Sigal, R. Nir Paz, I. G. Boneca and A. A. Herskovits, *J. Bacteriol.*, 2013, **195**, 5250-5261.
133. W. M. Smith, P. Thi Huong, L. Lei, J. Dou, A. H. Soomro, S. A. Beatson, G. A. Dykes and M. S. Turner, *Appl. Environ. Microbiol.*, 2012, **78**, 7753-7759.
134. B. Du, W. Ji, H. An, Y. Shi, Q. Huang, Y. Cheng, Q. Fu, H. Wang, Y. Yan and J. Sun, *Microbiol. Res.*, 2014.
135. K. Parvatiyar, Z. Zhang, R. M. Teles, S. Ouyang, Y. Jiang, S. S. Iyer, S. A. Zaver, M. Schenk, S. Zeng, W. Zhong, Z.-J. Liu, R. L. Modlin, Y.-J. Liu and G. Cheng, *Nat. Immunol.*, 2012, **13**, 1155-1161.
136. K. A. Archer, J. Durack and D. A. Portnoy, *PLoS Pathog.*, 2014, **10**, e1003861-e1003861.
137. G. Yi, V. P. Brendel, C. Shu, P. Li, S. Palanathan and C. C. Kao, *PLoS One*, 2013, **8**, e77846.
138. D. W. Green, *Expert. Opin. Ther. Targets*, 2002, **6**, 1-19.

139. M. Mac, A. Danel, K. Kizior, P. Nowak, A. Karocki and B. Tokarczyk, *Phys. Chem. Chem. Phys.*, 2003, **5**, 988-997.
140. W. F. McCoy, J. D. Bryers, J. Robbins and J. W. Costerton, *Can. J. Microbiol.*, 1981, **27**, 910-917.
141. A. Simeonov, A. Jadhav, C. J. Thomas, Y. Wang, R. Huang, N. T. Southall, P. Shinn, J. Smith, C. P. Austin, D. S. Auld and J. Inglese, *J. Med. Chem.*, 2008, **51**, 2363-2371.
142. A. Jadhav, R. S. Ferreira, C. Klumpp, B. T. Mott, C. P. Austin, J. Inglese, C. J. Thomas, D. J. Maloney, B. K. Shoichet and A. Simeonov, *J. Med. Chem.*, 2010, **53**, 37-51.
143. T. Hampton, *JAMA*, 2013, **310**, 1661-1663.
144. A. L. Vaccarino, D. Paul, P. K. Mukherjee, E. B. Rodríguez de Turco, V. L. Marcheselli, L. Xu, M. L. Trudell, J. M. Minguez, M. P. Matía, C. Sunkel, J. Alvarez-Builla and N. G. Bazan, *Bioorg. Med. Chem.*, 2007, **15**, 2206-2215.
145. D. Kalia, G. Merey, S. Nakayama, Y. Zheng, J. Zhou, Y. Luo, M. Guo, B. T. Roembke and H. O. Sintim, *Chem. Soc. Rev.*, 2013, **42**, 305-341.
146. U. Romling, *Sci. Signal.*, 2008, **1**, pe39.
147. R. M. Corrigan and A. Grundling, *Nat Rev Microbiol*, 2013, **11**, 513-524.
148. B. Dey and W. R. Bishai, *Semin. Immunol.*, 2014.
149. A. G. Bowie, *Nat. Immunol.*, 2012, **13**, 1137-1139.
150. K. Parvatiyar, Z. Zhang, R. M. Teles, S. Ouyang, Y. Jiang, S. S. Iyer, S. A. Zaver, M. Schenk, S. Zeng, W. Zhong, Z. J. Liu, R. L. Modlin, Y. J. Liu and G. Cheng, *Nat. Immunol.*, 2012, **13**, 1155-1161.
151. J. J. Woodward, A. T. Iavarone and D. A. Portnoy, *Science*, 2010, **328**, 1703-1705.
152. K. A. Fitzgerald, S. M. McWhirter, K. L. Faia, D. C. Rowe, E. Latz, D. T. Golenbock, A. J. Coyle, S. M. Liao and T. Maniatis, *Nat. Immunol.*, 2003, **4**, 491-496.
153. B. Dey, R. J. Dey, L. S. Cheung, S. Pokkali, H. Guo, J. H. Lee and W. R. Bishai, *Nat. Med.*, 2015, **21**, 401-406.
154. A. C. Collins, H. Cai, T. Li, L. H. Franco, X. D. Li, V. R. Nair, C. R. Scharn, C. E. Stamm, B. Levine, Z. J. Chen and M. U. Shiloh, *Cell Host Microbe*, 2015, **17**, 820-828.
155. B. Dey, R. J. Dey, L. S. Cheung, S. Pokkali, H. Guo, J. H. Lee and W. R. Bishai, *Nat. Med.*, 2015, **21**, 401-406.
156. D. Gao, J. Wu, Y. T. Wu, F. Du, C. Aroh, N. Yan, L. Sun and Z. J. Chen, *Science*, 2013, **341**, 903-906.
157. Y. Zhang, L. Yeruva, A. Marinov, D. Prantner, P. B. Wyrick, V. Lupashin and U. M. Nagarajan, *J. Immunol.*, 2014, **193**, 2394-2404.
158. R. Wassermann, M. F. Gulen, C. Sala, S. G. Perin, Y. Lou, J. Rybniker, J. L. Schmid-Burgk, T. Schmidt, V. Hornung, S. T. Cole and A. Ablasser, *Cell Host Microbe*, 2015, **17**, 799-810.
159. X. D. Li, J. Wu, D. Gao, H. Wang, L. Sun and Z. J. Chen, *Science*, 2013, **341**, 1390-1394.
160. L. Sun, J. Wu, F. Du, X. Chen and Z. J. Chen, *Science*, 2013, **339**, 786-791.

161. J. Wu, L. Sun, X. Chen, F. Du, H. Shi, C. Chen and Z. J. Chen, *Science*, 2013, **339**, 826-830.
162. K. Hansen, T. Prabakaran, A. Laustsen, S. E. Jorgensen, S. H. Rahbaek, S. B. Jensen, R. Nielsen, J. H. Leber, T. Decker, K. A. Horan, M. R. Jakobsen and S. R. Paludan, *EMBO J.*, 2014, **33**, 1654-1666.
163. X. Lahaye, T. Satoh, M. Gentili, S. Cerboni, C. Conrad, I. Hurbain, A. El Marjou, C. Lacabaratz, J. D. Lelievre and N. Manel, *Immunity*, 2013, **39**, 1132-1142.
164. M. H. Orzalli, N. A. DeLuca and D. M. Knipe, *Proc. Natl. Acad. Sci. U. S. A.*, 2012, **109**, e3008-3017.
165. T. Li, J. Chen and I. M. Cristea, *Cell Host Microbe*, 2013, **14**, 591-599.
166. J. J. Wu, W. Li, Y. Shao, D. Avey, B. Fu, J. Gillen, T. Hand, S. Ma, X. Liu, W. Miley, A. Konrad, F. Neipel, M. Sturzl, D. Whitby, H. Li and F. Zhu, *Cell Host Microbe*, 2015, **18**, 333-344.
167. L. Lau, E. E. Gray, R. L. Brunette and D. B. Stetson, *Science*, 2015, **350**, 568-571.
168. G. Postic, A. Danchin and U. Mechold, *RNA*, 2012, **18**, 155-165.
169. K. H. Cho and S. O. Kang, *PLoS One*, 2013, **8**, e69425.
170. F. Rao, R. Y. See, D. Zhang, D. C. Toh, Q. Ji and Z. X. Liang, *J. Biol. Chem.*, 2010, **285**, 473-482.
171. R. Srivastav, D. Kumar, A. Grover, A. Singh, B. A. Manjasetty, R. Sharma and B. Taneja, *Nucleic Acids Res.*, 2014, **42**, 7894-7910.
172. G. Lamichhane, M. Zignol, N. J. Blades, D. E. Geiman, A. Dougherty, J. Grosset, K. W. Broman and W. R. Bishai, *Proc. Natl. Acad. Sci. U. S. A.*, 2003, **100**, 7213-7218.
173. R. M. Corrigan, J. C. Abbott, H. Burhenne, V. Kaever and A. Grundling, *PLoS Pathog.*, 2011, **7**, e1002217.
174. C. E. Witte, A. T. Whiteley, T. P. Burke, J. D. Sauer, D. A. Portnoy and J. J. Woodward, *MBio*, 2013, **4**, e00282-00213.
175. L. Li, Q. Yin, P. Kuss, Z. Maliga, J. L. Millan, H. Wu and T. J. Mitchison, *Nat. Chem. Biol.*, 2014, **10**, 1043-1048.
176. P. Gao, M. Ascano, Y. Wu, W. Barchet, B. L. Gaffney, T. Zillinger, A. A. Serganov, Y. Liu, R. A. Jones, G. Hartmann, T. Tuschl and D. J. Patel, *Cell*, 2013, **153**, 1094-1107.
177. P. J. Kranzusch, A. S. Lee, S. C. Wilson, M. S. Solovykh, R. E. Vance, J. M. Berger and J. A. Doudna, *Cell*, 2014, **158**, 1011-1021.
178. K. Kubota, K. Nakahara, T. Ohtsuka, S. Yoshida, J. Kawaguchi, Y. Fujita, Y. Ozeki, A. Hara, C. Yoshimura, H. Furukawa, H. Haruyama, K. Ichikawa, M. Yamashita, T. Matsuoka and Y. Iijima, *J Biol Chem*, 2004, **279**, 37832-37841.
179. J. Rorbach, T. J. Nicholls and M. Minczuk, *Nucleic Acids Res.*, 2011, **39**, 7750-7763.
180. F. Bruni, P. Gramegna, J. M. Oliveira, R. N. Lightowlers and Z. M. Chrzanowska-Lightowlers, *PLoS One*, 2013, **8**, e64670.
181. B. Dey and W. R. Bishai, *Semin. Immunol.*, 2014, **26**, 486-496.

182. M. J. Kim, H. C. Wainwright, M. Locketz, L. G. Bekker, G. B. Walther, C. Dittrich, A. Visser, W. Wang, F. F. Hsu, U. Wiehart, L. Tsenova, G. Kaplan and D. G. Russell, *EMBO Mol. Med.*, 2010, **2**, 258-274.
183. H. Rachman, M. Strong, T. Ulrichs, L. Grode, J. Schuchhardt, H. Mollenkopf, G. A. Kosmiadi, D. Eisenberg and S. H. Kaufmann, *Infect. Immun.*, 2006, **74**, 1233-1242.
184. H. Konno, K. Konno and G. N. Barber, *Cell*, 2013, **155**, 688-698.
185. Q. Liang, G. J. Seo, Y. J. Choi, M. J. Kwak, J. Ge, M. A. Rodgers, M. Shi, B. J. Leslie, K. P. Hopfner, T. Ha, B. H. Oh and J. U. Jung, *Cell Host Microbe*, 2014, **15**, 228-238.
186. H. Malen, S. Pathak, T. Softeland, G. A. de Souza and H. G. Wiker, *BMC Microbiol.*, 2010, **10**, 132.
187. A. Ablasser, J. L. Schmid-Burgk, I. Hemmerling, G. L. Horvath, T. Schmidt, E. Latz and V. Hornung, *Nature*, 2013, **503**, 530-534.
188. R. H. Silverman and S. R. Weiss, *J. Interferon Cytokine Res.*, 2014, **34**, 455-463.
189. V. Hornung, R. Hartmann, A. Ablasser and K. P. Hopfner, *Nat. Rev. Immunol.*, 2014, **14**, 521-528.
190. X. Cai, Y. H. Chiu and Z. J. Chen, *Mol. Cell.*, 2014, **54**, 289-296.
191. Z. Zhang, B. L. Gaffney and R. A. Jones, *J. Am. Chem. Soc.*, 2004, **126**, 16700-16701.
192. P. D. Newell, R. D. Monds and G. A. O'Toole, *Proc. Natl. Acad. Sci. U. S. A.*, 2009, **106**, 3461-3466.
193. A. Boehm, M. Kaiser, H. Li, C. Spangler, C. A. Kasper, M. Ackermann, V. Kaever, V. Sourjik, V. Roth and U. Jenal, *Cell*, 2010, **141**, 107-116.
194. H. Kulasakara, V. Lee, A. Brencic, N. Liberati, J. Urbach, S. Miyata, D. G. Lee, A. N. Neely, M. Hyodo, Y. Hayakawa, F. M. Ausubel and S. Lory, *Proc. Natl. Acad. Sci. U. S. A.*, 2006, **103**, 2839-2844.
195. N. J. Shikuma, J. C. Fong and F. H. Yildiz, *PLoS Pathog*, 2012, **8**, e1002719.
196. S. Lindenberg, G. Klauck, C. Pesavento, E. Klauck and R. Hengge, *EMBO J.*, 2013, **32**, 2001-2014.
197. A. B. Roy, O. E. Petrova and K. Sauer, *J. Bacteriol.*, 2012, **194**, 2904-2915.
198. Y. Li, S. Heine, M. Entian, K. Sauer and N. Frankenberg-Dinkel, *J. Bacteriol.*, 2013, **195**, 3531-3542.
199. A. J. Schmidt, D. A. Ryjenkov and M. Gomelsky, *J. Bacteriol.*, 2005, **187**, 4774-4781.
200. J. L. Burns, D. D. Deer and E. E. Weinert, *Mol. Biosyst.*, 2014, **10**, 2823-2826.
201. J. R. Tuckerman, G. Gonzalez, E. H. Sousa, X. Wan, J. A. Saito, M. Alam and M. A. Gilles-Gonzalez, *Biochemistry*, 2009, **48**, 9764-9774.
202. G. Enomoto, Ni-Ni-Win, R. Narikawa and M. Ikeuchi, *Proc. Natl. Acad. Sci. U. S. A.*, 2015, **112**, 8082-8087.
203. P. Savakis, S. De Causmaecker, V. Angerer, U. Ruppert, K. Anders, L. O. Essen and A. Wilde, *Mol. Microbiol.*, 2012, **85**, 239-251.
204. T. Lahiri, B. Luan, D. P. Raleigh and E. M. Boon, *Biochemistry*, 2014, **53**, 2126-2135.
205. L. Plate and M. A. Marletta, *Mol. Cell*, 2012, **46**, 449-460.

206. A. Kader, R. Simm, U. Gerstel, M. Morr and U. Römling, *Mol. Microbiol.*, 2006, **60**, 602-616.
207. J. Overhage, M. Bains, M. D. Brazas and R. E. Hancock, *J. Bacteriol.*, 2008, **190**, 2671-2679.
208. F. Rao, Y. Qi, H. S. Chong, M. Kotaka, B. Li, J. Li, J. Lescar, K. Tang and Z.-X. Liang, *J. Bacteriol.*, 2009, **191**, 4722-4731.
209. N. Mesaros, P. Nordmann, P. Plesiat, M. Roussel-Delvallez, J. Van Eldere, Y. Glupczynski, Y. Van Laethem, F. Jacobs, P. Lebecque, A. Malfroot, P. M. Tulkens and F. Van Bambeke, *Clin. Microbiol. Infect.*, 2007, **13**, 560-578.
210. P. Vicini, L. Amoretti, V. Ballabeni, M. Tognolini and E. Barocelli, *Bioorg. Med. Chem.*, 2000, **8**, 2355-2358.
211. P. Gopinath, K. Ramalingam, K. M. Muraleedharan and D. Karunagaran, *MedChemComm*, 2013, **4**, 749-752.
212. S. O. Abdul-Hay, T. D. Bannister, H. Wang, M. D. Cameron, T. R. Caulfield, A. Masson, J. Bertrand, E. A. Howard, M. P. McGuire, U. Crisafulli, T. R. Rosenberry, C. L. Topper, C. R. Thompson, S. C. Schürer, F. Madoux, P. Hodder and M. A. Leissring, *ACS Chem. Biol.*, 2015, **10**, 2716-2724.
213. Z. Li, Y. Pan, W. Zhong, Y. Zhu, Y. Zhao, L. Li, W. Liu, H. Zhou and C. Yang, *Bioorg. Med. Chem.*, 2014, **22**, 6735-6745.
214. D. Zhulenkovs, Z. Rudevica, K. Jaudzems, M. Turks and A. Leonchiks, *Bioorg. Med. Chem.*, 2014, **22**, 5988-6003.
215. S. Sidique, R. P. Dhanya, D. J. Sheffler, H. H. Nickols, L. Yang, R. Dahl, A. Mangravita-Novo, L. H. Smith, M. S. D'Souza, S. Semenova, P. J. Conn, A. Markou and N. D. Cosford, *J. Med. Chem.*, 2012, **55**, 9434-9445.
216. R. Dahl, Y. Bravo, V. Sharma, M. Ichikawa, R. P. Dhanya, M. Hedrick, B. Brown, J. Rascon, M. Vicchiarelli, A. Mangravita-Novo, L. Yang, D. Stonich, Y. Su, L. H. Smith, E. Sergienko, H. H. Freeze and N. D. Cosford, *J. Med. Chem.*, 2011, **54**, 3661-3668.
217. S. L. Kuchma, K. M. Brothers, J. H. Merritt, N. T. Liberati, F. M. Ausubel and G. A. O'Toole, *J. Bacteriol.*, 2007, **189**, 8165-8178.
218. H. Mikkelsen, G. Ball, C. Giraud and A. Filloux, *PLoS One*, 2009, **4**, e6018.
219. A. Meissner, V. Wild, R. Simm, M. Rohde, C. Erck, F. Bredenbruch, M. Morr, U. Römling and S. Häussler, *Environ. Microbiol.*, 2007, **9**, 2475-2485.
220. R. P. Ryan, J. Lucey, K. O'Donovan, Y. McCarthy, L. Yang, T. Tolker-Nielsen and J. M. Dow, *Environ. Microbiol.*, 2009, **11**, 1126-1136.
221. S. J. Cole and V. T. Lee, *J. Bacteriol.*, 2015, **198**, 91-97.
222. D. Drake and T. C. Montie, *J. Gen. Microbiol.*, 1988, **134**, 43-52.
223. H. Kazemian, S. Ghafourian, H. Heidari, P. Amiri, J. K. Yamchi, A. Shavalipour, H. Houri, A. Maleki and N. Sadeghifard, *Rev. Soc. Bras. Med. Trop.*, 2015, **48**, 432-436.
224. T. Krishnan, W. F. Yin and K. G. Chan, *Sensors (Basel)*, 2012, **12**, 4016-4030.
225. S. N. Norizan, W. F. Yin and K. G. Chan, *Sensors (Basel)*, 2013, **13**, 5117-5129.
226. T. Inoue, R. Shingaki and K. Fukui, *FEMS Microbiol. Lett.*, 2008, **281**, 81-86.

227. M. Deforet, D. van Ditmarsch, C. Carmona-Fontaine and J. B. Xavier, *Soft Matter*, 2014, **10**, 2405-2413.
228. T. Köhler, L. K. Curty, F. Barja, C. van Delden and J. C. Pechère, *J. Bacteriol.*, 2000, **182**, 5990-5996.
229. M. H. Rashid and A. Kornberg, *Proc. Natl. Acad. Sci. U. S. A.*, 2000, **97**, 4885-4890.
230. D. B. Kearns, *Nat. Rev. Microbiol.*, 2010, **8**, 634-644.
231. T. Köhler, R. Guanella, J. Carlet and C. van Delden, *Thorax*, 2010, **65**, 703-710.
232. C. D. McClure and N. L. Schiller, *Curr. Microbiol.*, 1996, **33**, 109-117.
233. L. Zulianello, C. Canard, T. Köhler, D. Caille, J. S. Lacroix and P. Meda, *Infect. Immun.*, 2006, **74**, 3134-3147.
234. A. Ueda and T. K. Wood, *PLoS Pathog.*, 2009, **5**, e1000483.
235. H. O. Sintim, J. A. Smith, J. Wang, S. Nakayama and L. Yan, *Future Med. Chem.*, 2010, **2**, 1005-1035.
236. G. W. Lau, D. J. Hassett, H. Ran and F. Kong, *Trends Mol. Med.*, 2004, **10**, 599-606.
237. H. M. Hassan and I. Fridovich, *J. Bacteriol.*, 1980, **141**, 156-163.
238. G. W. Lau, H. Ran, F. Kong, D. J. Hassett and D. Mavrodi, *Infect. Immun.*, 2004, **72**, 4275-4278.
239. K. Kanthakumar, G. Taylor, K. W. Tsang, D. R. Cundell, A. Rutman, S. Smith, P. K. Jeffery, P. J. Cole and R. Wilson, *Infect. Immun.*, 1993, **61**, 2848-2853.
240. H. Ran, D. J. Hassett and G. W. Lau, *Proc. Natl. Acad. Sci. U. S. A.*, 2003, **100**, 14315-14320.
241. P. Visca, F. Imperi and I. L. Lamont, *Trends Microbiol.*, 2007, **15**, 22-30.
242. I. J. Schalk and L. Guillon, *Environ. Microbiol.*, 2013, **15**, 1661-1673.
243. E. Banin, M. L. Vasil and E. P. Greenberg, *Proc. Natl. Acad. Sci. U. S. A.*, 2005, **102**, 11076-11081.
244. I. L. Lamont, P. A. Beare, U. Ochsner, A. I. Vasil and M. L. Vasil, *Proc. Natl. Acad. Sci. U. S. A.*, 2002, **99**, 7072-7077.
245. E. O. KING, M. K. WARD and D. E. RANEY, *J. Lab. Clin. Med.*, 1954, **44**, 301-307.
246. W. Kong, J. Zhao, H. Kang, M. Zhu, T. Zhou, X. Deng and H. Liang, *Nucleic Acids Res.*, 2015, **43**, 8268-8282.
247. L. C. Miller, C. T. O'Loughlin, Z. Zhang, A. Siryaporn, J. E. Silpe, B. L. Bassler and M. F. Semmelhack, *J. Med. Chem.*, 2015, **58**, 1298-1306.
248. M. A. Welsh, N. R. Eibergen, J. D. Moore and H. E. Blackwell, *J. Am. Chem. Soc.*, 2015, **137**, 1510-1519.
249. S. M. Ching, W. J. Tan, K. L. Chua and Y. Lam, *Bioorg. Med. Chem.*, 2010, **18**, 6657-6665.
250. O. J. Lieberman, M. W. Orr, Y. Wang and V. T. Lee, *ACS Chem. Biol.*, 2014, **9**, 183-192.
251. S. L. Chua, K. Sivakumar, M. Rybtke, M. Yuan, J. B. Andersen, T. E. Nielsen, M. Givskov, T. Tolker-Nielsen, B. Cao, S. Kjelleberg and L. Yang, *Sci. Rep.*, 2015, **5**, 10052.

252. K. M. Naik, D. B. Kolli and S. T. Nandibewoor, *Springerplus*, 2014, **3**, 360.
253. D. G. Ha, S. L. Kuchma and G. A. O'Toole, *Methods Mol. Biol.*, 2014, **1149**, 59-65.
254. D. G. Ha, S. L. Kuchma and G. A. O'Toole, *Methods Mol. Biol.*, 2014, **1149**, 67-72.